5-2017

Fluorescence and UV-VIS studies of quinone-induced protein modifications

Charles A. Thomas Jr

University of Tennessee at Chattanooga, wjf783@mocs.utc.edu

FLUORESCENCE AND UV-VIS STUDIES OF QUINONE-INDUCED PROTEIN MODIFICATIONS

Charles Andrew Thomas, Jr.

Departmental Honors Thesis
The University of Tennessee at Chattanooga
Department of Chemistry

Examination Date:
3 April 2017

_____

Dr. Titus V. Albu
Thesis Director

_____

Dr. Jisook Kim
Department Examiner

_____

Dr. Manuel F. Santiago
Department Examiner

ABSTRACT

Quinones are the metabolites of a class of chemicals known as polycyclic aromatic hydrocarbons. These chemicals have been found to be toxic in the environment, especially when interacting with certain proteins. In this study, we investigated the modification of Lysozyme and Ribonuclease A by a series of benzoquinones as well as few naphthoquinones. Fluorescence spectroscopy was used to measure the degree of modification of Lysozyme and Ribonuclease A when incubated with quinones at differing concentrations and for various times. All reactions, unless noted, were carried out in a phosphate buffer (pH=7.0) at 37°C to mimic physiological conditions. The fluorescence intensity of modified protein was shown to be less than that of unmodified protein, and effects of quinone substituents were examined. UV-VIS spectroscopy was also utilized to monitor adduct formation and other protein modifications. This study adds to our understanding of the effects of quinones on biological systems.

TABLE OF CONTENTS

LIST OF ACRONYMNS

Lyz	Lysozyme
RNase A	Ribonuclease A
PBQ	1,4-benzoquinone
MBQ	*methyl*-1,4-benzoquinone
CBQ	*chloro*-1,4-benzoquinone
HNQ	2-hydroxy-1,4-naphthoquinone
TCBQ	tetrachloro-1,4-benzoquinone
PhBQ	*phenyl*-1,4-benzoquinone
ONQ	*ortho*-1,4-naphthoquinone
PNQ	*para*-1,4-naphthoquinone
SDS-PAGE	Sodium Dodecyl Sulfate Polyacrylamide Gel Electrophoresis
NIFI(s)	Normalized Integrated Fluorescence Intensity(ies)
RIFI(s)	Reduced Integrated Fluorescence Intensity(ies)
UV-VIS	Ultraviolet-Visible
PAH(s)	Polycyclic Aromatic Hydrocarbon(s)
RNA	Ribonucleic Acid
MeOH	Methanol (Methyl Alcohol)
DI	Deionized
Eq.	Equation
kDa	kilodalton(s)
pKa	logarithmic acid dissociation constant

mM	millimoles per liter
mol	mole
L	liter
mL	milliliter(s)
μL	microliter(s)
nm	nanometer
g	gram(s)
h	hour(s)
min	minute(s)
s	second(s)

LIST OF TABLES

LIST OF FIGURES

Figure

Figure

Figure

Figure

Figure

CHAPTER 1

INTRODUCTION

1.1 A Brief Description of Quinones

Quinones are six-membered carbon rings with two carbon-oxygen double bonds and two carbon-carbon double bonds within the ring itself. Examples of quinones used in this research are shown below in Figure 1.1.

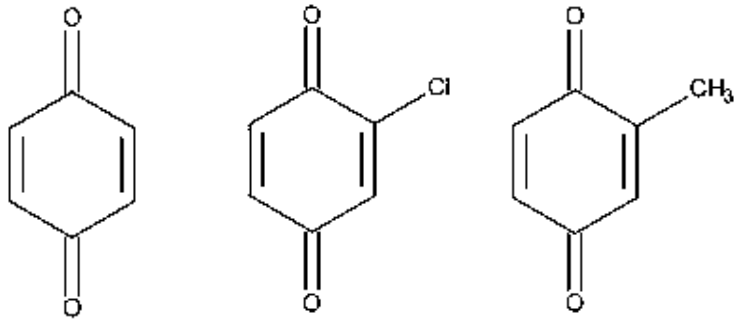

Figure 1.1 Quinones used in this research (1,4-benzoquinone (PBQ), 2-chloro-1,4-benzoquinone (CBQ), 2-methyl-1,4-benzoquinone (MBQ))

Quinones may originate from polycyclic aromatic hydrocarbons (PAHs) and exhibit toxic behavior in many ways [Snyder et al., 1989; Snyder & Hedli, 1996; Huff et al., 1989; Cornwell et al., 2003]. For example, quinones can exhibit their toxicity through redox cycling, adduct formation, and/or inducing enzyme polymerization [Kim et al., 2012; Kim et al., 2015]. Redox cycling is initiated by quinone reduction by a reductase, which then is followed by oxidation by molecular oxygen. Adduct formation is the process of quinone attacking and attaching covalently to a protein. Quinones can also act as a link between proteins leading to protein oligomerization and polymerization. In the body, quinones are highly reactive and can cause damage to healthy cells through DNA modification, lipid modification, and, the focus of this study, protein modification

[Kim et al. 2012; Vaughn, 2013; Bolton et al., 2000; Batra et al., 2006; Kim, 2013; Snyder et al., 1989].

Quinones used in this research are listed as follows: 1,4-benzoquinone (PBQ), 2-methyl-1,4-benzoquinone (MBQ), 2-chloro-1,4-benzoquinone (CBQ), tetrachloro-1,4-benzoquinone (TCBQ), phenyl-1,4-benzoquinone (PhBQ), 2-hydroxy-1,4-naphthoquinone (HNQ), 1,2-naphthoquinone (ONQ), and 1,4-naphthoquinone (PNQ). These quinones were selected due to the different electronic effects and various modifications they can produce when incubated with protein. For example, some quinone substituents exhibited greater electron donating effects versus electron withdrawing effects. This difference led to varying degrees of protein modification with electron withdrawing effects causing the most modification. Other differences between quinones were differences in consistency, color, and solubility. All quinones mentioned above were incubated with Lysozyme while only HNQ was incubated with Ribonuclease A.

1.2 Background Information on Proteins and Methods Used

Polycyclic aromatic hydrocarbons and their metabolites can specifically lead to protein aggregation. Studying PAH metabolites is interesting due to recent findings of the observed protein modifications to Ribonuclease A induced by PBQ as presented in Figure 1.2 [Kim et al., 2012; Kim et al., 2015].

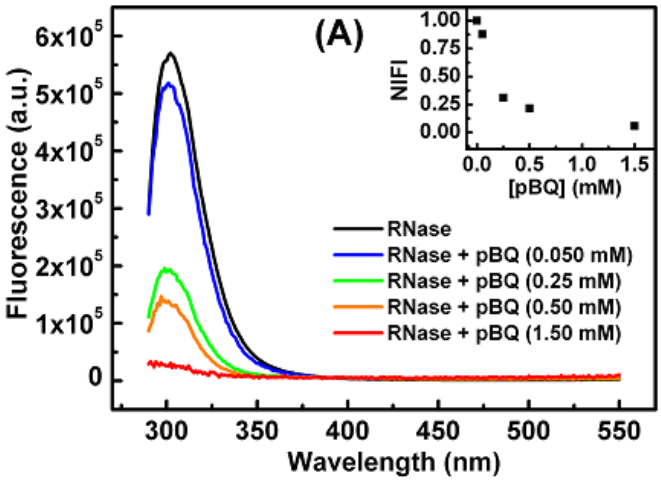

Figure 1.2 Fluorescence spectra of RNase A (0.050 mM) and RNase A (0.050 mM) modified by PBQ (0.050, 0.25, 0.50, or 1.50 mM) [Kim et al., 2012].

When proteins begin to aggregate, the result can disrupt encoding pathways leading to improper function of the cells. Protein aggregation occurs naturally as one gets older, and sometimes is the cause of Alzheimer's, Parkinson's, or Huntington's disease [Bemporad et al., 2006; Chiti & Dobson, 2006; Chiti & Dobson, 2009; Dobson, 2003; Ramirez-Alvarado, 2008; Gregersen et al., 2006]. It can easily be understood how mature protein aggregation can be toxic; however, recent research has shown that immature protein aggregations are much more toxic [Zhu et al., 2000; Nilsberth et al., 2001]. In this research, the interaction between a variety of quinones and two well-studied proteins, Lysozyme and Ribonuclease A, is investigated and quantified by use of fluorescence and UV-VIS spectroscopy.

Lysozyme is a model protein in biochemical research due to its relatively small size and ability to form crystals which are easy to manipulate [Swaminathan et al., 2011]. The function of Lysozyme is to hydrolyze glycosidic bonds between *N*-acetylmuramic acid and *N*-acetylglucosamine in Gram-positive bacteria, essentially acting as an

antibacterial agent [Willey et al., 2011]. Lysozyme was chosen for these studies due to its similar characteristics to proteins that have been found linked to neurodegenerative diseases. Specifically, Lysozyme is an amyloidogenic protein which makes it useful for comparison and understanding of such proteins that can generate plaques which cause bodily harm. In addition, Lysozyme exhibits good fluorescence behavior made possible by tyrosine and tryptophan residues which make up the protein.

Ribonuclease A is a model protein in biochemical research similar in size and crystal formation to Lysozyme. The function of Ribonuclease A is to degrade RNA strands into smaller parts. With a high affinity for single strand RNA, Ribonuclease A can exhibit its nuclease behavior both as an endonuclease and exonuclease [Voet et al., 2012]. Since Ribonuclease A is extremely common in our bodies and in the environment, it is an excellent protein to use in measuring the modification by other potentially harmful agents in the environment. In comparison with Lysozyme, Ribonuclease A is a non-amyloidogenic protein and therefore does not produce harmful plaques upon alteration of the protein structure. Though Ribonuclease A exhibits less fluorescence behavior than Lysozyme due to the absence of tryptophan, excess tyrosine residues contribute to the overall fluorescence behavior of the molecule.

Fluorescence spectroscopy is an analytical spectroscopic technique used to measure the fluorescence behavior of certain molecules at a highly sensitive level. Upon radiation with incident light, molecules absorb energy when their electrons are excited to higher energy levels and release energy when their electrons return to a more stable state. This process is known as fluorescence and can be used to identify molecules in addition to measuring changes molecules undergo [Skoog et al., 2007]. In this research, the

fluorescence behavior of proteins was measured to gain insight on the potential degree of modification caused by exposure to quinone molecules. The fluorescence of pure protein was compared with the fluorescence of altered protein as result of quinone molecules performing modification. Since both proteins used in this study contained amino acid residues with high quantum yields (tryptophan and tyrosine), the fluorescence behavior of the protein was dominated by these amino acids. It is believed any alteration to the fluorescence behavior of protein upon incubation with quinone is result of some structural change to the protein or an addition of quinone to the protein. This modification of protein affects the amino acid residues responsible for fluorescence, and ultimately cause a change in the fluorescence behavior of the protein.

UV-VIS spectroscopy is an analytical spectroscopic technique used to measure the absorbance of certain molecules in the UV-VIS region of the electromagnetic spectrum. Upon radiation with incident light, molecules absorb energy as their electrons are excited to higher energy levels and it is this absorbance that is measured with UV-VIS spectroscopy [Skoog et al., 2007]. Similar to fluorescence, certain amino acid residues, such as tryptophan and tyrosine, dominate in regard to the ability of absorbing energy. Due to UV-VIS spectroscopy being a technique of measuring absorbance, any addition of molecules that absorb in the UV-VIS range will affect the overall absorbance of the original molecule before addition of other molecules. It is believed that the addition of quinone to the proteins used in this study increases the absorbance of the modified protein because of covalently attached quinone molecules which, by themselves, absorb highly in the UV-VIS range.

1.3 Prior Studies in Our Lab

Much research has been performed at UTC over the past several years regarding Lysozyme, Ribonuclease A, and quinones. The results of these studies have paved the way for the understanding of the results presented in Chapters 2 and 3. Previous research has centered around the modification of protein specifically through protein crosslinking which results in protein oligomerization. This modification has been verified mainly through use of SDS-PAGE with fluorescence and UV-VIS spectroscopy as supporting analytical techniques. Several prior studies have utilized SDS-PAGE gels which support the results collected through this study. In this chapter, results from previous studies will be presented and discussed.

1.3.1 Modifications of ribonuclease A induced by *p*-benzoquinone

In these studies carried out by Kim et al., Ribonuclease A modifications were investigated upon exposure to PBQ at various concentrations [Kim et al., 2012]. Ribonuclease A was fixed at a concentration of 0.050 mM with PBQ used at 0.050, 0.25, 0.50, or 1.50 mM. Fluorescence spectroscopy along with UV-VIS spectroscopy was utilized to examine the spectrophotometric characteristics of Ribonuclease A after exposure to PBQ in addition to unmodified Ribonuclease A. SDS-PAGE was also utilized to visualize polymeric aggregates formed by the various reactions. All studies were performed using a phosphate buffer (50 mM) at pH=7.0 and 37°C.

The major findings of these studies are straight forward, PBQ does elicit modification of Ribonuclease A by forming both Ribonuclease A adducts and polymeric

aggregates. Figure 1.3 shows corresponding graphs of fluorescence and UV-VIS spectra of Ribonuclease A incubated with PBQ [Kim et al., 2012].

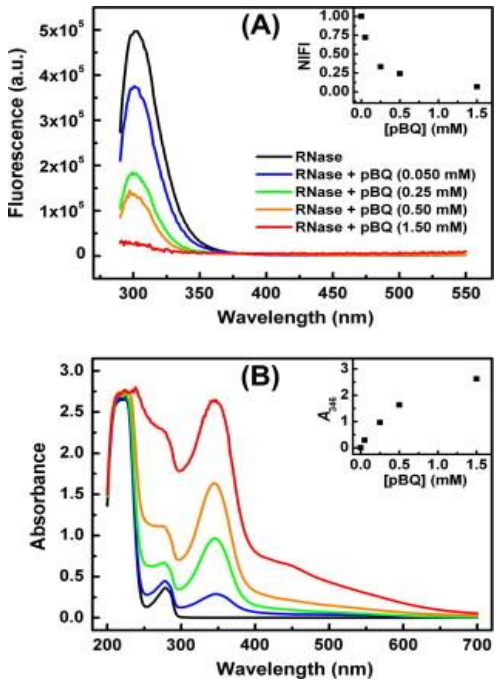

Figure 1.3 (A) Fluorescence and (B) UV-VIS spectra of RNase A (0.050 mM) and modified RNase A by PBQ (0.050, 0.25, 0.50, or 1.5 mM) for 24 h at 37°C [Kim et al., 2012].

The fluorescence behavior of modified Ribonuclease A is found to be less than unmodified Ribonuclease A indicating PBQ does elicit detectable modifications of Ribonuclease A. In addition, UV-VIS studies indicate PBQ formed covalent bonds to the modified Ribonuclease A supporting adduct formation induced by PBQ. As seen in Figure 1.4, SDS-PAGE results show PBQ is efficient in producing oligomers over time by observing the results of previously performed reactions involving PBQ and Ribonuclease A [Kim et al., 2012].

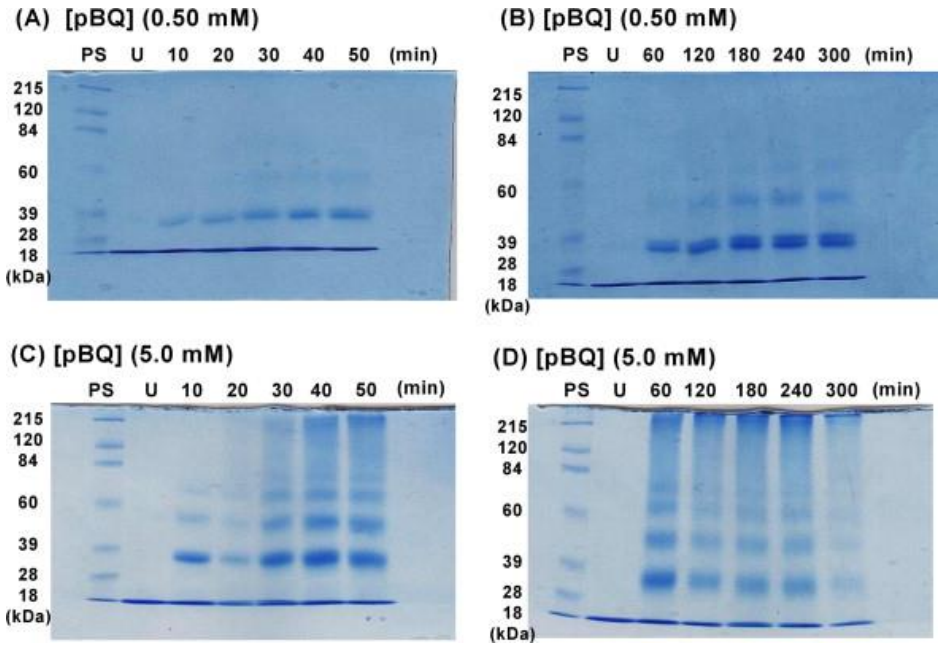

Figure 1.4 Concentration and time-dependent modification of RNase A upon exposure to PBQ at 0.50 mM and 5.0 mM in phosphate buffer (pH=7.0, 50 mM) at 37°C [Kim et al., 2012].

Overall, these results show PBQ can induce formation of both Ribonuclease A adducts and aggregates.

1.3.2 A comparison study on ribonuclease A modifications induced by substituted *p*-benzoquinones

In these studies carried out by Kim et al., Ribonuclease A modifications were investigated upon exposure to PBQ, MBQ, or CBQ [Kim et al., 2015]. Fluorescence spectroscopy along with UV-VIS spectroscopy was utilized to examine the spectrophotometric characteristics of Ribonuclease A after exposure to PBQ, MBQ, CBQ, and unmodified Ribonuclease A. SDS-PAGE was also utilized to visualize polymeric aggregates formed by the various reactions using each quinone. In SDS-PAGE experiments, Ribonuclease A was fixed at a concentration of 0.145 mM with each quinone used at 1.0 mM. All studies were performed using a phosphate buffer (50 mM) at pH=7.0 and 37°C.

As with previous studies, each quinone elicited modification of Ribonuclease A by forming polymeric aggregates and adducts. From these studies, it was found each quinone caused varying degrees of modification when incubated for the same amount of time. As seen in Figure 1.5, the fluorescence behavior of modified Ribonuclease A is found to be less than unmodified Ribonuclease A indicating that all quinones elicit modification of Ribonuclease A [Kim et al., 2015]. In addition, UV-VIS studies indicate all quinones covalently bond to Ribonuclease A supporting the previously described pathway of modification through adduct formation. As seen in Figure 1.6, SDS-PAGE results show all quinones modify Ribonuclease A through oligomerization [Kim et al., 2015]. CBQ was found to cause the quickest and most pronounced degree of modification and MBQ was found to cause the least degree of modification.

Overall, these studies show an order of increasing reactivity towards Ribonuclease A beginning with MBQ causing the least modification, PBQ causing an intermediate level of modification, and CBQ causing the greatest modification.

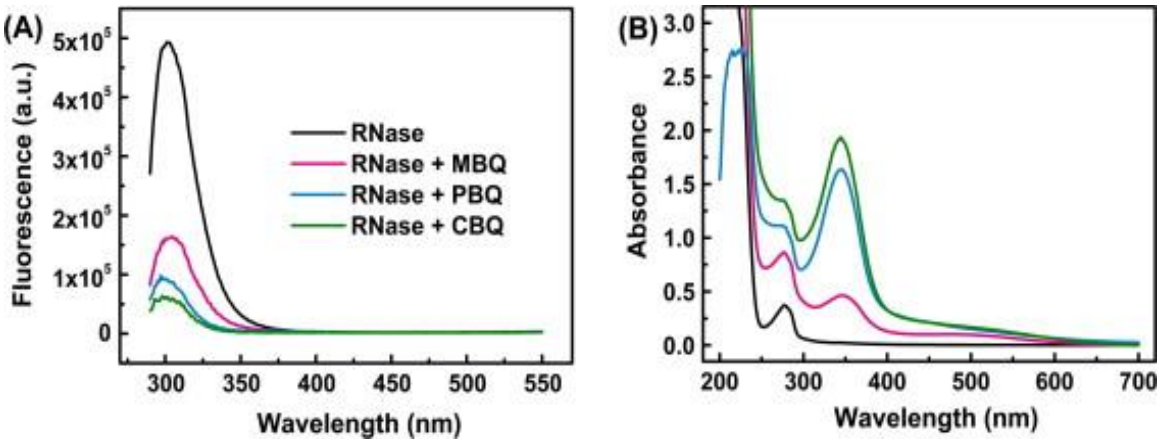

Figure 1.5 (A) Fluorescence and (B) UV-VIS spectra of RNase A (0.050 mM) and modified RNase A by PBQ, CBQ, or MBQ (0.50 mM) for 24 h at 37°C [Kim et al., 2015].

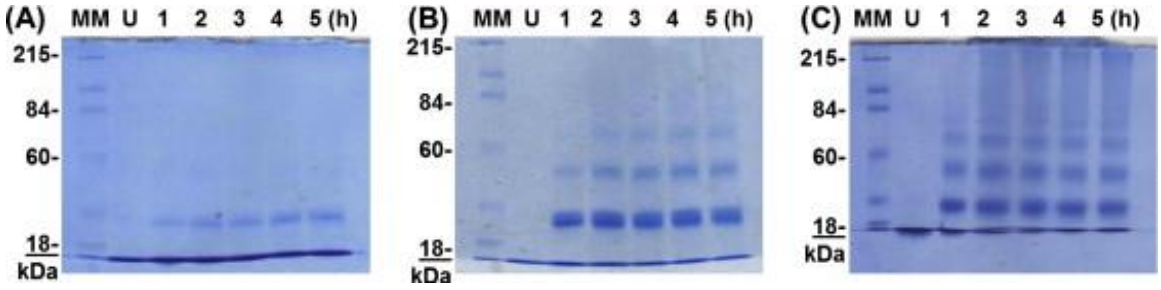

Figure 1.6 Time-dependent modification of RNase A (0.145 mM) treated with MBQ, PBQ, or CBQ (1.0 mM) for 1, 2, 3, 4 ,5 h at 37°C in phosphate buffer (pH=7.0, 50 mM). MM, protein standard molecular marker; U, RNase A; (A) RNase A + MBQ; (B) RNase A + PBQ; (C) RNase A + CBQ [Kim et al., 2015].

1.3.3 Modifications of Lysozyme by Substituted Benzoquinones

In these studies carried out by Greve & Kim presented in a Departmental Honors Thesis at UTC, Lysozyme modifications were investigated upon exposure to PBQ, CBQ, or MBQ [Greve & Kim, 2015]. SDS-PAGE was used to verify any modification of Lysozyme through induction of polymeric aggregation by PBQ, CBQ, or MBQ. Lysozyme was fixed at a concentration of 0.10 mM with quinones used at 0.10, 0.50, 1.0, and 3.0 mM. All studies were performed using a phosphate buffer (50 mM) at pH=7.0 and 37°C.

Due to the similarities of Lysozyme to Ribonuclease A, similar results were achieved regarding protein modification by PBQ, CBQ, and MBQ. Specifically, the amount of polymeric aggregate formation formed by CBQ opposed to PBQ and MBQ. In addition, aggregate formation was found to be decreasing with respect to decreasing concentration of quinone. This result was true for all quinones with the only difference being the degree of oligomerization each quinone was responsible for inducing. Figures 1.7 through 1.10 show PBQ elicits intermediate modification of Lysozyme through protein oligomerization leading to polymeric aggregation [Greve & Kim, 2015]. As seen in Figures 1.11 through 1.14, CBQ, having electron withdrawing properties, favors interaction with nucleophilic amino acid residues from Lysozyme and induces protein oligomerization [Greve & Kim, 2015]. However, as seen in Figures 1.15 through 1.18, the studies performed with MBQ showed little polymeric aggregation compared to PBQ and MBQ and suggest MBQ, having electron donating properties, does not produce significant modifications to Lysozyme [Greve & Kim, 2015].

Overall, SDS-PAGE studies show dimer, trimer, and polymeric aggregate formation across all reactions involving quinones and Lysozyme. Concentration of quinone plays an important role in determining the degree of protein crosslinking along with the length of incubation. Similar to previous studies performed by Kim et al., CBQ elicits the greatest modification of Lysozyme, PBQ elicits intermediate modification of Lysozyme, and MBQ elicits the least modification of Lysozyme [Kim et al., 2015].

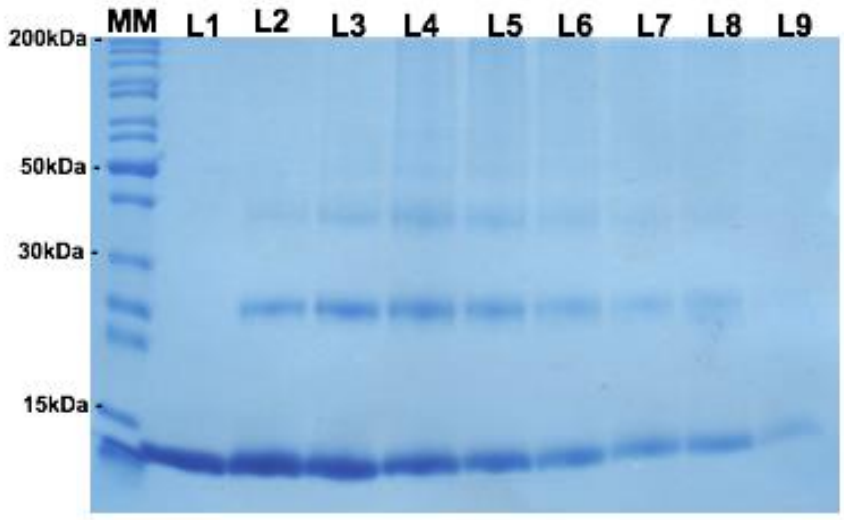

Figure 1.7 Time-dependent modification of Lyz (0.10 mM) treated with PBQ (3.0 mM) for 10, 30, 60, 120, 180, 240, and 300 min at 37°C in phosphate buffer (pH=7.0, 50 mM). MM, molecular marker; L1, Lyz (0.10 mM); L2-L8, Lyz + PBQ (3.0 mM) 10-300 min, L9, Lyz + PBQ (3.0 mM) 24 h [Greve & Kim, 2015].

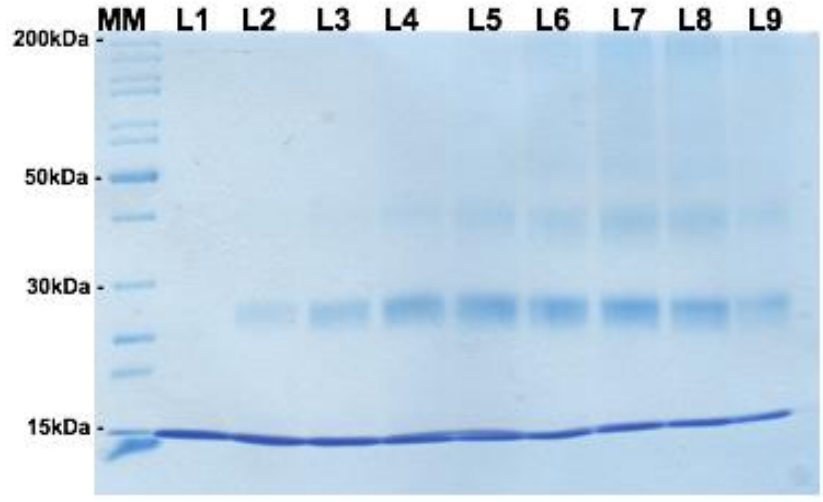

Figure 1.8 Time-dependent modification of Lyz (0.10 mM) treated with PBQ (1.0 mM) for 10, 30, 60, 120, 180, 240, and 300 min at 37°C in phosphate buffer (pH=7.0, 50 mM). MM, molecular marker; L1, Lyz (0.10 mM); L2-L8, Lyz + PBQ (1.0 mM) 10-300 min, L9, Lyz + PBQ (1.0 mM) 24 h [Greve & Kim, 2015].

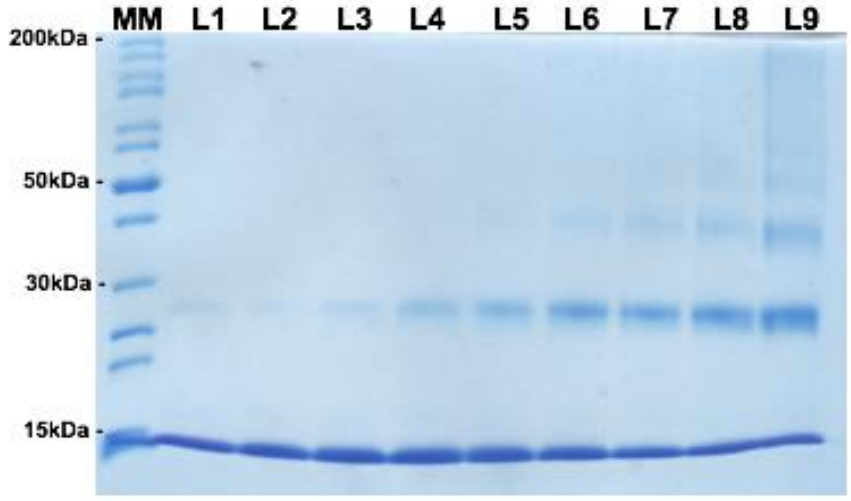

Figure 1.9 Time-dependent modification of Lyz (0.10 mM) treated with PBQ (0.50 mM) for 10, 30, 60, 120, 180, 240, and 300 min at 37°C in phosphate buffer (pH=7.0, 50 mM). MM, molecular marker; L1, Lyz (0.10 mM); L2-L8, Lyz + PBQ (0.50 mM) 10-300 min, L9, Lyz + PBQ (0.50 mM) 24 h [Greve & Kim, 2015].

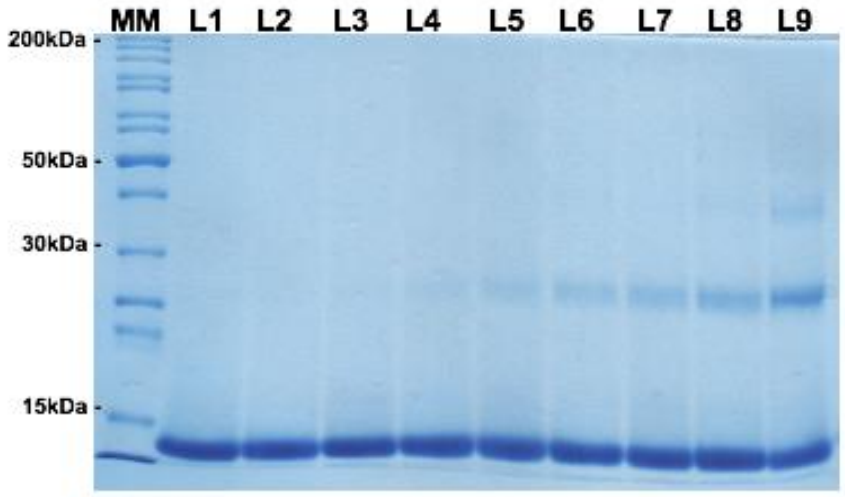

Figure 1.10 Time-dependent modification of Lyz (0.10 mM) treated with PBQ (0.10 mM) for 10, 30, 60, 120, 180, 240, and 300 min at 37°C in phosphate buffer (pH=7.0, 50 mM). MM, molecular marker; L1, Lyz (0.10 mM); L2-L8, Lyz + PBQ (0.10 mM) 10-300 min, L9, Lyz + PBQ (0.10 mM) 24 h [Greve & Kim, 2015].

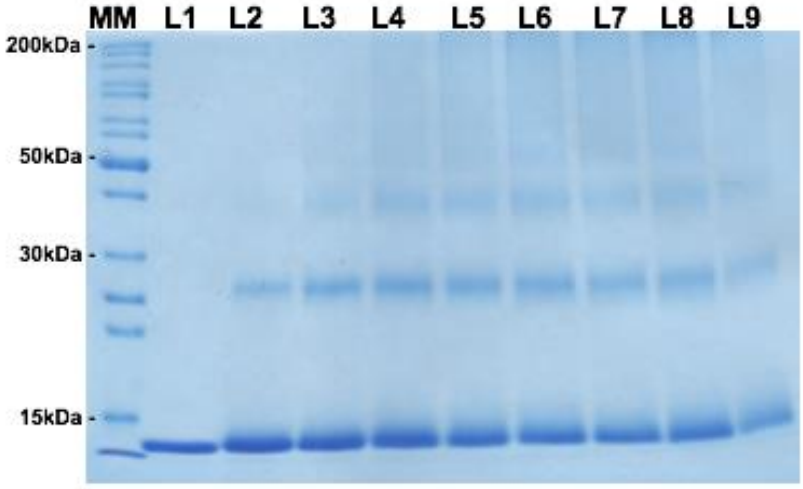

Figure 1.11 Time-dependent modification of Lyz (0.10 mM) treated with CBQ (3.0 mM) for 10, 30, 60, 120, 180, 240, and 300 min at 37°C in phosphate buffer (pH=7.0, 50 mM). MM, molecular marker; L1, Lyz (0.10 mM); L2-L8, Lyz + CBQ (3.0 mM) 10-300 min, L9, Lyz + CBQ (3.0 mM) 24 h [Greve & Kim, 2015].

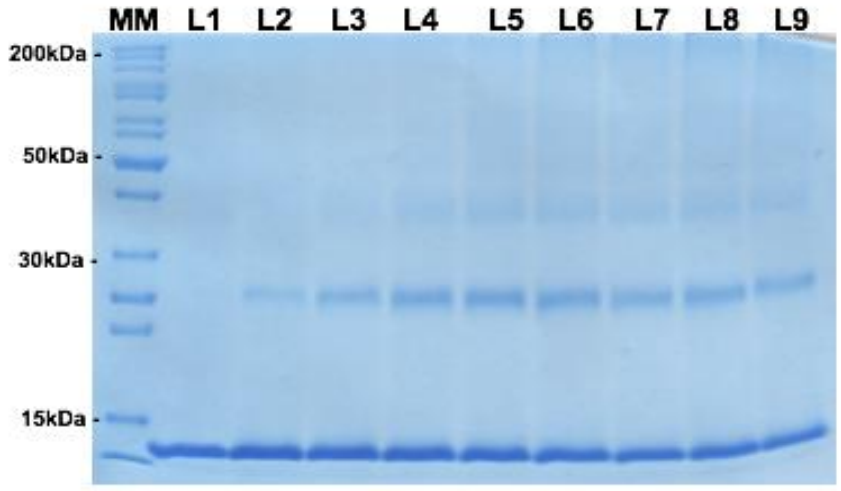

Figure 1.12 Time-dependent modification of Lyz (0.10 mM) treated with CBQ (1.0 mM) for 10, 30, 60, 120, 180, 240, and 300 min at 37°C in phosphate buffer (pH=7.0, 50 mM). MM, molecular marker; L1, Lyz (0.10 mM); L2-L8, Lyz + CBQ (1.0 mM) 10-300 min, L9, Lyz + CBQ (1.0 mM) 24 h [Greve & Kim, 2015].

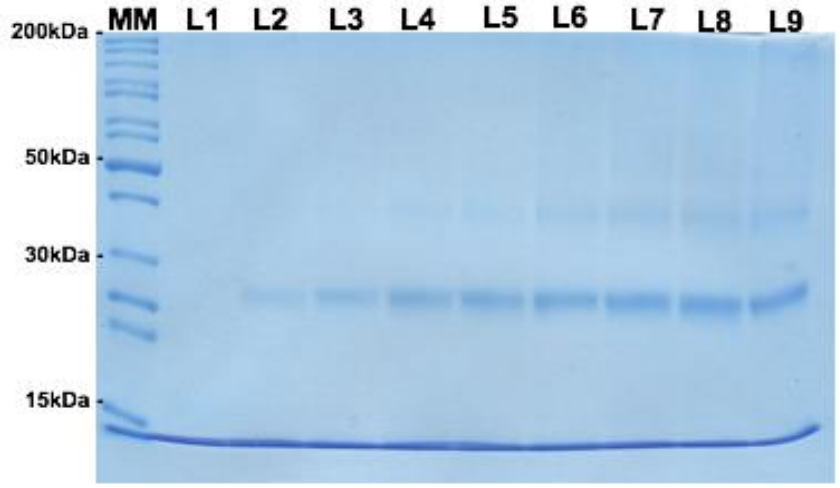

Figure 1.13 Time-dependent modification of Lyz (0.10 mM) treated with CBQ (0.50 mM) for 10, 30, 60, 120, 180, 240, and 300 min at 37°C in phosphate buffer (pH=7.0, 50 mM). MM, molecular marker; L1, Lyz (0.10 mM); L2-L8, Lyz + CBQ (0.50 mM) 10-300 min, L9, Lyz + CBQ (0.50 mM) 24 h [Greve & Kim, 2015].

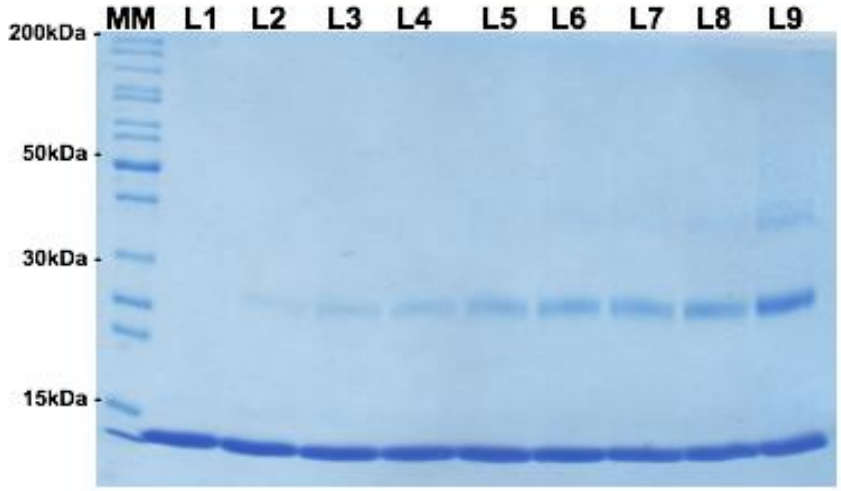

Figure 1.14 Time-dependent modification of Lyz (0.10 mM) treated with CBQ (0.10 mM) for 10, 30, 60, 120, 180, 240, and 300 min at 37°C in phosphate buffer (pH=7.0, 50 mM). MM, molecular marker; L1, Lyz (0.10 mM); L2-L8, Lyz + CBQ (0.10 mM) 10-300 min, L9, Lyz + CBQ (0.10 mM) 24 h [Greve & Kim, 2015].

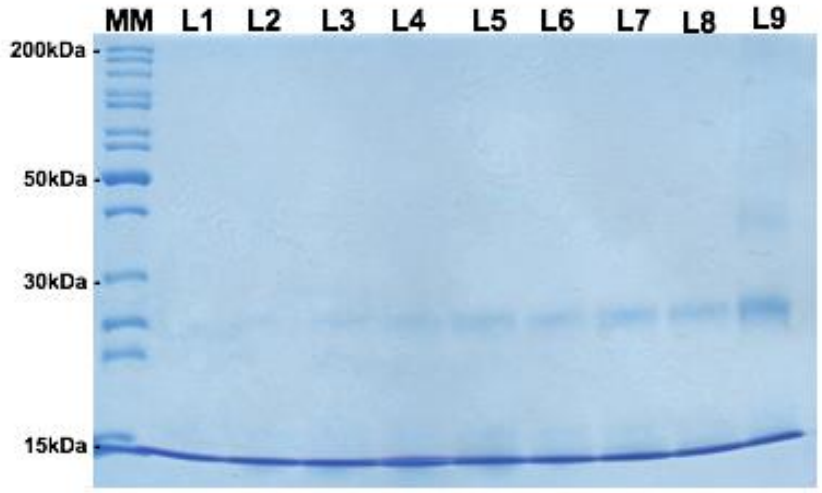

Figure 1.15 Time-dependent modification of Lyz (0.10 mM) treated with MBQ (3.0 mM) for 10, 30, 60, 120, 180, 240, and 300 min at 37°C in phosphate buffer (pH=7.0, 50 mM). MM, molecular marker; L1, Lyz (0.10 mM); L2-L8, Lyz + MBQ (3.0 mM) 10-300 min, L9, Lyz + MBQ (3.0 mM) 24 h [Greve & Kim, 2015].

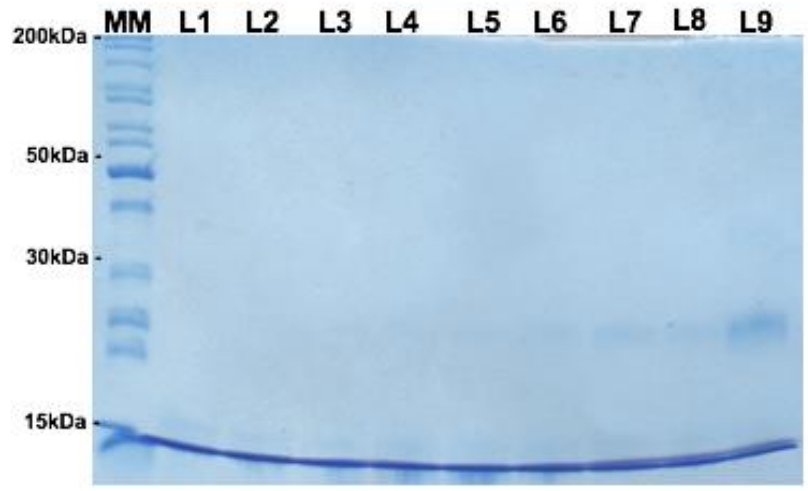

Figure 1.16 Time-dependent modification of Lyz (0.10 mM) treated with MBQ (1.0 mM) for 10, 30, 60, 120, 180, 240, and 300 min at 37°C in phosphate buffer (pH=7.0, 50 mM). MM, molecular marker; L1, Lyz (0.10 mM); L2-L8, Lyz + MBQ (1.0 mM) 10-300 min, L9, Lyz + MBQ (1.0 mM) 24 h [Greve & Kim, 2015].

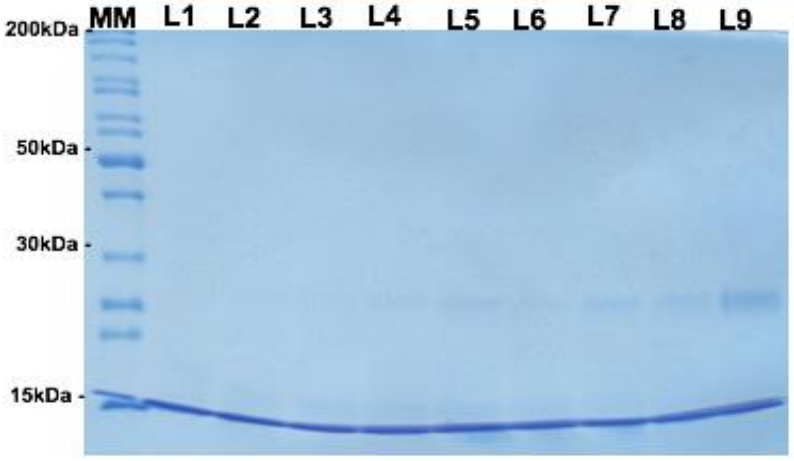

Figure 1.17 Time-dependent modification of Lyz (0.10 mM) treated with MBQ (0.50 mM) for 10, 30, 60, 120, 180, 240, and 300 min at 37°C in phosphate buffer (pH=7.0, 50 mM). MM, molecular marker; L1, Lyz (0.10 mM); L2-L8, Lyz + MBQ (0.50 mM) 10-300 min, L9, Lyz + MBQ (0.50 mM) 24 h [Greve & Kim, 2015].

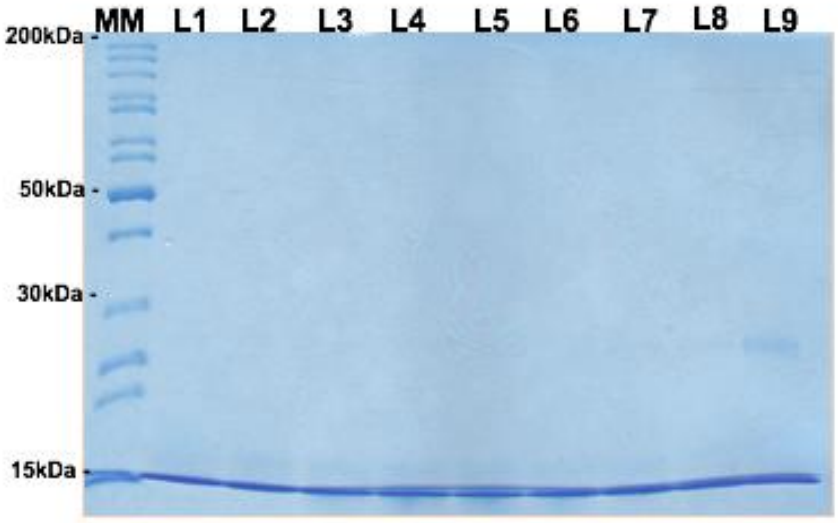

Figure 1.18 Time-dependent modification of Lyz (0.10 mM) treated with MBQ (0.10 mM) for 10, 30, 60, 120, 180, 240, and 300 min at 37°C in phosphate buffer (pH=7.0, 50 mM). MM, molecular marker; L1, Lyz (0.10 mM); L2-L8, Lyz + MBQ (0.10 mM) 10-300 min, L9, Lyz + MBQ (0.10 mM) 24 h [Greve & Kim, 2015].

1.3.4 Ribonuclease A Modification Induced by 1,2-Naphthoquinone and 2-Hydroxy-1,4-Naphthoquinone

In these studies carried out by Smith & Kim presented in a Departmental Honors Thesis at UTC, Ribonuclease A modifications were investigated upon exposure to ONQ and HNQ [Smith & Kim, 2015]. Ribonuclease A was fixed at a concentration of 0.10 mM with naphthoquinones used at 5.0 mM. SDS-PAGE was primarily used to examine the modification of Ribonuclease A through protein oligomerization induced by ONQ or HNQ. Reactions with Ribonuclease A were performed at pH=7.0 and 37°C to mimic physiological conditions. In addition, to fully understand the effects of each naphthoquinone on Ribonuclease A, the incubation conditions of Ribonuclease A were varied regarding pH. Considering HNQ, specifically the ionizable hydroxyl group, changes in the pH of the incubation condition would supposedly alter the functionality of both Ribonuclease A and HNQ.

As seen in Figure 1.19, SDS-PAGE results show ONQ to elicit greater activity towards Ribonuclease A resulting in protein oligomerization [Smith & Kim, 2015]. As seen in Figures 1.20 and 1.21, HNQ, regardless of pH change, was not found to cause protein oligomerization and was believed to carry out its protein modifying capabilities through other mechanisms [Smith & Kim, 2015]. It is these mechanisms that are investigated and discussed more in Chapter 3.

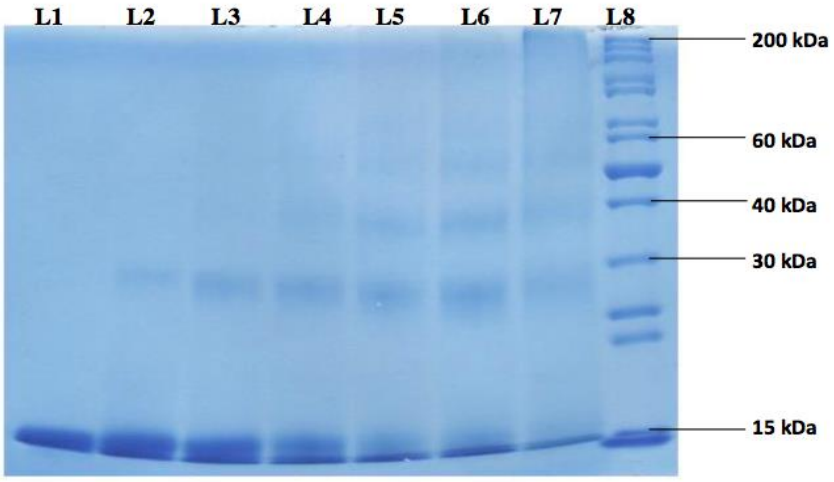

Figure 1.19 Time-dependent modification of RNase A (0.10 mM) treated with ONQ (5.0 mM) for 10 min, 30 min, 1, 2, 3, and 24 h at 37°C in phosphate buffer (pH=7.0, 50 mM). L1, RNase A (0.10 mM), L2-L7, RNase A + ONQ (5.0 mM) 30 min-24 h, L8, molecular marker [Smith & Kim, 2015].

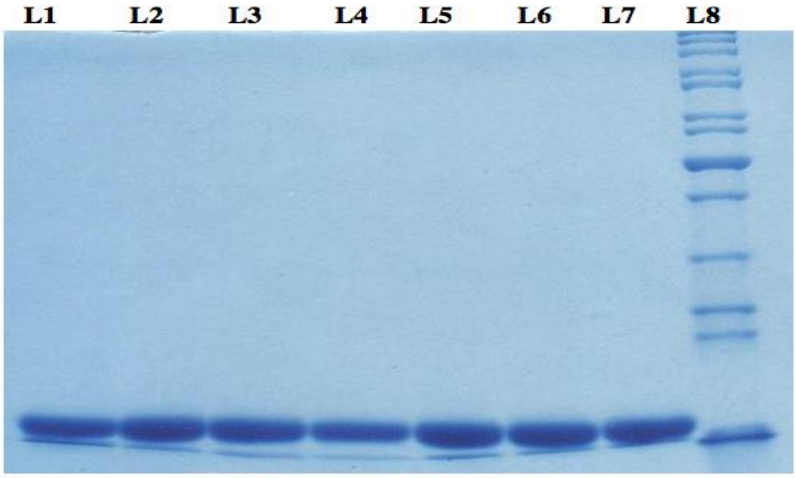

Figure 1.20 Time-dependent modification of RNase A (0.10 mM) treated with HNQ (5.0 mM) for 10 min, 30 min, 1, 2, 3, and 24 h at 37°C in phosphate buffer (pH=7.0, 50 mM). L1, RNase A (0.10 mM), L2-L7, RNase A + HNQ (5.0 mM) 30 min-24 h, L8, molecular marker [Smith & Kim, 2015].

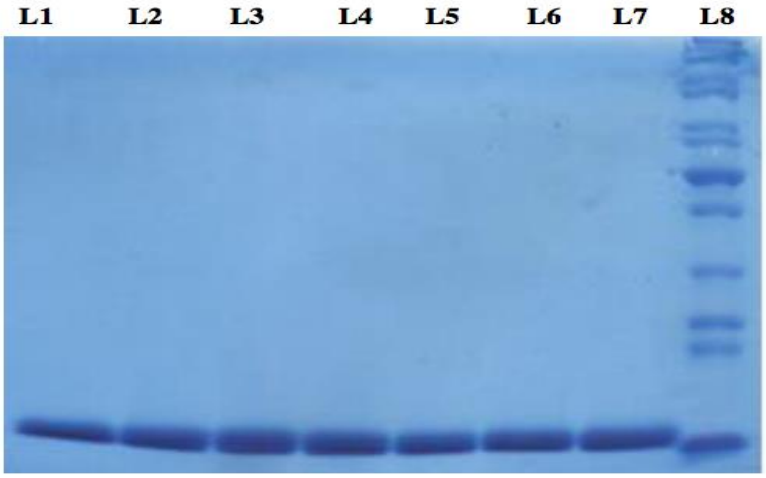

Figure 1.21 Time-dependent modification of RNase A (0.10 mM) treated with HNQ (5.0 mM) for 10 min, 30 min, 1, 2, 3, and 24 h at 37°C in phosphate buffer (pH=4.8, 50 mM). L1, RNase A (0.10 mM), L2-L7, RNase A + HNQ (5.0 mM) 30 min-24 h, L8, molecular marker [Smith & Kim, 2015].

CHAPTER 2

STUDIES OF LYSOZYME MODIFICATIONS INDUCED BY QUINONES

2.1 Introduction

In previous studies performed by Greve & Kim, certain quinones have been found to induce modification of Lysozyme [Greve & Kim, 2015]. So far, PBQ, MBQ, and CBQ have all been found to elicit modification of Lysozyme through protein crosslinking, which yields protein oligomerization, and adduct formation. This current study seeks to add to previous studies regarding the quinones mentioned above, as well as test several others on their modifying capabilities towards Lysozyme. Additional quinones include: TCBQ, PhBQ, HNQ, ONQ, and PNQ. In addition, certain parameters such as pH and temperature are altered to investigate their effects on the modification of Lysozyme incubated with PBQ. Fluorescence and UV-VIS spectroscopy were used to examine the modifications of Lysozyme induced by these quinones.

2.2 Methodology

All chemicals were purchased from Sigma Aldrich, Fisher, Acros Organics, or MP Biomedicals and were of reagent grade. The protein of interest, Lysozyme (from *hen egg white*), was purchased from MP Biomedicals and kept frozen for preservation until ready for use. All water used in this study was deionized (DI) water purified by a Millipore system (Milli-Q). All solutions were made in lab and kept sealed or covered until ready for use. All reactions were performed in a similar manner following the devised experimental protocol to keep error at a minimum. Each study was performed over a three-day period consisting of (1) preparing and starting the reaction, (2)

performing dialysis of the incubated solution, and (3) finishing the reaction. Quartz cuvettes, purchased from Starna Cells, Inc., were re-used after being thoroughly cleaned with Starna Cells, Inc. cuvette cleaner and allowed to dry. At times, when higher concentration reactions were performed, a film-like residue would build up on the inside of the reaction cuvette. This was cleaned by filling to the brim with concentrated nitric acid and allowed to soak overnight. The next day, the normal cleaning procedure with cuvette cleaner was performed to ensure a thorough cleaning of the cuvette. Physiological conditions (pH=7.0, 37°C) were modeled for all reactions except for studies in which the pH or temperature was varied. At all times, proper laboratory protocol was followed and the laboratory was kept in clean and functional condition.

2.2.1 Buffer Solution

A phosphate buffer (50 mM), comprised of a mixture of monobasic monosodium phosphate crystal ($NaH_2PO_4 \cdot H_2O$) and dibasic disodium phosphate anhydrous (Na_2HPO_4), was prepared and used for all reactions in this study. Most reactions were performed at pH=7.0 and 37°C to mimic physiological conditions. However, some reactions were performed at a different pH or temperature to study the effect of changing these factors. The phosphate buffer solution was used in every 3 mL reaction cuvette as well as in 1 L beakers when performing dialysis. Solutions of $NaH_2PO_4 \cdot H_2O$ (50 mM) and Na_2HPO_4 (50mM) were combined in ratios to produce a solution at a pH pre-determined by the Henderson-Hasselbalch equation (Eq. 2.1).

$$pH = pKa + log\frac{[base]}{[acid]} \qquad \text{(Eq. 2.1)}$$

A phosphate buffer solution was chosen primarily because of the multiple dissociation constants of phosphoric acid. Since the second deprotonation of phosphoric acid has a pKa around 7.2, an equilibrium between $NaH_2PO_4 \cdot H_2O$ and Na_2HPO_4 creates an effective buffering range around pH=7.0. Due to the physiological approach of the study, the use of phosphates in the buffer solution keeps the study in line with biological systems.

To perform a reaction, 4 L of buffer was made fresh the day before each reaction. 14.19 g of Na_2HPO_4 (50mM) was weighed and carefully poured in a 2 L volumetric flask followed by dilution to the line with deionized water. Following the same procedure, 13.79 g of $NaH_2PO_4 \cdot H_2O$ (50 mM) was weighed and carefully poured in a similar 2 L volumetric flask, again diluting to the line with deionized water. To have enough Na_2HPO_4 (50mM) for pH=7.0, an additional 0.500 L of Na_2HPO_4 (50mM) was made by weighing 3.55 g of Na_2HPO_4 (50mM) and following the same dilution and mixing protocol mentioned above. These flasks were subjected to stirring by mechanical means for roughly 30 min. Once fully dissolved, the two solutions of acid and base were combined in pre-determined ratios, 1 L at a time, to produce the desired pH of the buffer. For example, for a buffer solution at pH=7.0, 557 mL of Na_2HPO_4 (50 mM) was combined with 443 mL of $NaH_2PO_4 \cdot H_2O$ (50 mM), adequately mixed, and transferred into a 4 L plastic jug. This process was repeated three additional times to produce 4 L of buffer solution. The final pH of solution was checked using a Fisher AB15 Accumet pH meter equipped with an AccuTupH probe. After calibration with stock solutions at pH=4.00 and pH=10.01, if the pH of the buffer solution was within ± 0.05 units of the

desired pH, the solution was acceptable and was stored in the fridge at 4°C until ready for use.

2.2.2 Protein Solution

Lysozyme stock solutions were made to provide enough protein for the extent of this study. This involved carefully weighing an imprecise amount of Lysozyme, 0.0462 g, onto tared weigh-paper and quantitatively transferring into a 10 mL volumetric flask. Phosphate buffer (50 mM, pH=7.0) was used to wash any residual Lysozyme off the weigh-paper into the volumetric flask. Lysozyme, in the volumetric flask, was diluted to the line with phosphate buffer (50 mM, pH=7.0) and the flask was capped and sealed with ParaFilm. To facilitate the protein into solution, sonication was performed for 15 min in addition to inversion and shaking the volumetric flask by hand. After sonication, the protein solution was carefully transferred to Eppendorf tubes and stored in the freezer until needed.

The concentration of stock Lysozyme was calculated by converting 0.0462 g of Lysozyme to moles of Lysozyme and then dividing by 0.0100 L. To convert grams to moles, 0.0462 g of Lysozyme was divided by 14388 g/mol, the molecular weight of Lysozyme. This value was then divided by 0.0100 L to determine the molarity, or concentration, of the stock Lysozyme. Finally, this concentration was multiplied by 1000 to express the concentration in mM, a unit easier to manipulate during future calculations. As result, the concentration of stock Lysozyme was determined to be 0.321 mM.

To perform a reaction, one Eppendorf tube containing the stock Lysozyme was retrieved from the freezer and allowed to thaw out on ice for 20 min, on the counter for

20 min, and finally in the hand for a few minutes. Once completely thawed, the protein solution was vortexed for 1 min to ensure homogeneity before being ready for use.

For all studies involving the modification of Lysozyme by quinones, Lysozyme was fixed at a concentration of 0.010 mM. Calculations were performed to determine the exact volume of stock Lysozyme to add to each reaction cuvette to obtain a Lysozyme concentration of 0.010 mM. This was performed using Equation 2.2 where M_1 is the concentration of stock Lysozyme (0.321 mM), V_1 is the required aliquot of stock Lysozyme to be added to the reaction cuvette, M_2 is the desired concentration of Lysozyme (0.010 mM), and V_2 is the desired volume in the reaction cuvette (3000 µL).

$$M_1V_1 = M_2V_2 \qquad \text{(Eq. 2.2)}$$

As result, 93.5 µL of stock Lysozyme was transferred to a 3 mL reaction cuvette containing phosphate buffer (50 mM) to achieve a Lysozyme concentration of 0.010 mM used for all studies.

2.2.3 Quinone Solution

Quinone solutions were made fresh for every reaction performed. This involved weighing an imprecise amount of quinone on tared weigh-paper (a mass between 0.0100 g and 0.0200 g) and quantitatively transferring to a 10 mL, 50 mL, or even 100 mL volumetric flask. Phosphate buffer (50 mM) was used to wash any residual quinone off the weigh-paper into the volumetric flask. Quinone, in the volumetric flask, was diluted to the line with phosphate buffer (50 mM) and capped and sealed with ParaFilm. To facilitate the quinone into solution, sonication was performed for 10 min in addition to inversion and shaking the volumetric flask by hand. Halfway through the sonication

procedure, the volumetric flask was removed, inverted to mix the solution, and then placed back into the sonicator. After sonication, the quinone solution was transferred into a small holding beaker, covered with foil, and was ready for use.

Considering the quinones used, PBQ dissolved easily into solution with the techniques mentioned above, but MBQ, CBQ, TCBQ, PhBQ, HNQ, ONQ, and PNQ required an additional agent to aide with their solubility. For this, a 10% MeOH/90% phosphate buffer (50 mM) was used to help dissolve the quinones in the 10 mL, 50 mL, or 100 mL volumetric flasks. It is important to note only the volumetric flask containing the quinone solution contained 10% MeOH. Once the quinone, in solution, was transferred from the small holding beaker to the reaction cuvette, phosphate buffer (50 mM) was used to bring the reaction cuvette up to volume. When using the 10% MeOH/90% phosphate buffer solution for quinone preparation, the overall concentration of MeOH in the reaction cuvettes never exceeded 1%.

During the sonication procedure, the concentration of quinone prepared in solution was calculated by converting the mass of quinone to moles of quinone and then dividing by the volume of the volumetric flask the quinone was dissolved in. To convert grams of quinone to moles of quinone, the mass of quinone was divided by the molar mass of the quinone. This value was then divided by the volume of the volumetric flask used to determine the molarity, or concentration, of the quinone in solution. Finally, this concentration was multiplied by 1000 to express the concentration in mM, a unit easier to manipulate during future calculations.

In addition, further calculations were performed during the sonication process to determine the exact volume of quinone solution to add to the reaction cuvette containing

Lyz (0.010 mM) and phosphate buffer (50 mM) to achieve the desired concentration of quinone in the reaction cuvette. This was calculated using Equation 2.3 where, in this case, M_1 is the actual concentration of the quinone solution prepared, V_1 is the required aliquot of quinone solution to be added to the reaction cuvette, M_2 is the desired concentration of quinone, and V_2 is the desired volume in the reaction cuvette (3000 μL).

$$M_1V_1 = M_2V_2 \qquad \text{(Eq. 2.3)}$$

Since several concentrations of quinone were used across all studies, and the amount of quinone weighed out each time was different, the amount of quinone solution added to the reaction cuvette varied reaction to reaction.

For PBQ, aliquot volumes were calculated for desired concentrations of 0.010 mM, 0.050 mM, 0.10 mM, and 0.30 mM. For MBQ, CBQ, TCBQ, PhBQ, HNQ, ONQ, PNQ, and studies involving PBQ at different temperatures or pH, aliquot volumes were calculated for a fixed concentration of 0.050 mM. This concentration was determined to work with best when comparing different quinones or variables of reactions because it provided a concentration high enough to modify Lysozyme significantly.

Once the calculated volume of quinone solution was added to the reaction cuvette containing Lyz (0.010 mM) and phosphate buffer (50 mM), the reaction began, the cuvette was placed into the fluorimeter for scanning, and the reaction time was kept on a scientific timer.

2.2.4 Fluorescence Spectroscopy & Anisotropy Measurements

Fluorescence spectroscopy was performed using a Horiba Jobin Yvon Fluorolog spectrophotometer equipped with a Xenon lamp. The excitation wavelength was fixed at 280 nm with a 2 nm slit width to accommodate tryptophan and tyrosine residues in Lysozyme. The resulting emission was recorded every 1 nm with a slit width of 2 nm over the range of 290-600 nm. To draw correlations between all studies, each spectrum was normalized from 500-550 nm where little emission was recorded. Microsoft Excel was used to analyze the data and to produce graphs to visualize the fluorescence spectra.

All reactions were performed in a quartz cuvette in phosphate buffer (50 mM). The cuvette was equipped with a stir bar to ensure proper mixing and to minimize sedimentation of Lysozyme. The stirring motion was set to the 3rd level of power as indicated on the fluorimeter. Emission scanning lasted around 10 min and varied occasionally in duration due to mechanical motion inside of the fluorimeter. Initial scanning, or reaction scanning, of Lysozyme occurred over 24 h with scans occurring every hour for that duration. Post-modified Lysozyme was returned to a quartz cuvette after a 24 h dialysis and scanned an additional four times. This resulting data was recorded, averaged, and analyzed in Microsoft Excel to produce the graphs presented in this study. A control was produced by subjecting Lyz (0.010 mM) in phosphate buffer (50 mM) to the same procedure as every reaction performed.

The software to operate the fluorimeter was FluorEssence by Horiba Jobin Yvon. This software was capable of automating fluorescence and anisotropy scans which were utilized to accomplish the 24 h scans of each study. The first and second scans were always started manually with each consecutive scan being automatically started by the

programming. Since each emission scan lasted around 10 min (600 s), the instrument was programmed to scan the reaction every 2997 s for 24 h to accomplish 24 h of scanning each hour. Due to the mechanical motion of parts inside of the fluorimeter, an additional 3 s was added to accommodate the automated re-calibration of the instrument after each scan. Due to fluctuations in voltage supplied to the instrument, the timing of the scans slightly varied for each reaction and occasionally needed to be reset during the reaction.

The process of performing fluorescence measurements was performed in a similar manner for every reaction by following a pre-determined protocol. To begin, the fluorimeter was turned on by first switching on the water bath, the fan, the lamp, and then the software PC. The lamp was allowed to warm up for 1 h before any measurements took place. The instrument was initialized by selecting to perform a spectra study, specifically an emission study, and then by executing a trial scan (C1-Trial) with the cuvette containing only Lysozyme and phosphate buffer (50 mM). Once the initialization was complete and the trial scan was acceptable, the software was used to program the instrument for fluorescence measurements. A scientific timer was obtained and started as soon as the aliquot of quinone was administered to the reaction cuvette containing Lysozyme and phosphate buffer. After this, the reaction cuvette was capped, the sides wiped with Kimwipes, inverted 3 times, and placed in the fluorimeter for scanning. Once securely positioned inside the fluorimeter, the fluorescence scanning was started and the time on the scientific timer was recorded. This time was the delay between the actual start of the reaction of Lysozyme with quinone and the fluorescence scanning of the

reaction. In addition, the time of day was recorded to be able to monitor the start and stop of each consecutive measurement every hour.

Post-modified Lysozyme fluorescence measurements were performed using a different programmed scanning procedure as initial scanning. In these scans, modified Lysozyme was scanned four times in the time frame of 1 h at 37°C. Once these scans were complete, the cuvette was removed from the fluorimeter and the instrument was shut down in the reverse order in was turned on. This concluded the use of fluorescence spectroscopy to measure the modification of Lysozyme induced by quinones.

In addition to fluorescence measurements, anisotropy measurements were performed as well during initial and post-modified scanning of Lysozyme. Appendix A shows anisotropy measurements for each study performed using Lysozyme. A general trend can be seen in each graph indicating the correlation between increasing modification of Lysozyme and increasing anisotropy values of Lysozyme.

2.2.5 UV-VIS Spectroscopy

UV-VIS spectroscopy was performed using a double-beam UV-1800 Shimadzu UV Spectrophotometer. The instrument was always allowed to warm up for 20 min before any measurements took place. Excitation was achieved using a D_2/W lamp with the resulting spectra recorded at 1 nm sampling intervals over the range of 200-700 nm with the scan speed set to fast. The slit width was 1.0 nm and the D_2/W light change was set at 340.8 nm. The instrument was auto-zeroed and baselined prior to every scan to account for background noise. Microsoft Excel was used to analyze the data recorded and to produce the graphs presented in this study.

Immediately after fluorescence scanning was complete, the cuvette was transferred into the UV-VIS spectrophotometer for analysis. Absorbance of the analyte was recorded and immediately processed on screen using the software UV Probe 2.33. A reference cell containing phosphate buffer (50 mM, pH=7.0) was prepared at the beginning of the study and was used for every reaction throughout the study. This insured the absorbance calculated by the instrument was solely from Lysozyme and any bound or unbound quinone. Pre-dialysis Lysozyme exhibited larger absorbance than post-dialysis Lysozyme due to unbound quinone in solution absorbing light. Removal of unbound quinone by dialysis reduced the absorbance of the analyte and produced a more accurate representation of modified Lysozyme.

All UV-VIS measurements were performed in the same manner and used to measure the amount of modification (by adduct formation) of Lysozyme.

2.2.6 Dialysis

To accurately measure the modification of Lysozyme induced by quinones, dialysis was performed to remove unbound quinone that was not covalently bonded to Lysozyme. Spectroscopically measuring Lysozyme with bound quinone alone gives clear understanding of the modification of Lysozyme induced by quinones.

Dialysis was performed using a 5 mL Float-A-Lyzer purchased from Spectrum Laboratories. The membrane, with a molecular cutoff of 3.5 kDa, allowed unbound quinone to freely exit through the membrane. Lysozyme, with a molecular mass of 14.3 kDa, or modified Lysozyme, with a slightly higher molecular mass, remained inside of the dialysis membrane along with any quinone bound to the protein via ionic bonding,

covalent bonding, or H-bonding. Before use, each dialysis membrane was thoroughly soaked, washed, and rinsed with DI water and then temporarily held in phosphate buffer solution (50 mM) kept at 4°C. Before the reaction solution could be transferred into the dialysis membrane, the membrane was emptied of phosphate buffer solution to insure proper concentration of the protein and quinone in solution. Once the reaction solution was carefully transferred from the reaction cuvette to the dialysis membrane by a disposable pipette, the dialysis membrane was placed in 900 mL of phosphate buffer solution and kept at 4°C for 24 h. Facilitation of unbound quinone out of the dialysis membrane was accelerated by the concentration gradient between the phosphate buffer solution and the reaction solution as well as by stirring using a stir bar. Since the concentration of quinone outside of the dialysis membrane was less than the concentration of quinone inside of the dialysis membrane, simple diffusion occurred and the unbound quinone exited the dialysis membrane. This was further accelerated by changing out the phosphate buffer solution three times, typically every 2.5 h. By doing this, the concentration gradient became smaller each time and diffusion continued to take place. After three buffer changes, and considering the volume of reaction solution to phosphate buffer solution, it is safe to assume all unbound quinone had been washed from the reaction solution.

After 24 h of dialysis, the contents in the dialysis membrane were returned to a clean reaction cuvette and placed in the fluorimeter for post-dialysis fluorescence scanning. By removal of unbound quinone in solution, the modification of Lysozyme by bound quinone only was measured and quantified by fluorescence and UV-VIS spectroscopy.

2.3 Results and Discussion

The results of several reactions involving Lysozyme are presented below. Six different studies were conducted: (1) a study with PBQ at various concentrations, (2) a study with PBQ incubated for various lengths of time, (3) a study involving certain substituents on PBQ, (4) a study involving naphthoquinones, and (5-6) studies focused on the pH and temperature dependence of PBQ. Fluorescence and UV-VIS graphs are included for each study. The graphs depict the fluorescence intensity and absorbance of post-dialysis Lysozyme. Post-dialysis Lysozyme (i.e. modified Lysozyme) refers to Lysozyme which has completed a 24 h dialysis and contains only Lysozyme and any bound quinone to the protein.

Normalized integrated fluorescence intensity (NIFI) values were obtained by selecting a range of wavelengths and calculating the area under the curve of each fluorescence spectrum. Two separate wavelength ranges were chosen for all calculations of NIFI. The integration range of 300-410 nm spans the entire fluorescence area while the integration range of 320-360 nm narrows in on the maximum fluorescence intensity for each reaction. This was done to account for minor peaks in the fluorescence spectra and to measure uniformity when comparing results. Two reference NIFIs were used, Lyz (0.010 mM) for all studies except those with pH or temperature alterations, and Lyz + PBQ (0.050 mM) (pH=7.0, 37°C) for the studies with pH or temperature alterations. To quantify the modification of Lysozyme from different studies, a reduced integrated fluorescence intensity (RIFI) value was calculated by dividing the NIFI of the study in question by the reference NIFI, converting to a percentage, and then subtracting from

100%. Reference NIFIs have RIFIs of 0% since 100%-100% = 0% and negative RIFIs represent an increase in fluorescence intensity since the corresponding NIFI is greater than the reference NIFI.

Through observation of a reduction of fluorescence intensity and an increase in absorbance, modification of Lysozyme was confirmed from the results of these studies.

2.3.1 Lysozyme Modifications Induced by PBQ at Various Concentrations

In this study, Lyz (0.010 mM) was treated with PBQ (0.010, 0.050, 0.10, or 0.30 mM) and allowed to react while being monitored using fluorescence for 24 h. Following the 24 h incubation, dialysis was performed for an additional 24 h followed by a final spectroscopic measurement of modified Lysozyme. All reactions were performed in a phosphate buffer (50 mM) at 37°C and pH=7.0 to mimic physiological conditions. To investigate the influence of using methanol for increasing quinone solubility, one reaction was performed using a 10% MeOH/90% phosphate buffer when preparing the quinone solution.

Table 2.1 lists RIFI values calculated over 300-410 nm and 320-360 nm in addition to absorbance values for each reaction performed in this study. Figure 2.1 shows the fluorescence intensity of Lysozyme and Lysozyme modified by PBQ (0.010, 0.050, 0.10, or 0.30 mM) for 24 h at 37°C. All spectra were normalized in the 500-550 nm range where little emission is present to ensure proper comparison. Figure 2.2 shows the absorbance of Lysozyme and Lysozyme modified by PBQ (0.010, 0.050, 0.10, or 0.30 mM) for 24 h at 37°C.

Table 2.1 RIFI of Lyz (0.010 mM) and Lyz (0.010 mM) modified by PBQ (0.010, 0.050, 0.10, or 0.30 mM) for 24 h at 37°C. Absorbance at 346 nm of Lyz (0.010 mM) and Lyz (0.010 mM) modified by PBQ (0.010, 0.050, 0.10, or 0.30 mM) for 24 h at 37°C.

Reaction	RIFI[a] (%)	RIFI[b] (%)	A_{346} (a.u.)
Lyz (0.010 mM)	0	0	-0.001
Lyz + PBQ (0.010 mM)	28	29	0.039
Lyz + PBQ (0.050 mM) MeOH	53	53	0.082
Lyz + PBQ (0.050 mM)	57	58	0.094
Lyz + PBQ (0.10 mM) (150526)	65	66	0.125
Lyz + PBQ (0.10 mM) (150713)	66	67	0.123
Lyz + PBQ (0.10 mM) (150513)	70	71	No Data
Lyz + PBQ (0.30 mM)	81	82	0.134

a *integration between 300-410 nm*
b *integration between 320-360 nm*

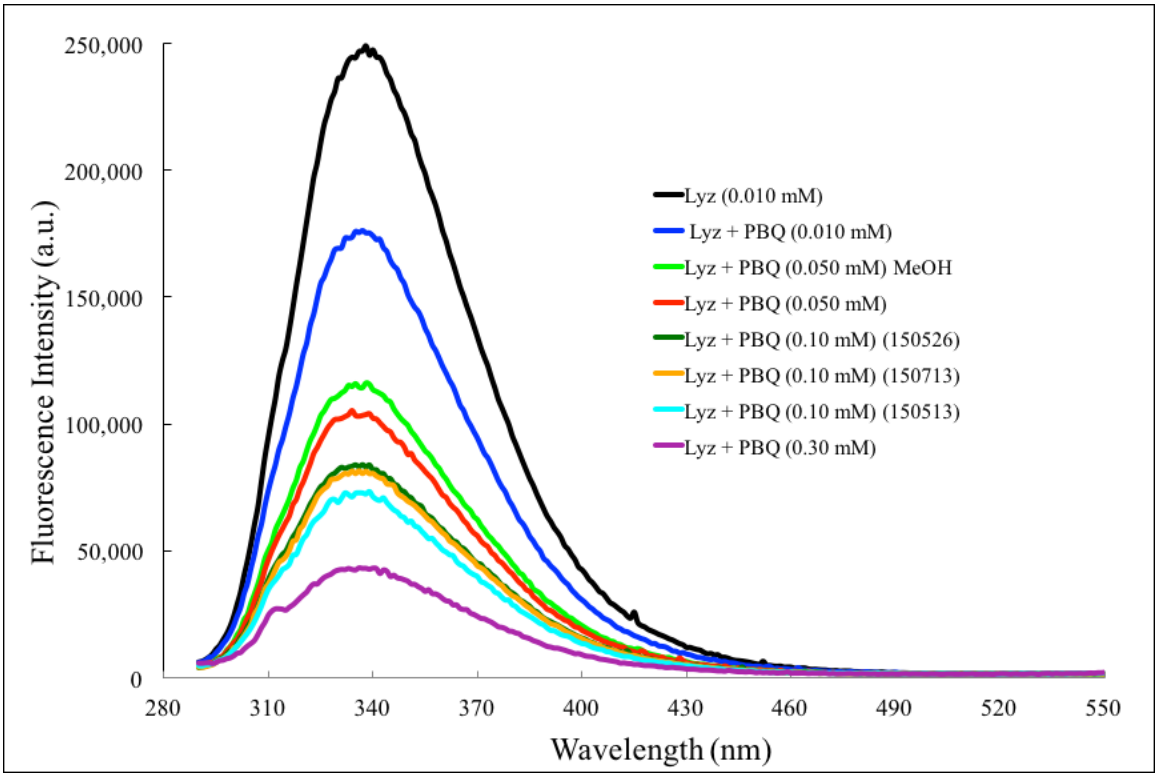

Figure 2.1 Fluorescence spectra of Lyz (0.010 mM) and Lyz (0.010 mM) modified by PBQ (0.010, 0.050, 0.10, or 0.30 mM) for 24 h at 37°C.

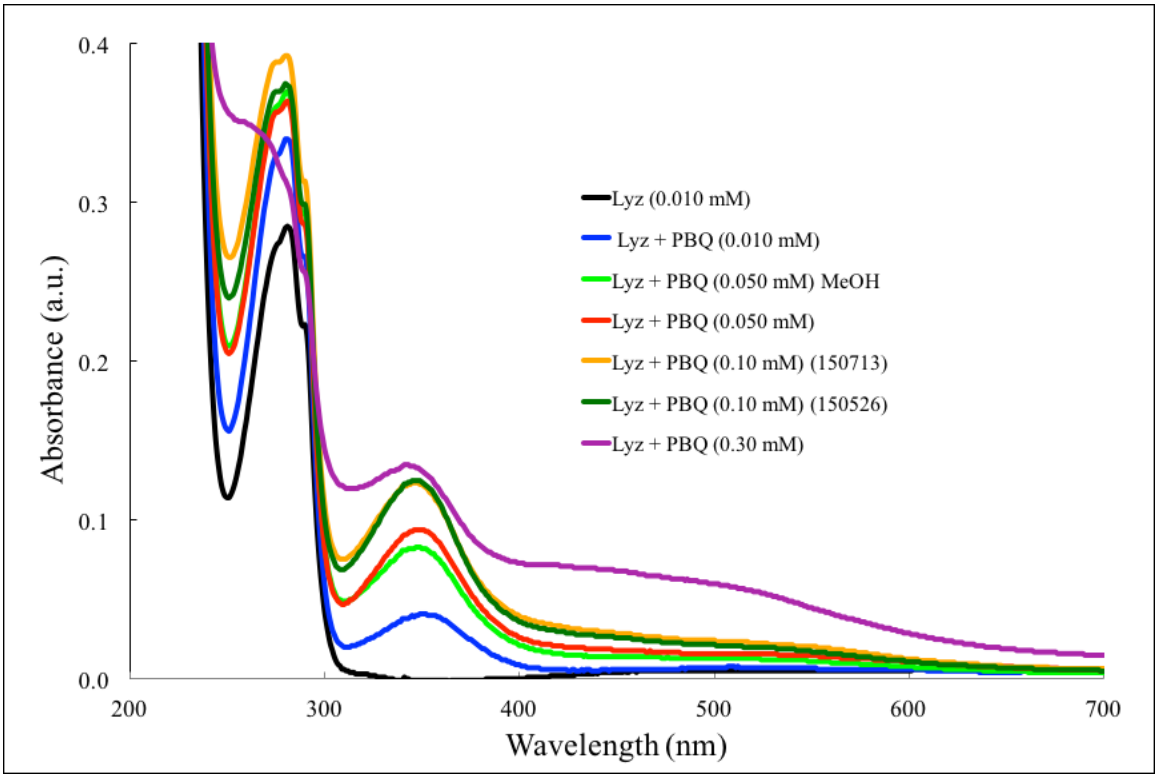

Figure 2.2 UV-VIS spectra of Lyz (0.010 mM) and Lyz (0.010 mM) modified by PBQ (0.010, 0.050, 0.10, or 0.30 mM) for 24 h at 37°C.

As seen in Figure 2.1, the fluorescence intensity decreases as the concentration of PBQ increases in the reaction solution. From the results of previous studies, it was found exposure of Lysozyme to PBQ elicits protein oligomerization over time. This oligomerization is believed to cause a decrease in the fluorescence intensity of Lysozyme. To quantify the degree of modification of Lysozyme, RIFI values were calculated using Lyz (0.010 mM) as the reference NIFI. As seen in Table 2.1, the RIFI increases as the concentration of PBQ in the reaction solution increases. This is interpreted as an increase in the modification of Lysozyme upon exposure to increasing concentration of PBQ. Considering all reactions performed in this study, Table 2.1 shows no more than a 1% difference in RIFI values calculated over the two integration ranges.

As seen in Figure 2.2, the absorbance in the 300-410 nm range increases as the concentration of PBQ increases in the reaction solution. Since quinone absorbs in this range, and any free quinone has already been removed through dialysis, the increase in absorbance is believed to be result of PBQ covalently bonded to Lysozyme. To monitor this, Table 2.1 shows the absorbance at 346 nm of Lysozyme and modified Lysozyme. From these results, increasing the concentration of PBQ increases the overall absorbance of Lysozyme. This is interpreted as an increase in the modification (in this case, adduct formation) of Lysozyme upon increasing concentration of PBQ.

When considering the effect of using 10% MeOH during quinone preparation, Table 2.1 shows RIFI values for Lyz + PBQ (0.050 mM) MeOH and Lyz + PBQ (0.050 mM) to be less than 5% of each other. Figures 2.1 and 2.2 support this by showing a slight difference in the fluorescence and absorbance spectra of the two reactions. Overall, it can be concluded that the use of 10% MeOH is minimal in affecting the modification of Lysozyme when exposed to PBQ.

Due to some experimental errors during the reaction PBQ (0.10 mM) (150513), the UV-VIS spectrum was not recorded. As result, the reaction was duplicated once, then twice, when differences were observed in the NIFI between the first and second run. The RIFI for the following two reactions Lyz + PBQ (0.10 mM) (150526) and Lyz + PBQ (0.10 mM) (150713) were almost identical and varied only by 1%. This confirmed the difference in NIFI of the first reaction involving Lysozyme incubated with PBQ (0.10 mM) as our method is reliable up to 3% difference in RIFI. As result of the duplications, it is believed Lysozyme incubated with PBQ (0.10 mM) yields a modification of Lysozyme by 65-67%.

In summary, Lysozyme modification was found to be increasing with the concentration of PBQ. In conjunction with the SDS-PAGE data presented in Chapter 1 [Greve & Kim, 2015], and similar to what was observed during previous studies with Ribonuclease A, this study shows PBQ exhibits its modifying capabilities through both induction of protein oligomerization and adduct formation.

2.3.2 Lysozyme Modifications Induced by PBQ Over Various Lengths of Time

In this study, Lyz (0.010 mM) was treated with PBQ (0.050 mM) and allowed to react while being monitored using fluorescence for 0, 1, 2, 3, and 24 h. Following each incubation, dialysis was performed for 24 h followed by a final spectroscopic measurement of modified Lysozyme. All reactions were performed in a phosphate buffer (50 mM) at 37°C and pH=7.0 to mimic physiological conditions.

Table 2.2 lists RIFI values calculated over 300-410 nm and 320-360 nm in addition to absorbance values for each reaction performed in this study. Figure 2.3 shows the fluorescence intensity of Lysozyme and Lysozyme modified by PBQ (0.050 mM) for 0, 1, 2, 3, and 24 h at 37°C. All spectra were normalized in the 500-550 nm range where little emission is present to ensure proper comparison. Figure 2.4 shows the absorbance of Lysozyme and Lysozyme modified by PBQ (0.050 mM) for 0, 1, 2, 3, and 24 h at 37°C.

Table 2.2 RIFI of Lyz (0.010 mM) and Lyz (0.010 mM) modified by PBQ (0.050 mM) for 0 h, 1 h, 2 h, 3 h, and 24 h at pH=7.0 and 37°C. Absorbance at 346 nm of Lyz (0.010 mM) and Lyz (0.010 mM) modified by PBQ (0.050 mM) for 0 h, 1 h, 2 h, 3 h, and 24 h at pH=7.0 and 37°C.

Reaction	RIFI[a] (%)	RIFI[b] (%)	A_{346} (a.u.)
Lyz + PBQ (0.050 mM) 1 h	-17	-18	-0.009
Lyz + PBQ (0.050 mM) 2 h	-13	-15	-0.007
Lyz + PBQ (0.050 mM) 0 h	-13	-13	-0.009
Lyz (0.010 mM) 0 h	-12	-12	0.003
Lyz + PBQ (0.050 mM) 3 h	-5	-5	0.007
Lyz (0.010 mM)	0	0	-0.001
Lyz + PBQ (0.050 mM)	57	58	0.094

a *integration between 300-410 nm*
b *integration between 320-360 nm*

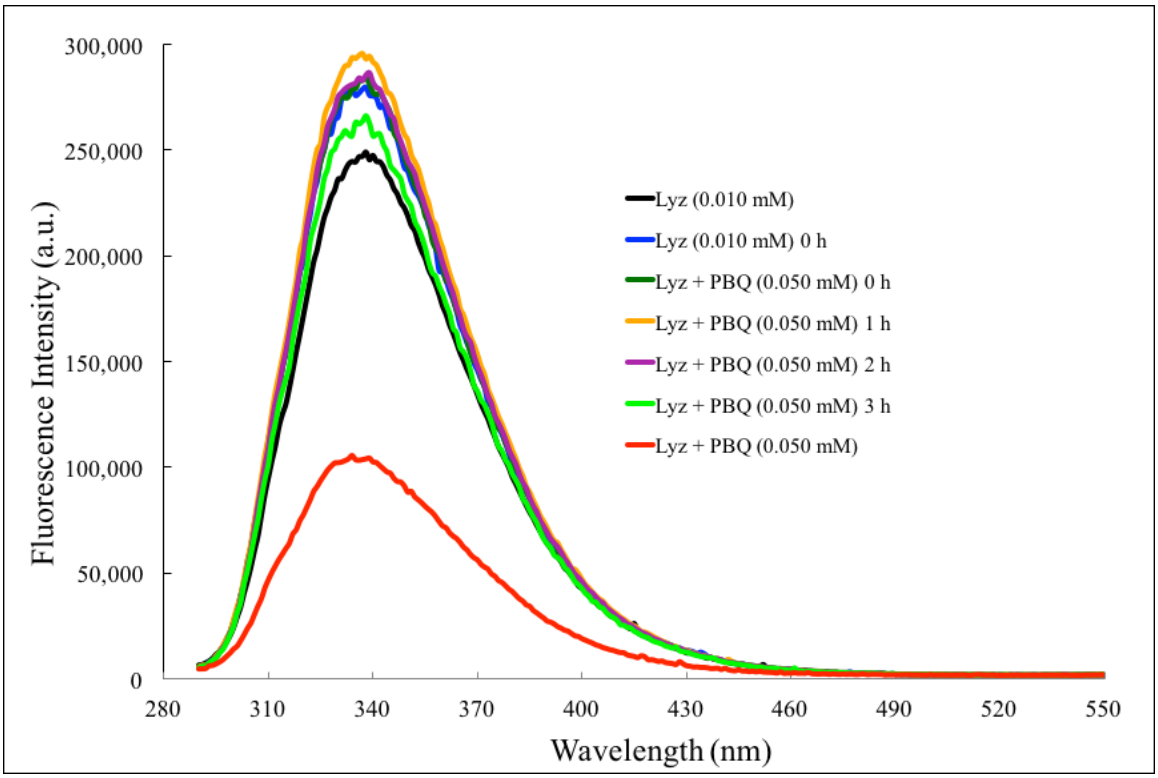

Figure 2.3 Fluorescence spectra of Lyz (0.010 mM) and Lyz (0.010 mM) modified by PBQ (0.050 mM) for 0 h, 1 h, 2 h, 3 h, and 24 h at pH=7.0 and 37°C.

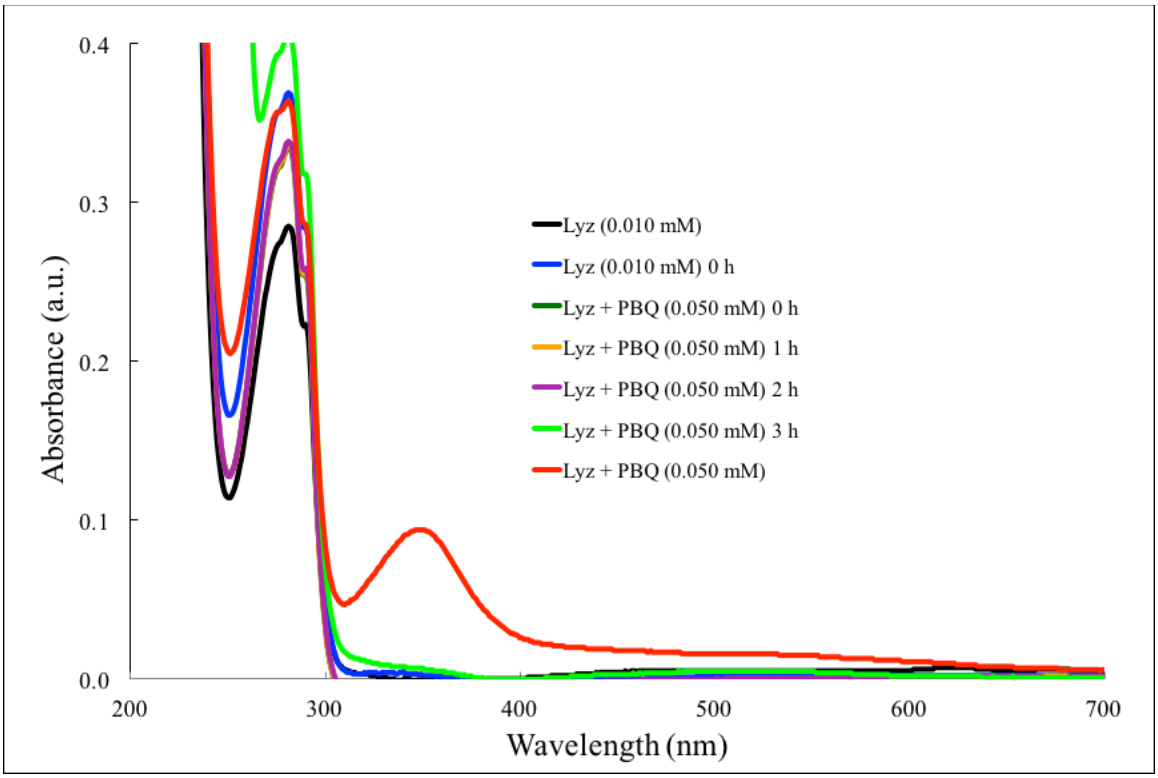

Figure 2.4 UV-VIS spectra of Lyz (0.010 mM) and Lyz (0.010 mM) modified by PBQ (0.050 mM) for 0 h, 1 h, 2 h, 3 h, and 24 h at pH=7.0 and 37°C.

As seen in Figure 2.3, the fluorescence intensity of Lysozyme and Lysozyme modified with PBQ increases during the first three hours of incubation. Since each reaction was performed for a specific amount of time, the results were assumed to vary according to the incubation time. The resulting increase in fluorescence intensity could be due to adduct formation or redox cycling of PBQ, both which may increase the quantum yield of Lysozyme. Since redox cycling results in higher concentrations of the reduced form of PBQ, the fluorescence intensity would be expected to increase as reduced PBQ exhibits fluorescence. No protein oligomerization (induced by PBQ) was assumed to occur during the first three hours as the fluorescence intensity did not decrease. To quantify the degree of modification of Lysozyme, RIFI values were calculated using Lyz (0.010 mM) as the reference NIFI. As seen in Table 2.2, the RIFI

decreases to a maximum during the first hour of incubation and then begins to increase over time. From the results of this study, one could safely assume the RIFI would continue increasing for the next several hours until similar results of the reactions Lyz (0.010 mM) and Lyz + PBQ (0.050 mM) in the previous study were observed. Considering all reactions performed in this study, Table 2.2 shows no more than a 2% difference in RIFI values calculated over the two integration ranges.

As seen in Figure 2.4, little to no absorbance occurs in the 300-410 nm range during the first three hours of incubation. Since quinone absorbs in this range, and any free quinone has already been removed through dialysis, little adduct formation is believed to occur during the first three hours of incubation. To monitor this, Table 2.2 shows the absorbance at 346 nm of Lysozyme and modified Lysozyme. From this data, it is confirmed that three hours of incubation is not enough time to produce lasting modification of Lysozyme through adduct formation.

When considering the reaction Lyz (0.010 mM) 0 h, Figure 2.3 and Table 2.2 indicate an increase in fluorescence intensity when compared to the reaction Lyz (0.010 mM). This increase could be due to the lack of protein-protein interaction which would occur over 24 h of incubation. Since the reaction Lyz (0.010 mM) 0 h underwent an immediate dialysis after Lysozyme was placed in solution, the results indicate the fluorescence intensity of Lysozyme increases and then decreases over time.

Considering the results of SDS-PAGE studies presented in Chapter 1 [Greve & Kim, 2015], Lysozyme modification was expected during the first three hours of incubation with PBQ. From the results of these studies, fluorescence and UV-VIS spectroscopy did not support previous results regarding the oligomerization of Lysozyme

during the first three hours of incubation with PBQ although the concentration of Lysozyme used in SDS-PAGE studies were higher. These results suggest the fluorescence intensity of Lysozyme is unaffected by PBQ within the first three hours of incubation but protein oligomerization, initiated by PBQ, still occurs.

2.3.3 Lysozyme Modifications Induced by Substituted Quinones

In this study, Lyz (0.010 mM) was treated with MBQ (0.050 mM), PBQ (0.050 mM), PhBQ (0.050 mM), CBQ (0.050 mM), and TCBQ (0.050 mM) and allowed to react while being monitored using fluorescence for 24 h. Following the 24 h incubation, dialysis was performed for an additional 24 h followed by a final spectroscopic measurement of modified Lysozyme. All reactions were performed in a phosphate buffer (50 mM) at 37°C and pH=7.0 to mimic physiological conditions.

Table 2.3 lists RIFI values calculated over 300-410 nm and 320-360 nm in addition to absorbance values for each reaction performed in this study. Figure 2.5 shows the fluorescence intensity of Lysozyme and Lysozyme modified by MBQ (0.050 mM), PBQ (0.050 mM), PhBQ (0.050 mM), CBQ (0.050 mM), and TCBQ (0.050 mM) for 24 h at 37°C. All spectra were normalized in the 500-550 nm range where little emission is present to ensure proper comparison. Figure 2.6 shows the absorbance of Lysozyme and Lysozyme modified by MBQ (0.050 mM), PBQ (0.050 mM), PhBQ (0.050 mM), CBQ (0.050 mM), and TCBQ (0.050 mM) for 24 h at 37°C.

Table 2.3 RIFI of Lyz (0.010 mM) and Lyz (0.010 mM) modified by MBQ (0.050 mM), PBQ (0.050 mM), PhBQ (0.050 mM), CBQ (0.050 mM), and TCBQ (0.050 mM) for 24 h at 37°C. Absorbance at 346 nm of Lyz (0.010 mM) and Lyz (0.010 mM) modified by MBQ (0.050 mM), PBQ (0.050 mM), PhBQ (0.050 mM), CBQ (0.050 mM), and TCBQ (0.050 mM) for 24 h at 37°C.

Reaction	RIFI[a] (%)	RIFI[b] (%)	A_{346} (a.u.)
Lyz (0.010 mM)	0	0	-0.001
Lyz + MBQ (0.050 mM)	36	37	0.019
Lyz + PBQ (0.050 mM)	57	58	0.094
Lyz + PhBQ (0.050 mM)	60	61	0.042
Lyz + CBQ (0.050 mM)	66	67	0.122
Lyz + TCBQ (0.50 mM)	78	79	0.173

a *integration between 300-410 nm*
b *integration between 320-360 nm*

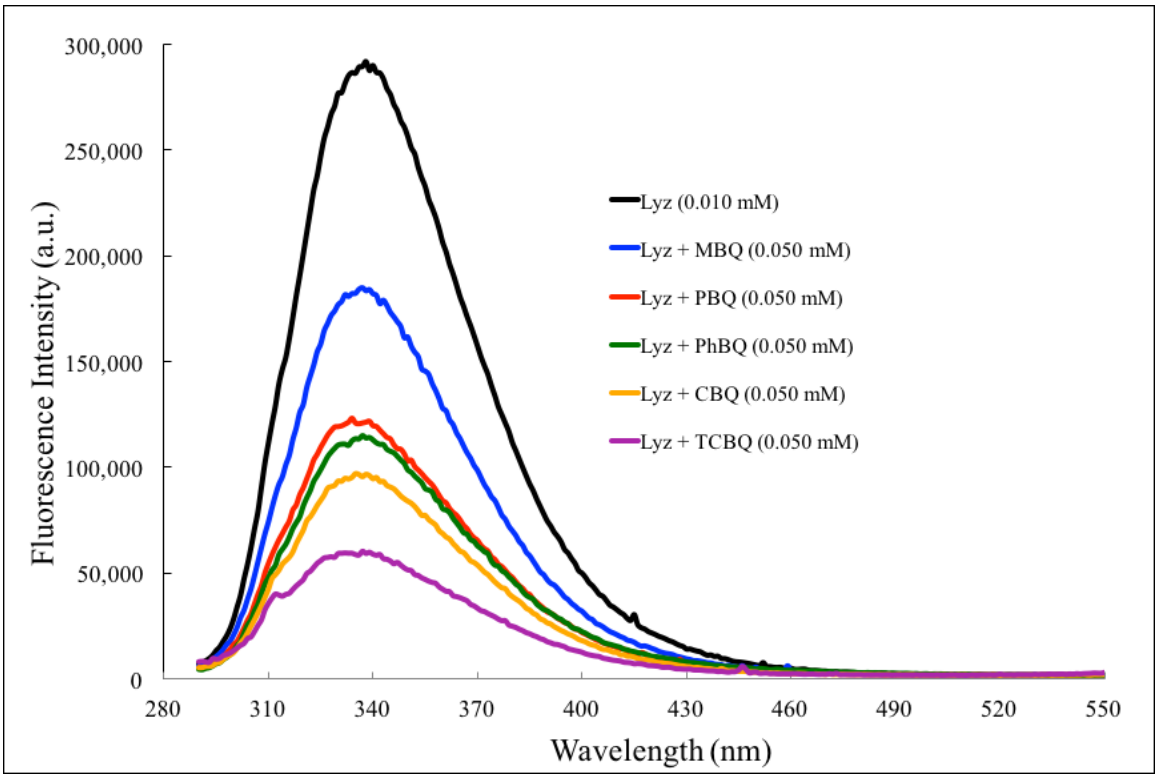

Figure 2.5 Fluorescence spectra of Lyz (0.010 mM) and Lyz (0.010 mM) modified by MBQ (0.050 mM), PBQ (0.050 mM), PhBQ (0.050 mM), CBQ (0.050 mM), and TCBQ (0.050 mM) for 24 h at 37°C.

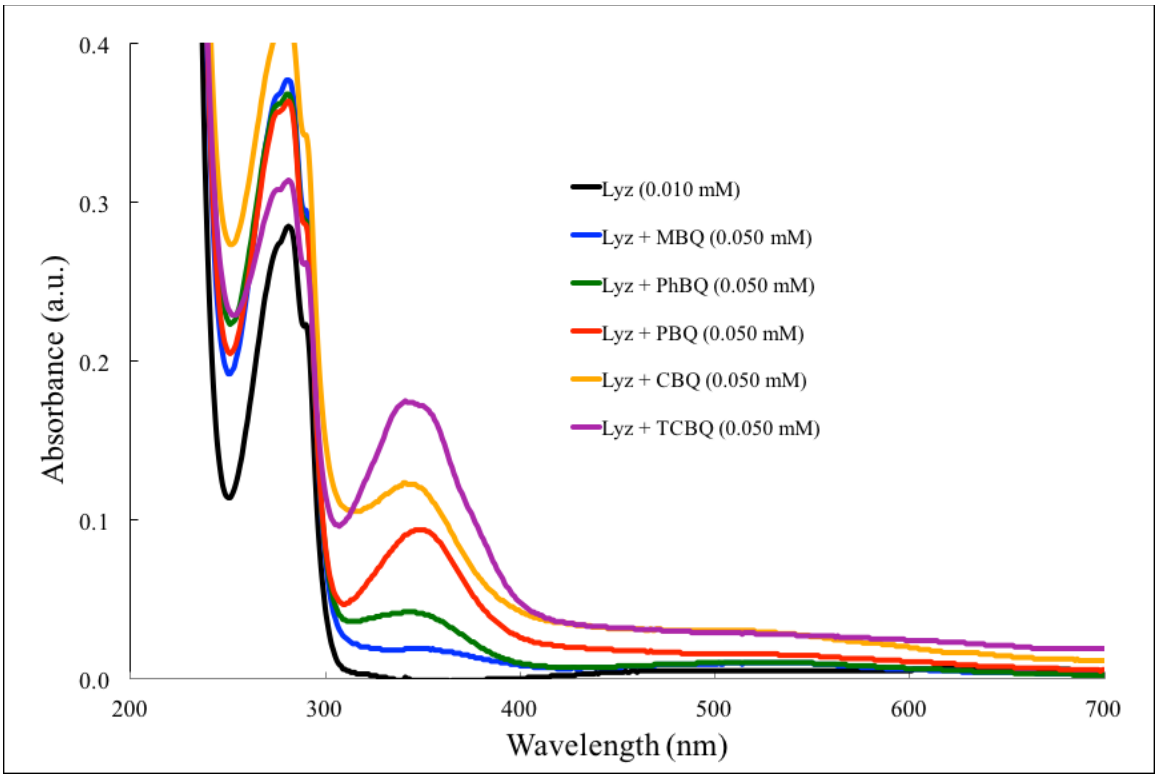

Figure 2.6 UV-VIS spectra of Lyz (0.010 mM) and Lyz (0.010 mM) modified by MBQ (0.050 mM), PBQ (0.050 mM), PhBQ (0.050 mM), CBQ (0.050 mM), and TCBQ (0.050 mM) for 24 h at 37°C.

As seen in Figure 2.5, the fluorescence intensity of Lysozyme decreases upon exposure to substituted quinones. MBQ was found to cause the smallest decrease in fluorescence intensity, followed by PBQ, PhBQ, CBQ, and TCBQ. This result is believed to be linked with the electron donating and electron withdrawing properties of each substituent. The substituents that are electron donating cause less modification of Lysozyme than the substituents that are electron withdrawing. MBQ, and to a lesser extent, PhBQ, have electron donating properties and are found to elicit moderate modification of Lysozyme. CBQ and TCBQ have electron withdrawing properties and are found to elicit severe modification of Lysozyme. To quantify the degree of modification of Lysozyme, RIFI values were calculated using Lyz (0.010 mM) as the

reference NIFI. As seen in Table 2.3, the RIFI increases as each substituent becomes more electron withdrawing. This is interpreted as an increase in modification of Lysozyme by molecules that possess electron withdrawing substituents. Considering all reactions performed in this study, Table 2.3 shows no more than a 1% difference in RIFI values calculated over the two integration ranges.

As seen in Figure 2.6, the absorbance in the 300-410 nm range increases in the same manner as mentioned above. Since quinone absorbs in this range, and any free quinone has already been removed through dialysis, the increase in absorbance is believed to be result of substituted quinones covalently bonded to Lysozyme. To monitor this, Table 2.3 shows the absorbance at 346 nm of Lysozyme and modified Lysozyme. From these results, as each substituent increases in electron withdrawing capability, the absorbance increases as well. This is interpreted as an increase in the modification (in this case, adduct formation) of Lysozyme upon exposure to substituted quinones with electron withdrawing properties.

Considering the reaction with PhBQ (0.050 mM), Figures 2.5 and 2.6 show interesting results when examining the order of modification each substituent produces. Figure 2.5 shows PhBQ to cause a greater decrease in fluorescence intensity than PBQ while Figure 2.6 shows PhBQ to exhibit less absorbance than PBQ. The results in previous studies have been found to have correlating results between fluorescence and UV-VIS spectra. In other words, as the fluorescence intensity decreases, the absorbance increases. PhBQ shows interesting results because its absorbance is less than what it supposedly should be. This is particularly interesting due to the structure of PhBQ and its potential energy absorbing capability.

In summary, Lysozyme modification was found to be increasing with the electron withdrawing capability of each substituted quinone. In conjunction with the SDS-PAGE data presented in Chapter 1 [Greve & Kim, 2015], this study shows substituted quinones exhibit modifying capabilities through both induction of protein oligomerization and adduct formation.

2.3.4 Lysozyme Modifications Induced by Naphthoquinones

In this study, Lyz (0.010 mM) was treated with HNQ (0.050 mM), PNQ (0.050 mM), and ONQ (0.050 mM) and allowed to react while being monitored using fluorescence for 24 h. Following the 24 h incubation, dialysis was performed for an additional 24 h followed by a final spectroscopic measurement of the modified Lysozyme. All reactions were performed in a phosphate buffer (50 mM) at 37°C and pH=7.0 to mimic physiological conditions.

Table 2.4 lists RIFI values calculated over 300-410 nm and 320-360 nm in addition to absorbance values for each reaction performed in this study. Figure 2.7 shows the fluorescence intensity of Lysozyme and Lysozyme modified by HNQ (0.050 mM), PNQ (0.050 mM), and ONQ (0.050 mM) for 24 h at 37°C. All spectra were normalized in the 500-550 nm range where little emission is present to ensure proper comparison. Figure 2.8 shows the absorbance of Lysozyme and Lysozyme modified by HNQ (0.050 mM), PNQ (0.050 mM), and ONQ (0.050 mM) for 24 h at 37°C.

Table 2.4 RIFI of Lyz (0.010 mM) and Lyz (0.010 mM) modified by HNQ (0.050 mM), PNQ (0.050 mM), and ONQ (0.050 mM) for 24 h at 37°C. Absorbance at 346 nm of Lyz (0.010 mM) and Lyz (0.010 mM) modified by HNQ (0.050 mM), PNQ (0.050 mM), and ONQ (0.050 mM) for 24 h at 37°C.

Reaction	RIFI[a] (%)	RIFI[b] (%)	A_{346} (a.u.)
Lyz (0.010 mM)	0	0	-0.001
Lyz + HNQ (0.050 mM)	29	29	0.025
Lyz + PNQ (0.050 mM)	43	43	0.014
Lyz + ONQ (0.050 mM)	60	61	0.081

a *integration between 300-410 nm*
b *integration between 320-360 nm*

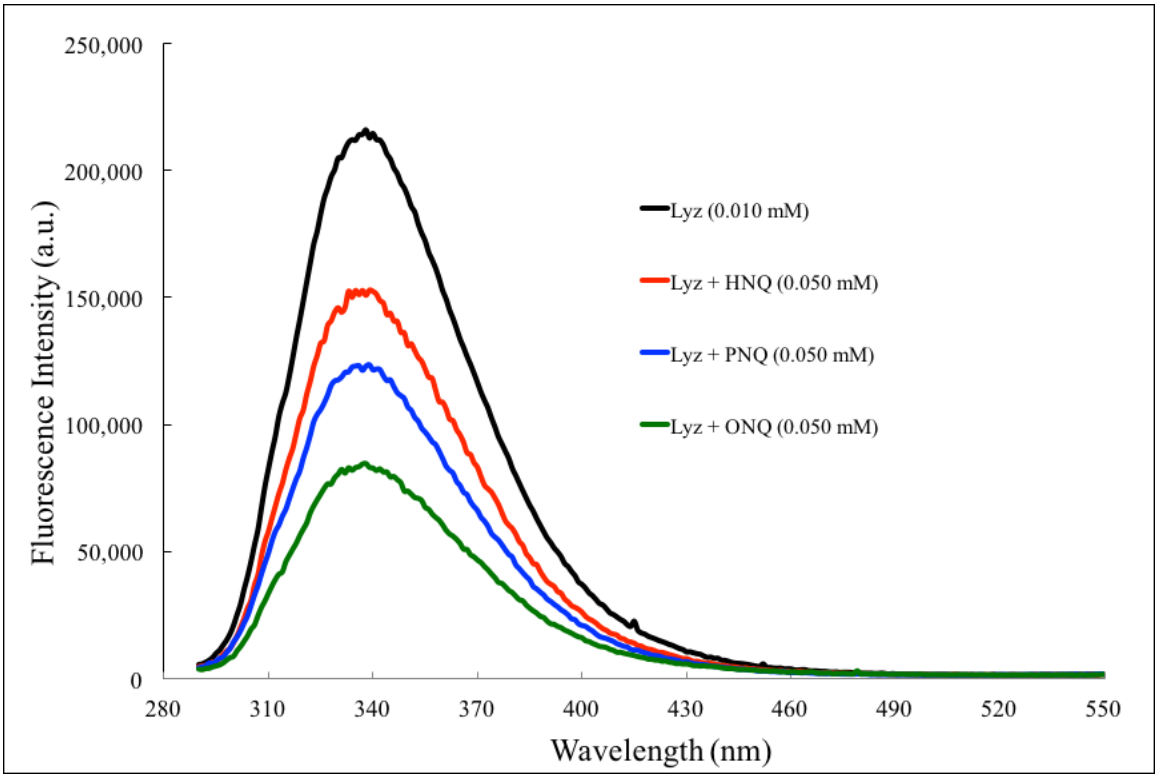

Figure 2.7 Fluorescence spectra of Lyz (0.010 mM) and Lyz (0.010 mM) modified by HNQ (0.050 mM), PNQ (0.050 mM), and ONQ (0.050 mM) for 24 h at 37°C.

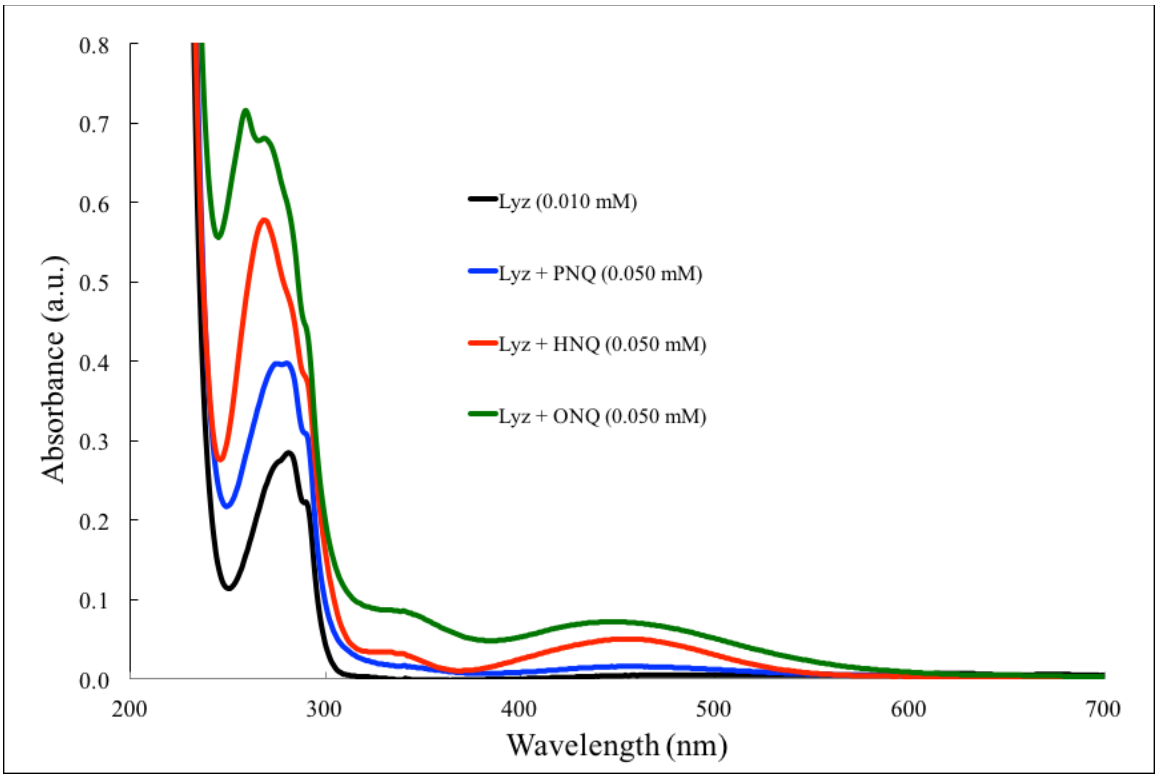

Figure 2.8 UV-VIS spectra of Lyz (0.010 mM) and Lyz (0.010 mM) modified by HNQ (0.050 mM), PNQ (0.050 mM), and ONQ (0.050 mM) for 24 h at 37°C.

As seen in Figure 2.7, the fluorescence intensity of Lysozyme decreases upon exposure to naphthoquinones. From the results of previous SDS-PAGE studies mentioned in Chapter 1, naphthoquinones have been found to produce little, if not any, protein modifying behavior [Smith & Kim, 2015]. In this study, HNQ, PNQ, and ONQ were all found to produce modification of Lysozyme. To quantify the degree of modification of Lysozyme, RIFI values were calculated using Lyz (0.010 mM) as the reference NIFI. As seen in Table 2.4, ONQ produced the largest RIFI followed by PNQ and HNQ, respectively. This is interpreted as HNQ causing the least modification of Lysozyme and ONQ causing the greatest modification of Lysozyme. Considering all

reactions performed in this study, Table 2.4 shows no more than a 1% difference in RIFI values calculated over the two integration ranges.

As seen in Figure 2.8, the absorbance in the 300-410 nm range increases as usual for quinone-incubated solutions with an additional increase in the 400-500 nm range due to the color of solution. Since naphthoquinone absorbs in this range, and any free naphthoquinone has already been removed through dialysis, the increase in absorbance is believed to be result of naphthoquinone covalently bonded to Lysozyme. To monitor this, Table 2.4 shows the absorbance at 346 nm of Lysozyme and modified Lysozyme. From these results, ONQ shows the largest absorbance, followed by HNQ then PNQ, respectively. This is interpreted as ONQ causing the largest degree of Lysozyme modification and HNQ and PNQ exhibiting a similar phenomenon as seen in the study with quinone substituents.

Considering the structure of each naphthoquinone used in this study, the results of this study demonstrate how the position of the double bonded oxygen on the naphthoquinone plays a role in its protein modifying capability. Figures 2.7 and 2.8 show ONQ to elicit the greatest modification of Lysozyme and PNQ and HNQ to elicit varying degrees of modification of Lysozyme. Since the UV-VIS absorbance of PNQ in the 300-410 nm range is relatively absent, it can be assumed PNQ does not exhibit its protein modifying behavior through adduct formation but rather by induction of protein oligomerization. In contrast, since the UV-VIS absorbance of HNQ in the 300-410 nm range is prominent, and the RIFI of HNQ is less than PNQ, it can be assumed HNQ exhibits its protein modifying behavior through adduct formation rather than induction of protein oligomerization. Going further, the double bonded oxygen at the *ortho*- position

seems to elicit the largest degree of Lysozyme modification. Comparing HNQ with PNQ, it appears the hydroxyl group on HNQ favors adduct formation while the double bonded oxygen at the *para*- position acts much like PBQ regarding induction of protein oligomerization.

In summary, Lysozyme modification, regardless of degree, was found with all naphthoquinones used in this study. Consistent with SDS-PAGE data presented in Chapter 1 [Smith & Kim, 2015], this study suggests naphthoquinones, specifically ONQ, HNQ, and PNQ, exhibit modifying capabilities towards Lysozyme through both induction of protein oligomerization and adduct formation.

2.3.5 Lysozyme Modifications Induced by PBQ at Various pH

In this study, Lyz (0.010 mM) was treated with PBQ (0.050 mM) and allowed to react at pH=6.0, pH=7.0, and pH=8.0 while being monitored using fluorescence for 24 h. Following the 24 h incubation, dialysis was performed for an additional 24 h followed by a final spectroscopic measurement of modified Lysozyme. All reactions were performed in a phosphate buffer (50 mM) at 37°C.

Table 2.5 lists RIFI values calculated over 300-410 nm and 320-360 nm in addition to absorbance values for each reaction performed in this study. Figure 2.9 shows the fluorescence intensity of Lysozyme and Lysozyme modified by PBQ (0.050 mM) at pH=6.0, pH=7.0, and pH=8.0 for 24 h at 37°C. All spectra were normalized in the 500-550 nm range where little emission is present to ensure proper comparison. Figure 2.10 shows the absorbance of Lysozyme and Lysozyme modified by PBQ (0.050 mM) at pH=6.0, pH=7.0, and pH=8.0 for 24 h at 37°C.

Table 2.5 RIFI of Lyz (0.010 mM) and Lyz (0.010 mM) modified by HNQ (0.050 mM), PNQ (0.050 mM), and ONQ (0.050 mM) for 24 h at 37°C. Absorbance at 346 nm of Lyz (0.010 mM) and Lyz (0.010 mM) modified by HNQ (0.050 mM), PNQ (0.050 mM), and ONQ (0.050 mM) for 24 h at 37°C.

Reaction	RIFI[a] (%)	RIFI[b] (%)	A_{346} (a.u.)
Lyz + PBQ (0.050 mM) pH=6.0	-20	-21	0.049
Lyz + PBQ (0.050 mM) pH=7.0	0	0	0.094
Lyz + PBQ (0.050 mM) pH=8.0	47	48	0.171

a integration between 300-410 nm
b integration between 320-360 nm

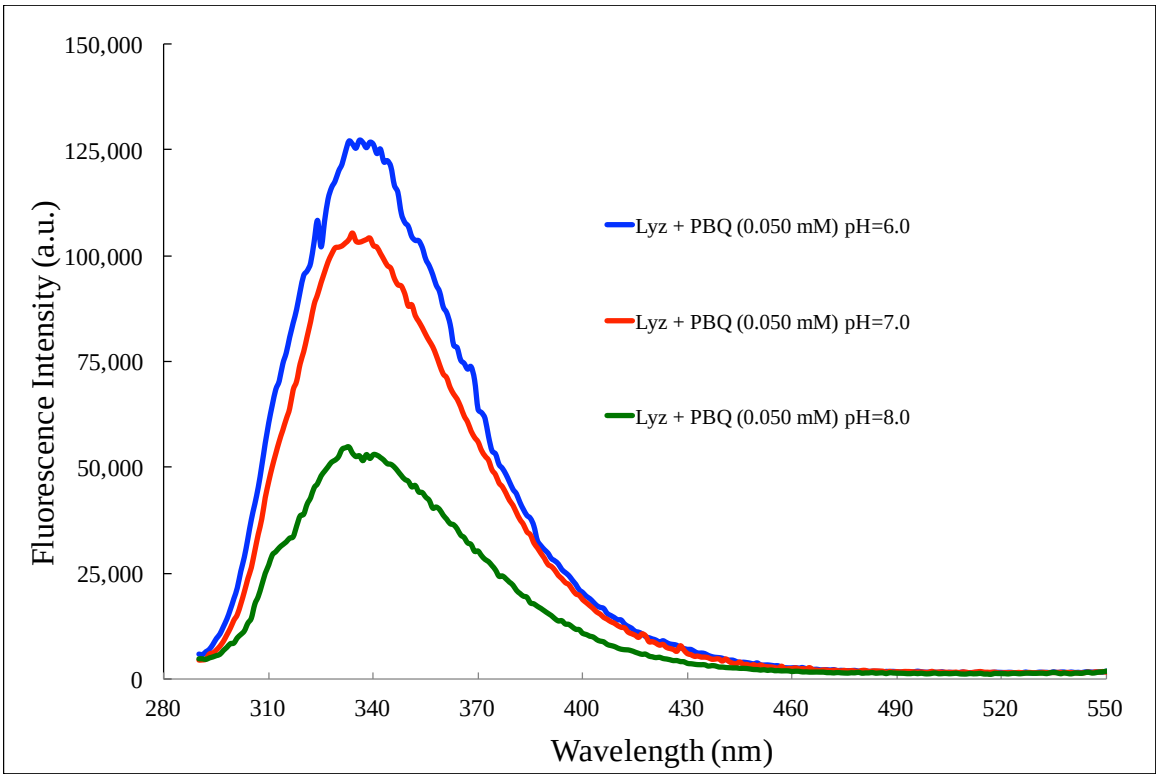

Figure 2.9 Fluorescence spectra of Lyz (0.010 mM) modified by PBQ (0.050 mM) at pH=6.0, pH=7.0, and pH=8.0 for 24 h at 37°C.

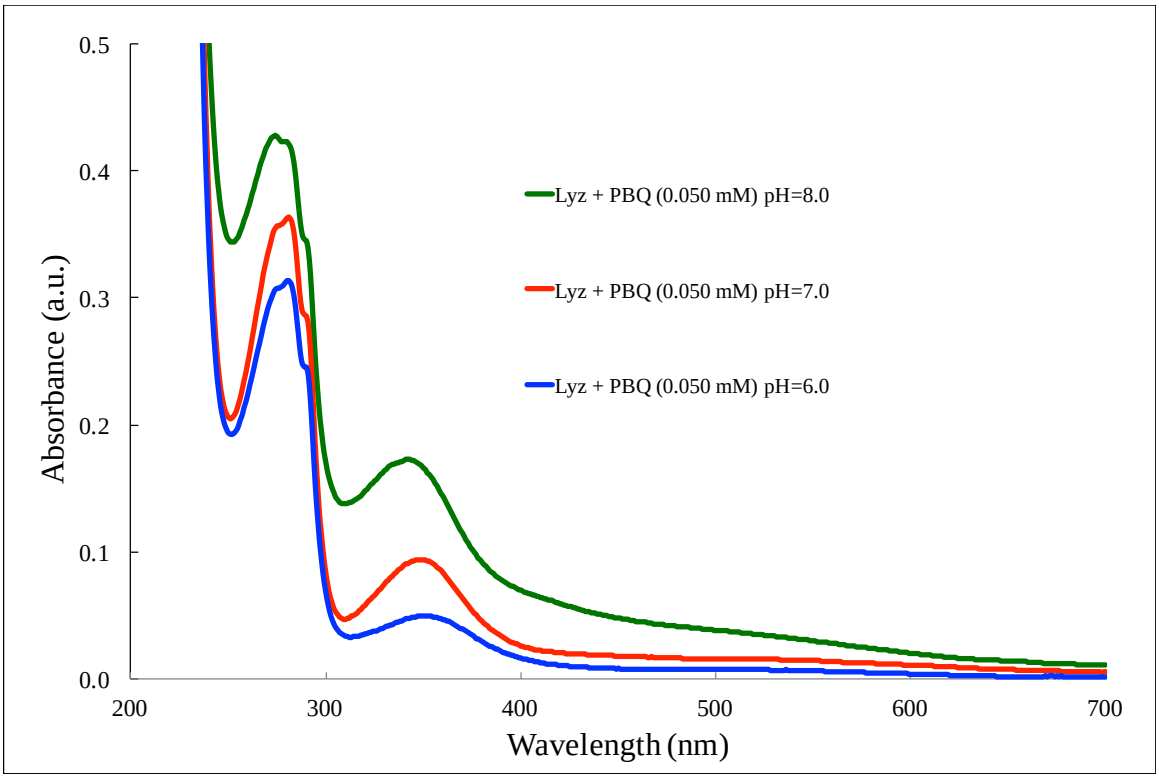

Figure 2.10 UV-VIS spectra of Lyz (0.010 mM) modified by PBQ (0.050 mM) at pH=6.0, pH=7.0, and pH=8.0 for 24 h at 37°C.

As seen in Figure 2.9, the fluorescence intensity decreases as the pH of the reaction solution increases. This is believed to be due to increasing the nucleophilic character of the protein as the pH increases and therefore increasing the association of Lysozyme and PBQ. To quantify this degree of modification of Lysozyme, RIFI values were calculated using Lyz + PBQ (0.050 mM) pH=7.0 as the reference NIFI. As seen in Table 2.5, the RIFI increases as the pH increases and decreases as the pH decreases. This is interpreted as an increase of modification of Lysozyme when increasing the pH and a decrease of modification of Lysozyme when decreasing the pH. Obviously, incubating Lysozyme with PBQ regardless of the pH causes a modification of Lysozyme. However, considering conditions at physiological pH, a decrease in pH causes less modification of Lysozyme and an increase in pH causes a greater modification of Lysozyme.

Considering all reactions performed in this study, Table 2.5 shows no more than a 1% difference in RIFI values calculated over the two integration ranges.

As seen in Figure 2.10, the absorbance in the 300-410 nm range increases as the pH of the reaction solution increases. Since quinone absorbs in this range, and any free quinone has already been removed through dialysis, the increase and decrease in absorbance is believed to be result of PBQ covalently bonded to Lysozyme. To monitor this, Table 2.5 shows the absorbance at 346 nm of Lysozyme incubated with PBQ at pH=6.0, pH=7.0, and pH=8.0. From these results, increasing the pH of the reaction solution increases the absorbance. Again, any incubation of Lysozyme with PBQ will cause an increase in the overall absorbance of Lysozyme, however, in this study, comparisons to physiological pH were made, and increases and decreases in absorbance were noted as result.

Considering the results of this study, several assumptions can be made. For example, increasing the pH of solution gives rise to increasing deprotonation of Lysozyme which results in greater attractive forces between PBQ and Lysozyme. In addition, decreasing the pH of solution gives rise to increasing protonation of Lysozyme and PBQ which results in greater repulsive forces between PBQ and Lysozyme.

In summary, Lysozyme modification was found to be dependent on varying the pH of the reaction. This study suggests PBQ exhibits its modifying capabilities through both induction of protein oligomerization and adduct formation at multiple pH values.

2.3.6 Lysozyme Modifications Induced by PBQ at Various Temperatures

In this study, Lyz (0.010 mM) was treated with PBQ (0.050 mM) and allowed to react at 27°C, 37°C, and 42°C while being monitored using fluorescence for 24 h. Following the 24 h incubation, dialysis was performed for an additional 24 h followed by a final spectroscopic measurement of modified Lysozyme. All reactions were performed in a phosphate buffer (50 mM) at pH=7.0.

Table 2.6 lists RIFI values calculated over 300-410 nm and 320-360 nm in addition to absorbance values for each reaction performed in this study. Figure 2.11 shows the fluorescence intensity of Lysozyme and Lysozyme modified by PBQ (0.050 mM) at 27°C, 37°C, and 42°C for 24 h at pH=7.0. All spectra were normalized in the 500-550 nm range where little emission is present to ensure proper comparison. Figure 2.12 shows the absorbance of Lysozyme and Lysozyme modified by PBQ (0.050 mM) at 27°C, 37°C, and 42°C for 24 h at pH=7.0.

Table 2.6 RIFI of Lyz (0.010 mM) modified by PBQ (0.050 mM) at 27°C, 37°C, and 42°C for 24 h at pH=7.0. Absorbance at 346 nm of Lyz (0.010 mM) modified by PBQ (0.050 mM) at 27°C, 37°C, and 42°C for 24 h at pH=7.0.

Reaction	RIFI[a] (%)	RIFI[b] (%)	A_{346} (a.u.)
Lyz + PBQ (0.050 mM) 27°C	-32	-34	0.057
Lyz + PBQ (0.050 mM) 37°C	0	0	0.094
Lyz + PBQ (0.050 mM) 42°C	21	22	0.119

a *integration between 300-410 nm*
b *integration between 320-360 nm*

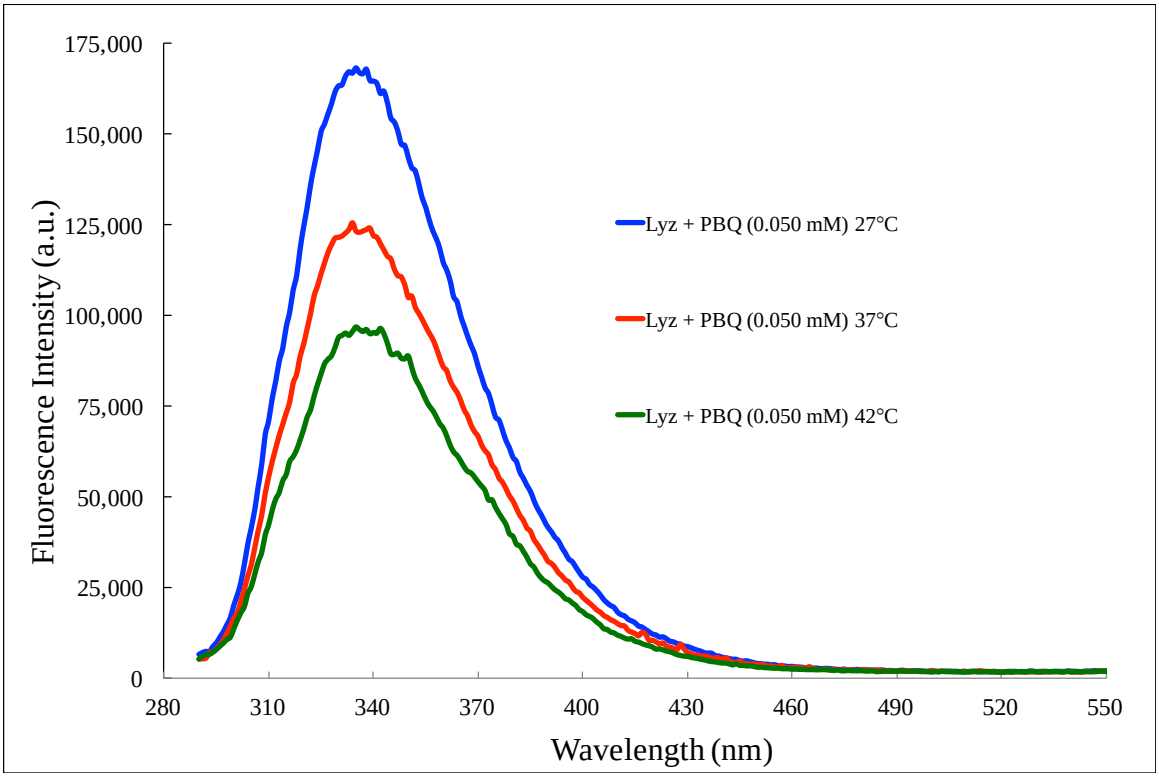

Figure 2.11 Fluorescence spectra of Lyz (0.010 mM) modified by PBQ (0.050 mM) at 27°C, 37°C, and 42°C for 24 h at pH=7.0.

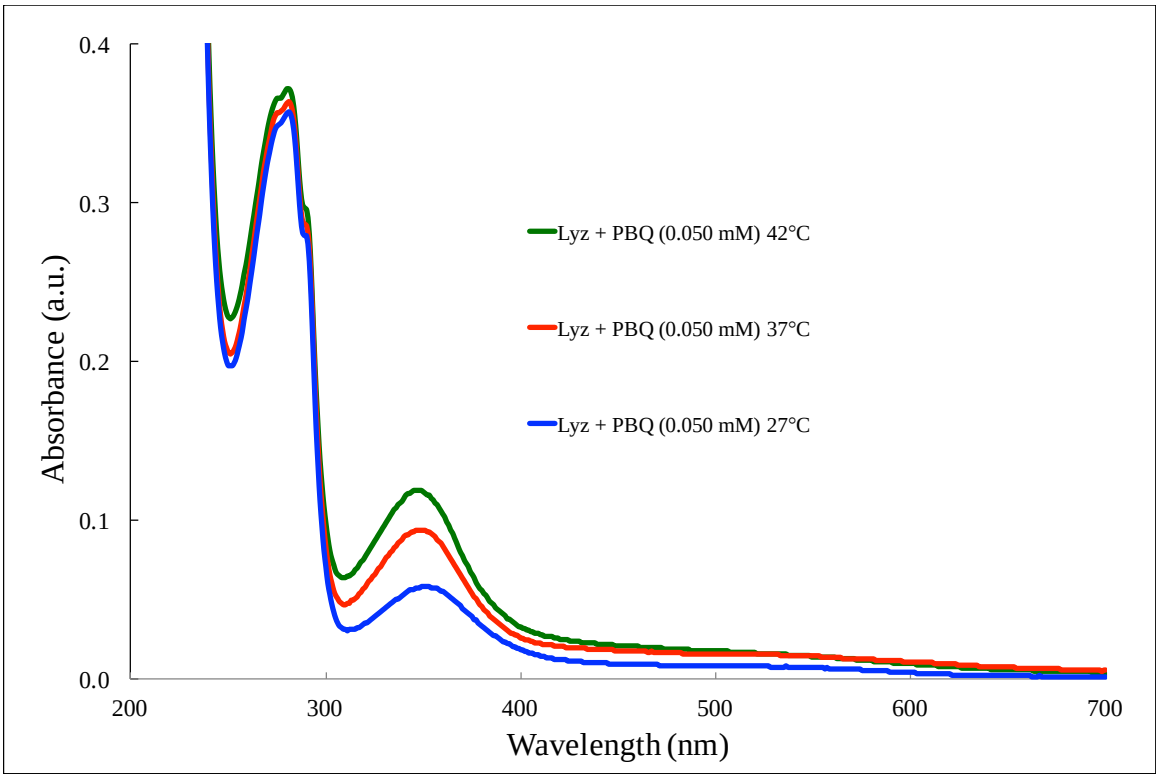

Figure 2.12 UV-VIS spectra of Lyz (0.010 mM) modified by PBQ (0.050 mM) at 27°C, 37°C, and 42°C for 24 h at pH=7.0.

As seen in Figure 2.11, the fluorescence intensity decreases as the temperature of the reaction solution increases. This is believed to be due to speeding up the kinetics of the reaction and possibly altering the shape and size of Lysozyme by changing the temperature. When Lysozyme and PBQ in solution are moving around at a greater speed due to an increase in the temperature of the reaction solution, a greater possibility of association can occur. Conversely, when Lysozyme and PBQ in solution are moving around at a reduced speed due to a decrease in the temperature of the reaction solution, a reduced possibility of association can occur. To quantify this degree of modification of Lysozyme, RIFI values were calculated using Lyz + PBQ (0.050 mM) 37°C as the reference NIFI. As seen in Table 2.6, the RIFI increases as the temperature increases and decreases as the temperature decreases. This is interpreted as an increase of modification

of Lysozyme when increasing the temperature and a decrease of modification of Lysozyme when decreasing the temperature. Similar to the previous study, incubating Lysozyme with PBQ regardless of the temperature of the reaction solution causes a modification of Lysozyme. However, considering conditions at physiological temperature (37°C), a decrease in temperature causes less modification of Lysozyme and an increase in temperature causes a greater modification of Lysozyme. Considering all reactions performed in this study, Table 2.6 shows no more than a 2% difference in RIFI values calculated over the two integration ranges.

As seen in Figure 2.12, the absorbance in the 300-410 nm range increases as the temperature of the reaction solution increases. Since quinone absorbs in this range, and any free quinone has already been removed through dialysis, the increase in absorbance is believed to be result of PBQ covalently bonded to Lysozyme. To monitor this, Table 2.6 shows the absorbance at 346 nm of Lysozyme incubated with PBQ at 27°C, 37°C, and 42°C. From these results, increasing the temperature of the reaction solution increases the absorbance at 346 nm. Again, any incubation of Lysozyme with PBQ will cause an increase in the overall absorbance of Lysozyme due to covalently bonded PBQ molecules, however, in this study, comparisons to physiological temperature were made, and increases in absorbance were noted as temperature increases.

In summary, Lysozyme modification was found to be increasing with respect to increasing temperature. This study shows again that PBQ exhibits its modifying capabilities through both induction of protein oligomerization and adduct formation at multiple temperatures.

2.4 Conclusions

Lysozyme modifications were observed with all quinone incubations as well as when environmental conditions were altered for reactions involving Lysozyme and PBQ. Six different studies were performed and each study provided insight on the modification of Lysozyme. Lysozyme modification, through protein oligomerization and adduct formation, was found to be increasing with the concentration of PBQ. Specifically, Lysozyme modification appears to be dominated by redox cycling and adduct formation within the first 3 h of incubation with PBQ. As the electron withdrawing capability of substituents on PBQ increases, so does modification of Lysozyme through protein oligomerization and adduct formation. Naphthoquinones elicit similar modification to Lysozyme with ONQ producing the largest modification. Considering environmental conditions, Lysozyme modification was found to be dependent on varying both the pH and temperature of the reaction solution.

CHAPTER 3

STUDIES OF RIBONUCLEASE A MODIFICATIONS INDUCED BY 2-HYDROXY-1,4-NAPHTHOQUINONE

3.1 Introduction

In previous SDS-PAGE studies performed by Smith & Kim, HNQ was not found to produce protein crosslinking of Ribonuclease A [Smith & Kim, 2015]. Instead, HNQ was assumed to elicit adduct formation which was too sensitive of a modification to be detected by SDS-PAGE. In the study here, fluorescence and UV-VIS spectroscopy were used to aid previous research by investigating the modification of Ribonuclease A by HNQ.

3.2 Methodology

All chemicals were purchased from Acros Organics and were of reagent grade. The protein of interest, Ribonuclease A (from *bovine pancreas*), was purchased from Fisher and kept frozen for preservation until ready for use. All water used in this study was deionized (DI) water purified by a Millipore system (Milli-Q). All solutions were made in lab and kept sealed or covered until ready for use. All reactions were performed in a similar manner following the devised experimental protocol to keep error at a minimum. Each study was performed over a three-day period consisting of (1) preparing and starting the reaction, (2) performing dialysis of the incubated solution, and (3) finishing the reaction. Quartz cuvettes, purchased from Starna Cells, Inc., were re-used after being thoroughly cleaned with Starna Cells, Inc. cuvette cleaner and allowed to dry. Physiological conditions (pH=7.0, 37°C) were modeled for all reactions except

for the studies in which the pH was varied. At all times, proper laboratory protocol was followed and the laboratory was kept in clean and functional condition.

3.2.1 Buffer Solution

A phosphate buffer (50 mM), comprised of a mixture of monobasic monosodium phosphate crystal ($NaH_2PO_4 \cdot H_2O$) and dibasic disodium phosphate anhydrous (Na_2HPO_4), was prepared and used for all reactions in this study. Most reactions were performed at pH=7.0 and 37°C to mimic physiological conditions; however, additional reactions were performed at a different pH to study the effect of changing the environmental factors. The phosphate buffer solution was used in every 3 mL reaction cuvette as well as in 1 L beakers when performing dialysis. Solutions of $NaH_2PO_4 \cdot H_2O$ (50 mM) and Na_2HPO_4 (50mM) were combined in ratios to produce a solution at a pH pre-determined by the Henderson-Hasselbalch equation (Eq. 3.1).

$$pH = pKa + log\frac{[base]}{[acid]} \qquad \text{(Eq. 3.1)}$$

A phosphate buffer solution was chosen primarily because of the multiple dissociation constants of phosphoric acid. Since the second deprotonation of phosphoric acid has a pKa around 7.2, an equilibrium between $NaH_2PO_4 \cdot H_2O$ and Na_2HPO_4 creates an effective buffering range around pH=7.0. Due to the physiological approach of the study, the use of phosphates in the buffer solution keeps the study in line with biological systems.

To perform a reaction, 4 L of buffer was made fresh the day before each reaction. 14.19 g of Na_2HPO_4 (50mM) was weighed and carefully poured in a 2 L volumetric flask followed by dilution to the line with deionized water. Following the same procedure,

13.79 g of $NaH_2PO_4 \cdot H_2O$ (50 mM) was weighed and carefully poured in a similar 2 L volumetric flask, again diluting to the line with deionized water. To have enough Na_2HPO_4 (50 mM) for pH=7.0, an additional 0.0500 L of Na_2HPO_4 (50 mM) was made by weighing 3.55 g of Na_2HPO_4 (50 mM) and following the same dilution and mixing protocol mentioned above. These flasks were subjected to stirring by mechanical means for roughly 30 min. Once fully dissolved, the two solutions of acid and base were combined in pre-determined ratios, 1 L at a time, to produce the desired pH of the buffer. For example, for a buffer solution at pH=7.0, 557 mL of Na_2HPO_4 (50 mM) was combined with 443 mL of $NaH_2PO_4 \cdot H_2O$ (50 mM), adequately mixed, and transferred into a 4 L plastic jug. This process was repeated three additional times to produce 4 L of buffer solution. The final pH of solution was checked using a Fisher AB15 Accumet pH meter equipped with an AccuTupH probe. After calibration with stock solutions at pH=4.00 and pH=10.01, if the pH of the buffer solution was within ± 0.05 units of the desired pH, the solution was acceptable and was stored in the fridge at 4°C until ready for use.

3.2.2 Protein Solution

Ribonuclease A stock solutions were made to provide enough protein for the extent of this study. This involved carefully weighing an imprecise amount of Ribonuclease A, 0.1221 g, onto tared weigh-paper and quantitatively transferring into a 10 mL volumetric flask. Phosphate buffer (50 mM, pH=7.0) was used to wash any residual Ribonuclease A off the weigh-paper into the volumetric flask. Ribonuclease A, in the volumetric flask, was diluted to the line with phosphate buffer (50 mM, pH=7.0)

and the flask was capped and sealed with ParaFilm. To facilitate the protein into solution, sonication was performed for 15 min in addition to inversion and shaking the volumetric flask by hand. After sonication, the protein solution was carefully transferred to Eppendorf tubes and stored in the freezer until needed.

The concentration of stock Ribonuclease A was calculated by converting 0.1221 g of Ribonuclease A to moles of Ribonuclease A and then dividing by 0.0100 L. To convert grams to moles, 0.1221 g of Ribonuclease A was divided by 13682 g/mol, the molecular weight of Ribonuclease A. This value was then divided by 0.0100 L to determine the molarity, or concentration, of the stock Ribonuclease A. Finally, this concentration was multiplied by 1000 to express the concentration in mM, a unit easier to manipulate during future calculations. As result, the concentration of stock Ribonuclease A was determined to be 0.8924 mM.

To perform a reaction, one Eppendorf tube containing the stock Ribonuclease A was retrieved from the freezer and allowed to thaw out on ice for 20 min, on the counter for 20 min, and finally in the hand for a few minutes. Once completely thawed, the protein solution was vortexed for 1 min to ensure homogeneity before being ready for use.

For all studies involving the modification of Ribonuclease A by HNQ, Ribonuclease A was fixed at a concentration of 0.050 mM. Calculations were performed to determine the exact volume of stock Ribonuclease A to add to each reaction cuvette to obtain a Ribonuclease A concentration of 0.050 mM. This was performed using Equation 3.2 where M_1 is the concentration of stock Ribonuclease A (0.8924 mM), V_1 is the required aliquot of stock Ribonuclease A to be added to the reaction cuvette, M_2 is the

desired concentration of RNase A (0.050 mM), and V_2 is the desired volume in the reaction cuvette (3000 μL).

$$M_1V_1 = M_2V_2 \qquad \text{(Eq. 3.2)}$$

As result, 168 μL of stock Ribonuclease A was transferred to a 3 mL reaction cuvette containing phosphate buffer (50 mM) to achieve a Ribonuclease A concentration of 0.050 mM used for all studies.

3.2.3 Quinone Solution

Solutions of HNQ were made fresh for every reaction performed. This involved weighing an amount of HNQ on tared weigh-paper (a mass between 0.0100 g and 0.0200 g) and quantitatively transferring to a 10 mL volumetric flask. To ensure all protein was transferred into the volumetric flask, 10% MeOH/90% phosphate buffer (50 mM) was used to wash any residual HNQ off the weigh-paper into the volumetric flask. HNQ, in the volumetric flask, was diluted to the line with 10% MeOH/90% phosphate buffer (50 mM) and capped and sealed with ParaFilm. To facilitate HNQ into solution, sonication was performed for 10 min in addition to inversion and shaking the volumetric flask by hand. Halfway through the sonication procedure, the volumetric flask was removed, inverted to mix the solution, and then placed back into the sonicator. After sonication, the HNQ solution was transferred into a small holding beaker, covered with foil, and was ready for use.

It is important to note that only the volumetric flask containing the HNQ solution contained 10% MeOH. Once the HNQ, in solution, was transferred from the small holding beaker to the reaction cuvette, phosphate buffer (50 mM) was used to bring the

reaction cuvette up to volume. Over all studies performed, the relative concentration of 10% MeOH in the reaction cuvette was minimal and not enough to influence the reaction being performed.

During the sonication procedure, the concentration of HNQ prepared in solution was calculated by converting the mass of HNQ to moles of HNQ and then dividing by 0.0100 L. To convert grams of HNQ to moles of HNQ, the mass of HNQ was divided by the molar mass of HNQ. This value was then divided by 0.0100 L to determine the molarity, or concentration, of the quinone in solution. Finally, this concentration was multiplied by 1000 to express the concentration in mM, a unit easier to manipulate during future calculations.

In addition, further calculations were performed during the sonication process to determine the exact volume of HNQ solution to add to the reaction cuvette containing RNase A (0.050 mM) and phosphate buffer (50 mM) to achieve the desired concentration of HNQ in the reaction cuvette. This was calculated using Equation 3.3 where, in this case, M_1 is the actual concentration of the HNQ solution prepared, V_1 is the required aliquot of HNQ solution to be added to the reaction cuvette, M_2 is the desired concentration of HNQ, and V_2 is the desired volume in the reaction cuvette (3000 μL).

$$M_1V_1 = M_2V_2 \qquad \text{(Eq. 3.3)}$$

Since several concentrations of HNQ were used across all studies, and the amount of HNQ weighed out each time was not the same, the amount of HNQ solution added to the reaction cuvette varied reaction to reaction.

For the study involving different concentrations of HNQ, aliquot volumes were calculated for desired concentrations of 0.050 mM, 0.10 mM, 0.25 mM, 0.50 mM, and

1.5 mM. For the study involving HNQ incubated with Ribonuclease A at different pH, aliquot volumes were calculated for a fixed concentration of 0.10 mM. This concentration was determined best to work with when comparing different variables of reactions because it provided a concentration high enough to interact well with Ribonuclease A.

Once the calculated volume of HNQ solution was added to the reaction cuvette containing RNase A (0.050 mM) and phosphate buffer (50 mM), the reaction began, the cuvette was placed into the fluorimeter for scanning, and the reaction time was kept on a scientific timer.

3.2.4 Fluorescence Spectroscopy & Anisotropy Measurements

Fluorescence spectroscopy was performed using a Horiba Jobin Yvon Fluorolog spectrophotometer equipped with a Xenon lamp. The excitation wavelength was fixed at 280 nm with a 2 nm slit width to accommodate the tyrosine residues in Ribonuclease A. The resulting emission was recorded every 1 nm with a slit width of 2 nm over the range of 290-600 nm. To draw correlations between all studies, each spectrum was normalized from 500-550 nm where little emission was recorded. Microsoft Excel was used to analyze the data and to produce graphs to visualize the fluorescence spectra.

All reactions were performed in a quartz cuvette in phosphate buffer (50 mM). The cuvette was equipped with a stir bar to ensure proper mixing and to minimize sedimentation of Ribonuclease A. The stirring motion was set to the 3rd level of power as indicated on the fluorimeter. Emission scanning lasted around 10 min and varied occasionally in duration due to mechanical motion inside of the fluorimeter. Initial

scanning, or reaction scanning, of Ribonuclease A occurred over 24 h with scans occurring every hour for that duration. Post-modified Ribonuclease A was returned to a quartz cuvette after a 24 h dialysis and scanned an additional four times. This resulting data was recorded, averaged, and analyzed in Microsoft Excel to produce the graphs presented in this study. A control was produced by subjecting RNase A (0.050 mM) in phosphate buffer (50 mM) to the same procedure as every reaction performed.

The software to operate the fluorimeter was FluorEssence by Horiba Jobin Yvon. This software was capable of automating fluorescence and anisotropy scans which were utilized to accomplish the 24 h scans of each study. The first and second scans were always started manually with each consecutive scan being automatically started by the programming. Since each emission scan lasted around 10 min (600 s), the instrument was programmed to scan the reaction every 2997 s for 24 h to accomplish 24 h of scanning each hour. Due to the mechanical motion of parts inside of the fluorimeter, an additional 3 s was added to accommodate the automated re-calibration of the instrument after each scan. Due to fluctuations in voltage supplied to the instrument, the timing of the scans slightly varied for each reaction and occasionally needed to be reset during the reaction.

The process of performing fluorescence measurements was performed in a similar manner for every reaction by following a pre-determined protocol. To begin, the fluorimeter was turned on by first switching on the water bath, the fan, the lamp, and then the software PC. The lamp was allowed to warm up for 1 h before any measurements took place. The instrument was initialized by selecting to perform a spectra study, specifically an emission study, and then by executing a trial scan (C1-Trial) with the

cuvette containing only Ribonuclease A and phosphate buffer (50 mM). Once the initialization was complete and the trial scan was acceptable, the software was used to program the instrument for fluorescence measurements. A scientific timer was obtained and started as soon as the aliquot of HNQ was administered to the reaction cuvette containing Ribonuclease A and phosphate buffer. After this, the reaction cuvette was capped, the sides wiped with Kimwipes, inverted 3 times, and placed in the fluorimeter for scanning. Once securely positioned inside the fluorimeter, the fluorescence scanning was started and the time on the scientific timer was recorded. This time was the delay between the actual start of the reaction of Ribonuclease A with HNQ and the initial emission scanning of the reaction. In addition, the time of day was recorded to be able to monitor the start and stop of each consecutive measurement every hour.

Post-modified Ribonuclease A fluorescence measurements were performed using a different programmed scanning procedure as initial scanning. In these scans, modified Ribonuclease A was scanned four times in the time frame of 1 h at 37°C. Once these scans were complete, the cuvette was removed from the fluorimeter and the instrument was shut down in the reverse order in was turned on. This concluded the use of fluorescence spectroscopy to measure the modification of Ribonuclease A induced by HNQ.

In addition to fluorescence measurements, anisotropy measurements were performed as well during initial and post-modified scanning of Ribonuclease A. Appendix B shows anisotropy measurements for each study performed using Ribonuclease A. A general trend can be seen in each graph indicating the correlation

between increasing modification of Ribonuclease A and increasing anisotropy values of Ribonuclease A.

Overall, the studies performed with fluorescence spectroscopy helped aid previous research in positively confirming modification of Ribonuclease A by HNQ.

3.2.5 UV-VIS Spectroscopy

UV-VIS spectroscopy was performed using a double-beam UV-1800 Shimadzu UV Spectrophotometer. The instrument was allowed to warm up for 20 min before any measurements took place. Excitation was achieved using a D_2/W lamp with the resulting spectra recorded at 1 nm sampling intervals over the range of 200-700 nm with the scan speed set to fast. The slit width was 1.0 nm and the D_2/W light change was set at 340.8 nm. The instrument was auto-zeroed and baselined prior to every scan to account for background noise. Microsoft Excel was used to analyze the data recorded and to produce the graphs presented in this study.

Immediately after fluorescence scanning was complete, the cuvette was transferred into the UV-VIS spectrophotometer for analysis. Absorbance of the analyte was recorded and immediately processed on screen using the software UV Probe 2.33. A reference cell containing phosphate buffer (50 mM, pH=7.0) was prepared at the beginning of the study and was used for every reaction throughout the study. This insured the absorbance calculated by the instrument was solely from Ribonuclease A and any bound or unbound HNQ. Pre-dialysis Ribonuclease A exhibited larger absorbance than post-dialysis Ribonuclease A due to unbound HNQ in solution absorbing light.

Removal of unbound HNQ by dialysis reduced the absorbance of the analyte and produced a more accurate representation of modified Ribonuclease A.

All UV-VIS measurements were performed in the same manner and used to measure the amount of modification (by adduct formation) of Ribonuclease A. Overall, the studies performed with UV-VIS spectroscopy helped aid previous research in positively confirming modification of Ribonuclease A by HNQ.

3.2.6 Dialysis

To accurately measure the modification of Ribonuclease A induced by HNQ, dialysis was performed to remove unbound HNQ that was not covalently bonded to Ribonuclease A. Spectroscopically measuring Ribonuclease A with bound HNQ alone gives clear understanding of the modification of Ribonuclease A induced by HNQ.

Dialysis was performed using a 5 mL Float-A-Lyzer purchased from Spectrum Laboratories. The membrane, with a molecular cutoff of 3.5 kDa, allowed unbound HNQ to freely exit through the membrane. Ribonuclease A, with a molecular mass of 13.6 kDa, or modified Ribonuclease A, with a slightly higher molecular mass, remained inside of the dialysis membrane along with any HNQ bound to the protein via ionic bonding, covalent bonding, or H-bonding. Before use, each dialysis membrane was thoroughly soaked, washed, and rinsed with DI water and then temporarily held in phosphate buffer solution (50 mM) kept at 4°C. Before the reaction solution could be transferred into the dialysis membrane, the membrane was emptied of phosphate buffer solution to insure proper concentration of the protein and HNQ in solution. Once the reaction solution was carefully transferred from the reaction cuvette to the dialysis

membrane by a disposable pipette, the dialysis membrane was placed in 900 mL of phosphate buffer solution and kept at 4°C for 24 h. Facilitation of unbound HNQ out of the dialysis membrane was accelerated by the concentration gradient between the phosphate buffer solution and the reaction solution as well as by stirring using a stir bar. Since the concentration of quinone outside of the dialysis membrane was less than the concentration of quinone inside of the dialysis membrane, simple diffusion occurred and the unbound HNQ exited the dialysis membrane. This was further accelerated by changing out the phosphate buffer solution three times, typically every 2.5 h. By doing this, the concentration gradient became smaller each time and diffusion continued to take place. After three buffer changes, and considering the volume of reaction solution to phosphate buffer solution, it is safe to assume all unbound HNQ had been washed from the reaction solution.

After 24 h of dialysis, the contents in the dialysis membrane were returned to a clean reaction cuvette and placed in the fluorimeter for post-dialysis fluorescence scanning. By removal of unbound quinone in solution, the modification of Ribonuclease A by bound HNQ was measured and quantified by fluorescence and UV-VIS spectroscopy.

3.3 Results and Discussion

The results of several reactions involving Ribonuclease A are presented below. Two official studies were conducted: (1) a study with HNQ at various concentrations, and (2) a study focused on the pH dependence of HNQ. Fluorescence and UV-VIS graphs are

included for each study. The graphs depict the fluorescence intensity and absorbance of post-dialysis Ribonuclease A. Post-dialysis Ribonuclease A (i.e. modified Ribonuclease A) refers to Ribonuclease A which has completed a 24 h dialysis and contains only Ribonuclease A and any bound quinone to the protein.

Normalized integrated fluorescence intensity (NIFI) values were obtained by selecting a range of wavelengths and calculating the area under the curve of each fluorescence spectrum. Two separate wavelength ranges were chosen for all calculations of NIFI. The integration range of 290-400 nm spans the entire emission area while the integration range 300-330 nm narrows in on the maximum fluorescence intensity for each reaction. This was done to account for minor blips in the fluorescence spectra and to measure uniformity when comparing results. Two reference NIFIs were used, RNase A (0.050 mM) for the study with HNQ at various concentrations and RNase A + HNQ (0.10 mM) pH=7.0 for the study focused on the pH dependence of HNQ. To quantify the modification of Ribonuclease A from different studies, a reduced integrated fluorescence intensity (RIFI) value was calculated by dividing the NIFI of the study in question by the reference NIFI, converting to a percentage, and then subtracting from 100%. Reference NIFIs have RIFIs of 0% since 100%-100% = 0% and negative RIFIs represent an increase in fluorescence intensity since the corresponding NIFI is greater than the reference NIFI.

Through observation of a reduction of fluorescence intensity and an increase in absorbance, modification of Ribonuclease A was confirmed from the results of these studies.

3.3.1 Ribonuclease A Modifications Induced by HNQ at Various Concentrations

In this study, RNase A (0.050 mM) was treated with HNQ (0.050, 0.10, 0.25, 0.50, or 1.5 mM) and allowed to react while being monitored using fluorescence for 24 h. Following the 24 h incubation, dialysis was performed for an additional 24 h followed by a final spectroscopic measurement of modified Ribonuclease A. All reactions were performed in a phosphate buffer (50 mM) at 37°C and pH=7.0 to mimic physiological conditions.

Table 3.1 lists RIFI values calculated over 290-400 nm and 300-330 nm in addition to absorbance values for each reaction performed in this study. Figure 3.1 shows the fluorescence intensity of Ribonuclease A and Ribonuclease A modified by HNQ (0.050, 0.10, 0.25, 0.50, or 1.5 mM) for 24 h at 37°C. All spectra were normalized in the 500-550 nm range where little emission is present to ensure proper comparison. Figure 3.2 shows the absorbance of Ribonuclease A and Ribonuclease A modified by HNQ (0.050, 0.10, 0.25, 0.50, or 1.5 mM) for 24 h at 37°C.

As seen in Figure 3.1, the fluorescence intensity decreases as the concentration of HNQ increases in the reaction solution. From the results of previous studies, it was found exposure of Ribonuclease A to HNQ does not elicit protein oligomerization over time. However, from the results of this study, a decrease in fluorescence intensity was observed. This reduction of fluorescence intensity is believed to be result of other means of protein modification, such as adduct formation.

Table 3.1 RIFI of RNase A (0.050 mM) and RNase A (0.050 mM) modified by HNQ (0.050, 0.10, 0.25, 0.50, or 1.5 mM) for 24 h at 37°C. Absorbance at 346 nm of RNase A (0.050 mM) and RNase A (0.050 mM) modified by HNQ (0.050, 0.10, 0.25, 0.50, or 1.5 mM) for 24 h at 37°C.

Reaction	RIFI[a] (%)	RIFI[b] (%)	A_{346} (a.u.)
RNase A (0.050 mM)	0	0	-0.002
RNase A + HNQ (0.050 mM)	11	11	0.029
RNase A + HNQ (0.10 mM)	32	31	0.057
RNase A + HNQ (0.25 mM)	47	46	0.088
RNase A + HNQ (0.50 mM)	90	91	0.283
RNase A + HNQ (1.5 mM)	97	98	1.035

a *integration between 290-400 nm*
b *integration between 300-330 nm*

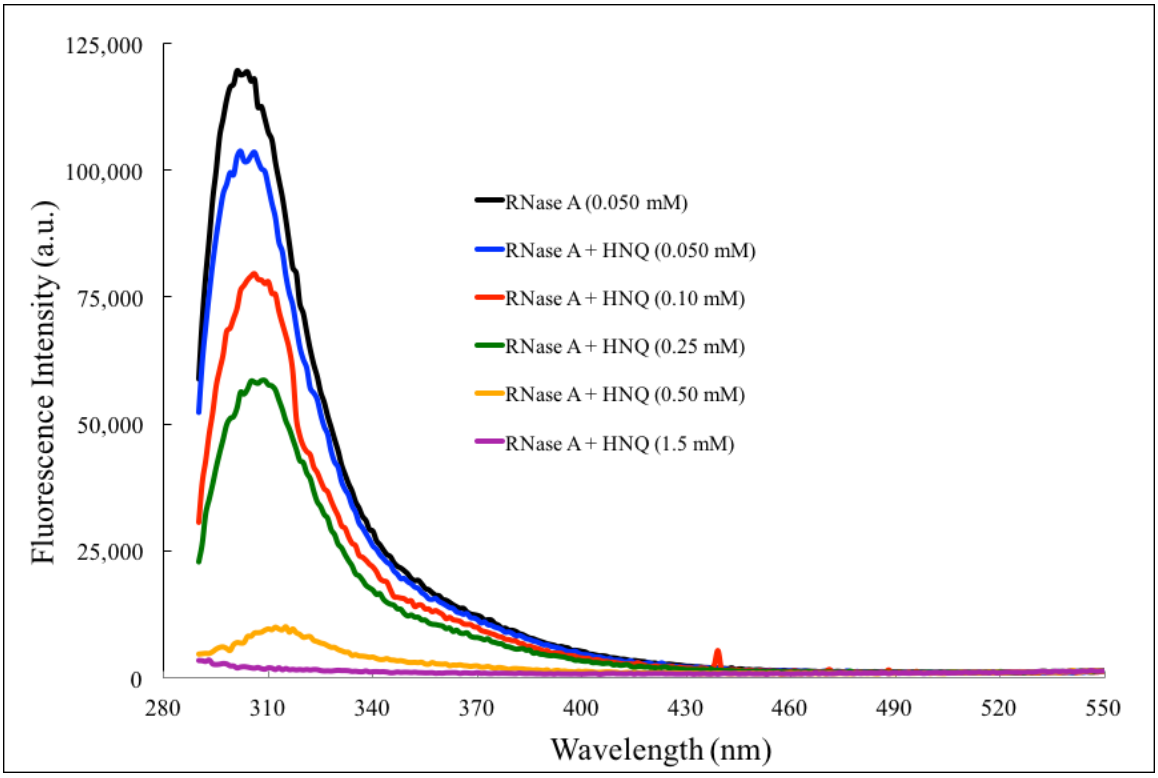

Figure 3.1 Fluorescence spectra of RNase A (0.050 mM) and RNase A (0.050 mM) modified by HNQ (0.050, 0.10, 0.25, 0.50, or 1.5 mM) for 24 h at 37°C.

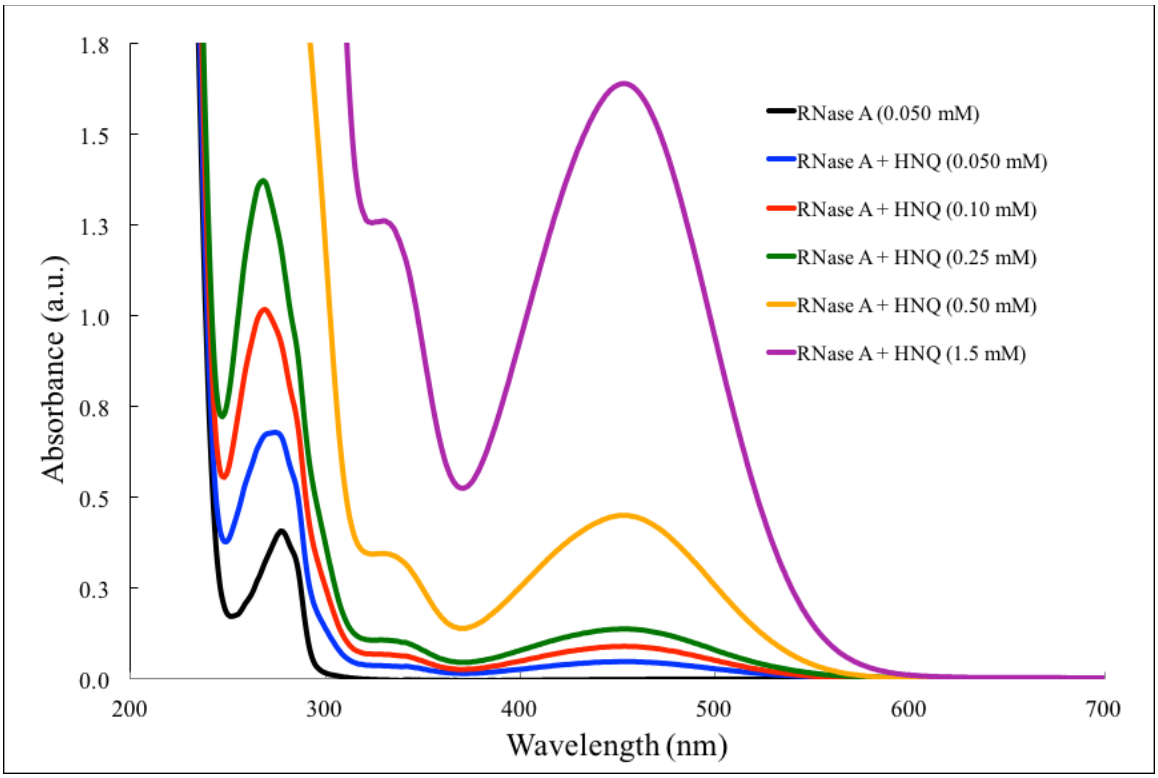

Figure 3.2 UV-VIS spectra of RNase A (0.050 mM) and RNase A (0.050 mM) modified by HNQ (0.050, 0.10, 0.25, 0.50, or 1.5 mM) for 24 h at 37°C.

To quantify the degree of modification of Ribonuclease A, RIFI values were calculated using RNase A (0.050 mM) as the reference NIFI. As seen in Table 3.1, the RIFI increases as the concentration of HNQ in the reaction solution increases. This is interpreted as an increase in the modification of Ribonuclease A upon exposure to increasing concentration of HNQ. Considering all reactions performed in this study, Table 3.1 shows no more than a 1% difference in RIFI values calculated over the two integration ranges.

As seen in Figure 3.2, the absorbance in the 320-550 nm range increases as the concentration of HNQ increases in the reaction solution. Since HNQ absorbs in this range, and any free HNQ has already been removed through dialysis, the increase in absorbance is believed to be result of HNQ covalently bonded to Ribonuclease A. To

monitor this, Table 3.1 shows the absorbance at 346 nm of Ribonuclease A and modified Ribonuclease A. From these results, increasing the concentration of HNQ increases the overall absorbance of modified Ribonuclease A. This is interpreted as an increase in the modification of Ribonuclease A upon increasing concentration of HNQ.

In summary, Ribonuclease A modification was found to be increasing with the concentration of HNQ. In addition to the SDS-PAGE data presented in Chapter 1 [Smith & Kim, 2015], and similar to what was observed during previous studies with Ribonuclease A, this study shows HNQ exhibits its modifying capabilities solely through adduct formation.

3.3.2 Ribonuclease A Modifications Induced by HNQ at Various pH

In this study, RNase A (0.050 mM) was treated with HNQ (0.010 mM) at pH=6.0, pH=7.0, and pH=8.0 and allowed to react while being monitored using fluorescence for 24 h. Following the 24 h incubation, dialysis was performed for an additional 24 h followed by a final spectroscopic measurement of modified Ribonuclease A. All reactions were performed in a phosphate buffer (50 mM) at 37°C.

Table 3.2 lists RIFI values calculated over 290-400 nm and 300-330 nm in addition to absorbance values for each reaction performed in this study. Figure 3.3 shows the fluorescence intensity of Ribonuclease A and Ribonuclease A modified by HNQ (0.10 mM) at pH=6.0, pH=7.0, and pH=8.0 for 24 h at 37°C. All spectra were normalized in the 500-550 nm range where little emission is present to ensure proper comparison. Figure 3.4 shows the absorbance of Ribonuclease A and Ribonuclease A modified by HNQ (0.10 mM) at pH=6.0, pH=7.0, and pH=8.0 for 24 h at 37°C.

Table 3.2 RIFI of RNase A (0.050 mM) modified by HNQ (0.10 mM) at pH=6.0, pH=7.0, and pH=8.0 for 24 h at 37°C. Absorbance at 346 nm of RNase A (0.050 mM) modified by HNQ (0.10 mM) at pH=6.0, pH=7.0, and pH=8.0 for 24 h at 37°C.

Reaction	RIFI[a] (%)	RIFI[b] (%)	A_{346} (a.u.)
RNase A + HNQ (0.10 mM) pH=6.0	-1	-2	0.048
RNase A + HNQ (0.10 mM) pH=7.0	0	0	0.057
RNase A + HNQ (0.10 mM) pH=8.0	52	53	0.109

a integration between 290-400 nm
b integration between 300-330 nm

As seen in Figure 3.3, the fluorescence intensity decreases as the pH of the reaction solution increases from 7.0 to 8.0 and remains much the same as the pH of the reaction solution decreases from 7.0 to 6.0. This is believed to be due to increasing and decreasing the nucleophilic character of the protein and therefore increasing and decreasing the likelihood of association of Ribonuclease A and HNQ. In addition, since protein oligomerization is not induced by HNQ, or influenced by pH changes, increasing the pH of the reaction solution encourages other means of protein modification to occur, such as adduct formation. To quantify this degree of modification of Ribonuclease A, RIFI values were calculated using RNase A + HNQ (0.10 mM) pH=7.0 as the reference NIFI. As seen in Table 3.2, the RIFI increases only as the pH of the reaction solution increases from 7.0 to 8.0 and is found to have little change when the pH of the reaction solution is decreased from 7.0 to 6.0. This is interpreted as an increase of modification of Ribonuclease A only upon increasing the pH of the reaction solution.

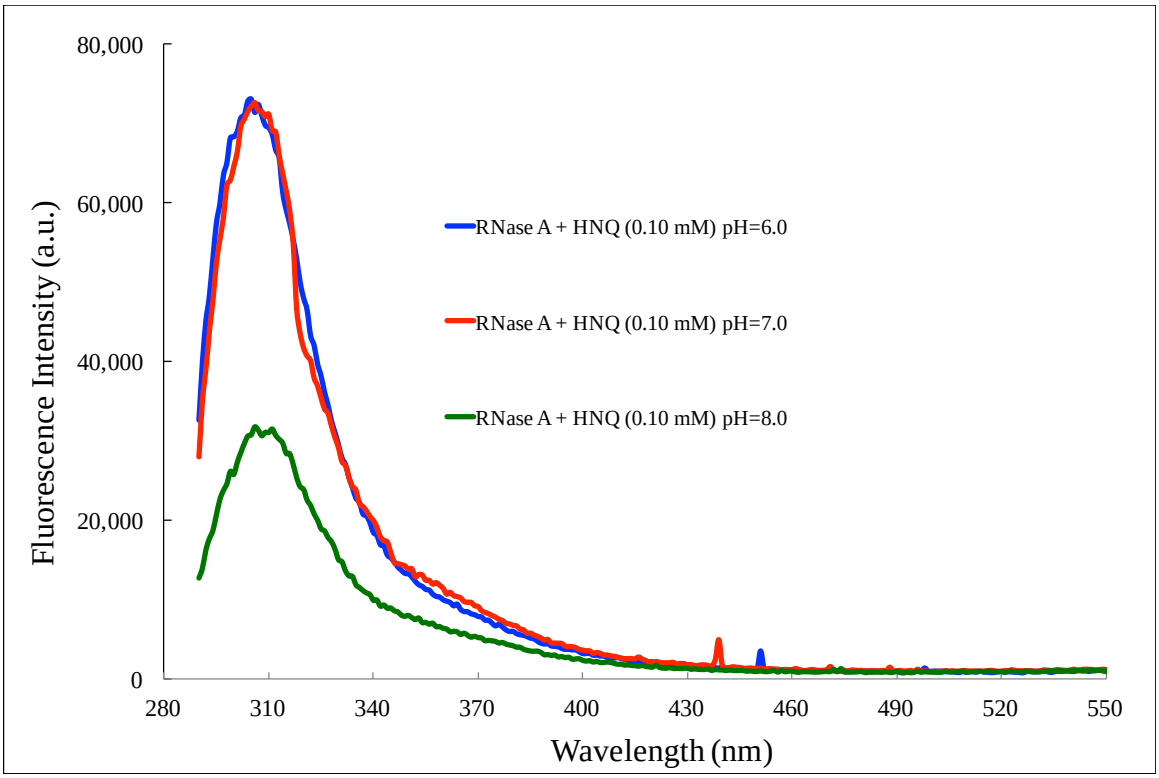

Figure 3.3 Fluorescence spectra of RNase A (0.050 mM) modified by HNQ (0.10 mM) at pH=6.0, pH=7.0, and pH=8.0 for 24 h at 37°C.

Obviously, incubating Ribonuclease A with HNQ regardless of the pH causes a modification of Ribonuclease A. However, considering conditions at physiological pH, an increase in pH causes greater modification of Ribonuclease A and a decrease in pH causes little to no change in the modification of Ribonuclease A. Considering all reactions performed in this study, Table 3.2 shows no more than a 1% difference in RIFI values calculated over the two integration ranges.

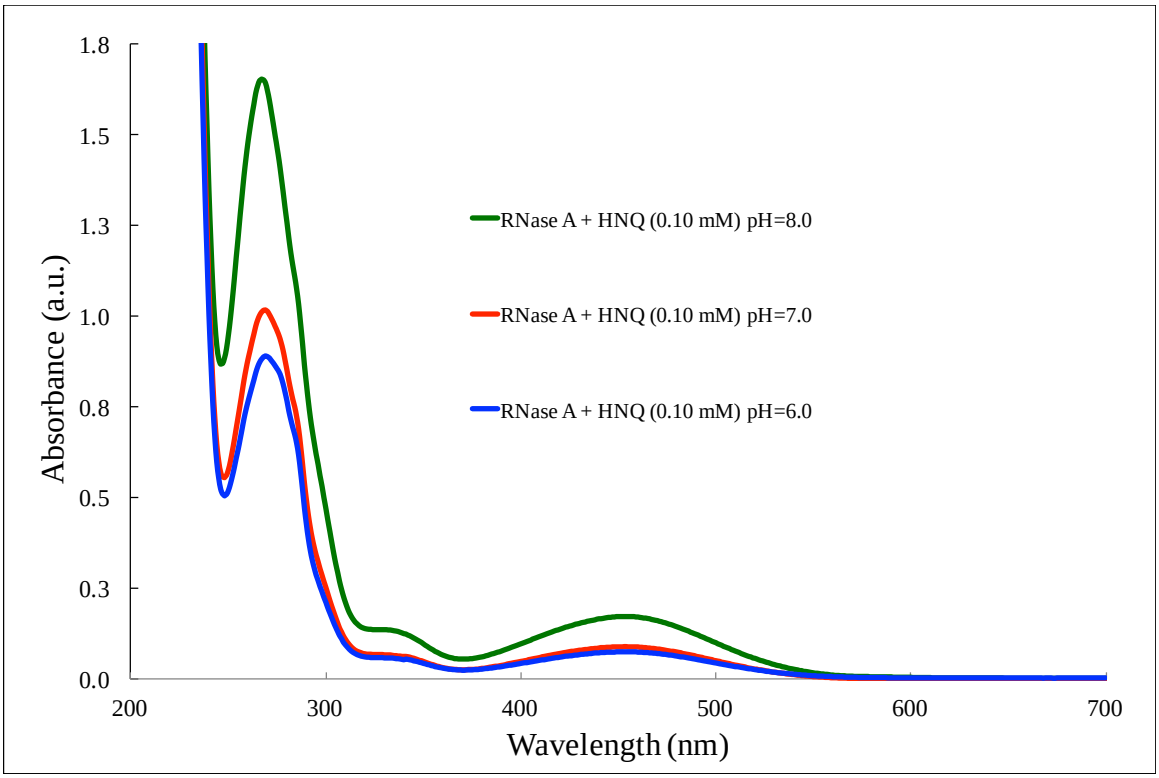

Figure 3.4 UV-VIS spectra of RNase A (0.050 mM) modified by HNQ (0.10 mM) at pH=6.0, pH=7.0, and pH=8.0 for 24 h at 37°C.

As seen in Figure 3.4, the absorbance in the 320-550 nm range increases as the pH of the reaction solution increases from 7.0 to 8.0 and decreases slightly as the pH of the reaction solution decreases from 7.0 to 6.0. Since HNQ absorbs in this range, and any free HNQ has already been removed through dialysis, the increase and decrease in absorbance is believed to be result of HNQ covalently bonded to Ribonuclease A. To monitor this, Table 3.2 shows the absorbance at 346 nm of Ribonuclease A incubated with HNQ at pH=6.0, pH=7.0, and pH=8.0. From these results, increasing the pH of the reaction solution from 7.0 to 8.0 increases the absorbance and decreasing the pH of the reaction solution from 7.0 to 6.0 decreases the absorbance. Again, any incubation of Ribonuclease A with HNQ will cause an increase in the overall absorbance of

Ribonuclease A, however, in this study, comparisons to physiological pH were made, and increases and decreases in absorbance were noted as result.

Considering the results of this study, several assumptions can be made. For example, increasing the pH of solution gives rise to increasing deprotonation of Ribonuclease A which results in greater attractive forces between HNQ and Ribonuclease A. In addition, because the pKa of the hydrogen on hydroxyl group of HNQ is 4.3, HNQ assumes a negative partial charge in all incubations at pH=6.0, pH=7.0, and pH=8.0 [Scifinder]. This would result in greater association of HNQ to positively charged amino acid residues of Ribonuclease A upon increasing the pH and less association of HNQ to positively charged amino acid residues of Ribonuclease A upon decreasing the pH. In contrast, decreasing the pH of solution gives rise to increasing protonation of HNQ and Ribonuclease A which would result in greater repulsive forces and lessen the interaction between the two. Although Figure 3.3 does not show a large increase in fluorescence spectroscopy of the reaction RNase A + HNQ (0.10 mM) pH=6.0, Figure 3.4 does show slight differences between the reactions performed at pH=6.0 and pH=7.0. Because UV-VIS spectroscopy is believed to detect changes due to adduct formation, the reaction performed at pH=6.0 shows supporting results of less modification due to greater amounts of HNQ and Ribonuclease A repelling one another as result of protonation caused by the lower pH.

In summary, Ribonuclease A modification was found to be increasing with respect to increasing the pH of the reaction solution from 7.0 to 8.0 and unchanged when decreasing the pH of the reaction solution from 7.0 to 6.0. In addition to SDS-PAGE data presented in Chapter 1 [Smith & Kim, 2015], this study shows HNQ exhibits its

modifying capabilities solely through adduct formation and is largely unaffected by decreases in pH.

3.4 Conclusions

Ribonuclease A modifications were observed with HNQ incubations as well as when environmental conditions were altered. Ribonuclease A modification, through adduct formation, was found to be increasing with the concentration of HNQ. In addition, Ribonuclease A modification was found to be increasing with respect to increasing the pH of the reaction solution from 7.0 to 8.0 and unchanged when decreasing the pH of the reaction solution from 7.0 to 6.0. In support of previous studies [Smith & Kim, 2015], HNQ was observed to exhibit its protein modifying capabilities solely through adduct formation and does not produce protein oligomerization.

BIBLIOGRAPHY

Batra, M.; et al. An efficient synthesis and biological activity of substituted p-benzoquinones. *Bioorg. Med. Chem.* **2006**, 14, 8519-8526.

Bemporad, F.; Calloni, G.; Camponi, S.; Plakoutsi, G.; Taddei, N. Chiti, F. *Acc. Chem. Res.* **2006**, 39, 620-627.

Bolton, J.L; et al. Role of quinones in toxicology. *Chem. Res. Toxicol.* **2000**, 13, 135-160.

Chiti, F.; Dobson, C.M. *Annu. Rev. Biochem.* **2006**, 75, 333-366.

Chiti, F.; Dobson, C.M. *Nat. Chem. Biol.* **2009**, 5, 15-22.

Cornwell, D.G.; et al. Electrophile tocopheryl quinones in apoptosis and mutagenesis: Thermochemolysis of thiol adducts with proteins and in cells. *Lipids*, **2003**, 38, 973-979.

Dobson, C.M. *Nature***. 2003**, 426, 884-890.

Gregersen, N.; Bross, P.; Vang, S.; Christensen, J.H. *Annu. Rev. Genom. Human Genet.* **2006**, 7, 103-124.

Greve, H. J.; Kim, J. Modifications of Lysozyme by Substituted Benzoquinones. Undergraduate Departmental Honors Thesis, University of Tennessee at Chattanooga, Chattanooga, TN, 2015

Huff, J.E.; et al. Multiple-Site Carcinogenicity of Benzene in Fischer-344 Rats and B6c3f1 Mice. *Environ. Health Perspect.* **1989,** 82, 125-163.

Kim, J. *Biological Implications of Benzoquinones*, in *Quinones: Occurrence, Medicinal Uses and Physiological Importance*, S.C.J. Ervin R. Price, Editor. 2013, Nova Science Pub Inc.

Kim, J.; Albu, T.V.; Vaughn, A.R.; Kang, M.; Carver, E.A.; Stickle, D.M. *Bioorg. Chem.* **2015**, 59, 106-116.

Kim, J.; Vaughn, A.R.; Cho, C.; Albu, T.V.; Carver, E.A. *Bioorg. Chem.* **2012**, 40, 92-98.

Nilsberth, C.; Westlind-Danielsson, A.; Eckman, C.B.; Condron, M.M.; Axelman, K.; Forsell, C.; Stenh, C.; Luthman, J.; et al. *Nat Neurosci.* **2001**, 4, 887-893.

Ramirez-Alvarado, M. *Prog. Mol. Biol. Transl. Sci.* **2008**, 84, 115-160.

Scifinder, Chemical Abstracts Service, RN 83-72-7. 2015: Columbus, OH.

Skoog, D.A.; Holler, F.J.; Crouch, S. R. *Principles of Instrumental Analysis*, 6th ed.; Cengage Learning: Andover, 2007.

Smith, M.; Kim, J. Ribonuclease A Modification Induced by 1,2-Naphthoquinone and 2-Hydroxy-1,4-Napthoquinone. Undergraduate Departmental Honors Thesis, University of Tennessee at Chattanooga, Chattanooga, TN, 2015

Snyder, R.; C.C. Hedli. An overview of benzene metabolism. *Environ. Health Perspect.* **1996**, 104, 1165-1171.

Snyder, R.; et al. Studies on the Mechanism of Benzene Toxicity. *Environ. Health Perspect.* **1989**, 82, 31-35.

Swaminathan, R.; et al. Lysozyme: a model protein for amyloid research. *Adv. Protein Chem Struct. Biol*. **2011**, 84, 63-111.

Vaughn, A.R. Biological implications of 2-chlorocyclohexa-2,5-diene-1,4-dione toward ribonuclease A. *Adv. Biosci. Biotechnol*. **2013**, 4.

Voet, D.; Voet, J.G.; Pratt, C.W. *Fundamentals of Biochemistry: Life at the Molecular Level*, 4th ed.; John Wiley & Sons: Hoboken, 2012.

Willey, J.M.; et al. *Prescott's microbiology*, 8th ed.; McGraw-Hill: New York, 2011.

Zhu, Y.J.; Lin, H.; Lal, R. *FASEB J.* **2000**, 14, 1244-1254.

APPENDICES

APPENDIX A

Anisotropy measures the non-sphericity of a molecule by recording the amount of emitted light that passes through different polarized planes. In these studies, larger values of anisotropy correspond to Lysozyme that has been modified resulting in polymerization or an overall non-spherical shape, while smaller values of anisotropy correspond to Lysozyme that has been modified resulting in an increased spherical shape.

Anisotropy values of post-dialysis Lysozyme recorded from 300-450 nm corresponding to each of the six different studies performed are presented in the following pages. These values were averaged and general trends in anisotropy were observed as result.

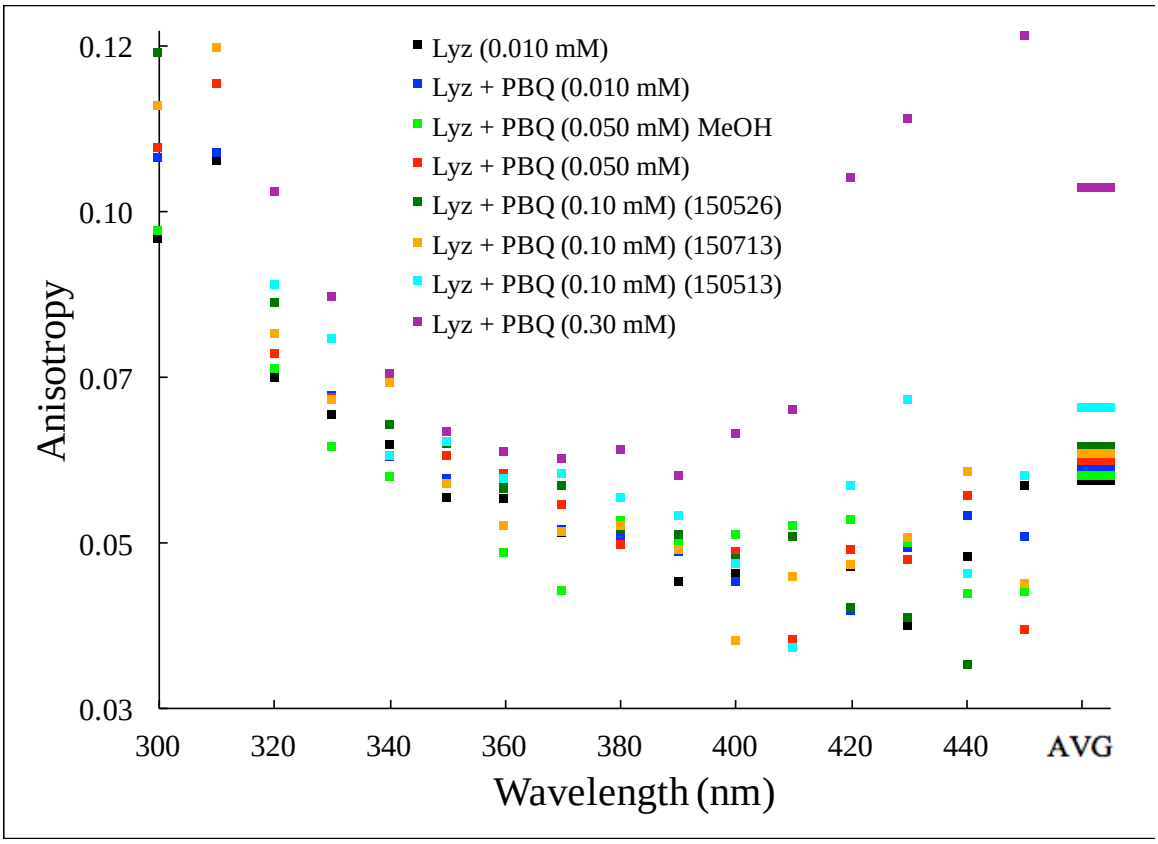

Figure A.1 Anisotropy values recorded from 300-450 nm with an average anisotropy value of Lyz (0.010 mM) and Lyz (0.010 mM) modified by PBQ (0.010, 0.050, 0.10, or 0.30 mM) for 24 h at 37°C.

A general trend of increasing anisotropy with increasing concentration of PBQ is observed. These results suggest PBQ alters the structure of Lysozyme by oligomerization and adduct formation resulting in an overall non-spherical shape of the protein.

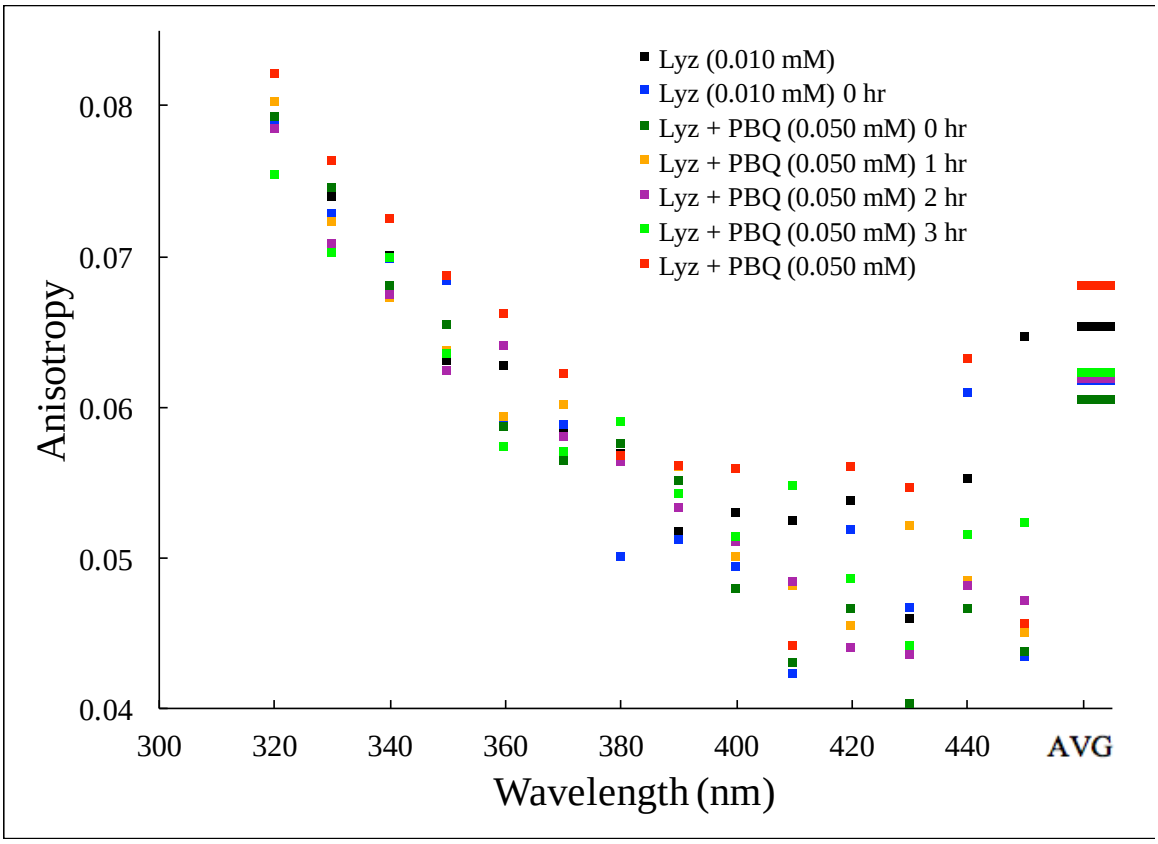

Figure A.2 Anisotropy values recorded from 300-450 nm with an average anisotropy value of Lyz (0.010 mM) and Lyz (0.010 mM) modified by PBQ (0.050 mM) for 0 h, 1 h, 2 h, 3 h, and 24 h at pH=7.0 and 37°C.

These results suggest the overall sphericity of Lysozyme increases upon initial exposure to PBQ and becomes non-spherical after several hours of incubation.

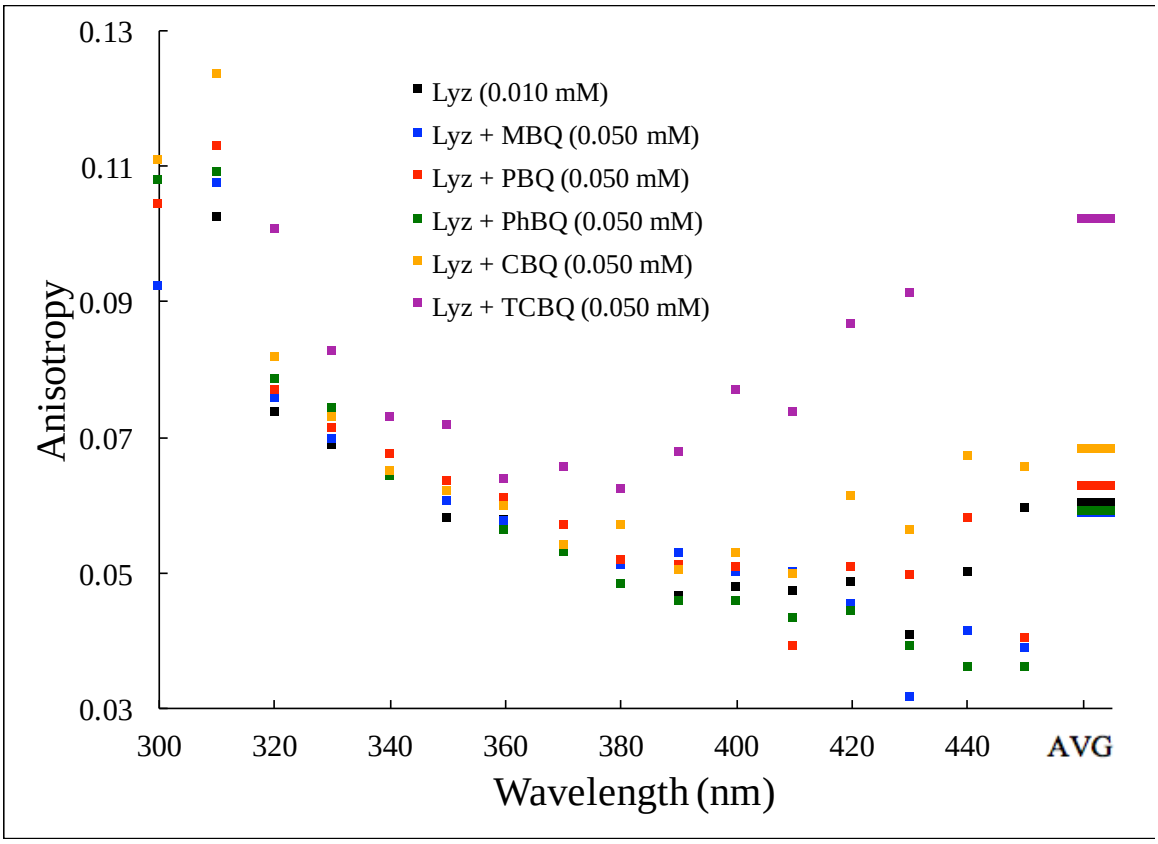

Figure A.3 Anisotropy values recorded from 300-450 nm with an average anisotropy value of Lyz (0.010 mM) and Lyz (0.010 mM) modified by MBQ (0.050 mM), PBQ (0.050 mM), PhBQ (0.050 mM), CBQ (0.050 mM), and TCBQ (0.050 mM) for 24 h at 37°C.

A general trend of increasing anisotropy with increasing electron withdrawing capability of each substituted quinone is observed. These results suggest substituted quinones alter the structure of Lysozyme by oligomerization and adduct formation resulting in an overall non-spherical shape of the protein. Consistent with Figures 2.5 and 2.6, PhBQ modifies Lysozyme in a way that increases the sphericity of the protein.

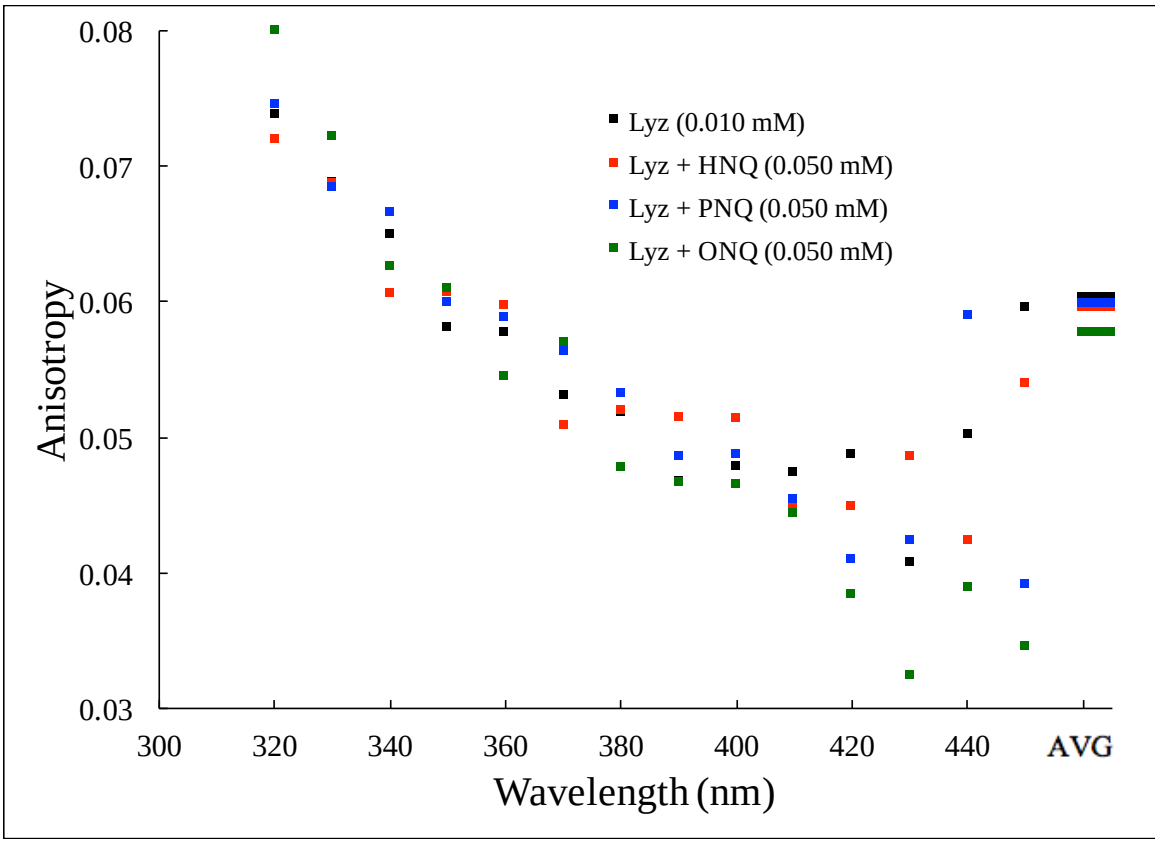

Figure A.4 Anisotropy values recorded from 300-450 nm with an average anisotropy value of Lyz (0.010 mM) and Lyz (0.010 mM) modified by HNQ (0.050 mM), PNQ (0.050 mM), and ONQ (0.050 mM) for 24 h at 37°C.

The results of these studies indicate naphthoquinones modify Lysozyme resulting in an increased spherical shape of the protein. Specifically, with support of Figures 2.7 and 2.8, ONQ elicits the largest degree of modification and is shown to modify Lysozyme in a way that increases the sphericity of the protein.

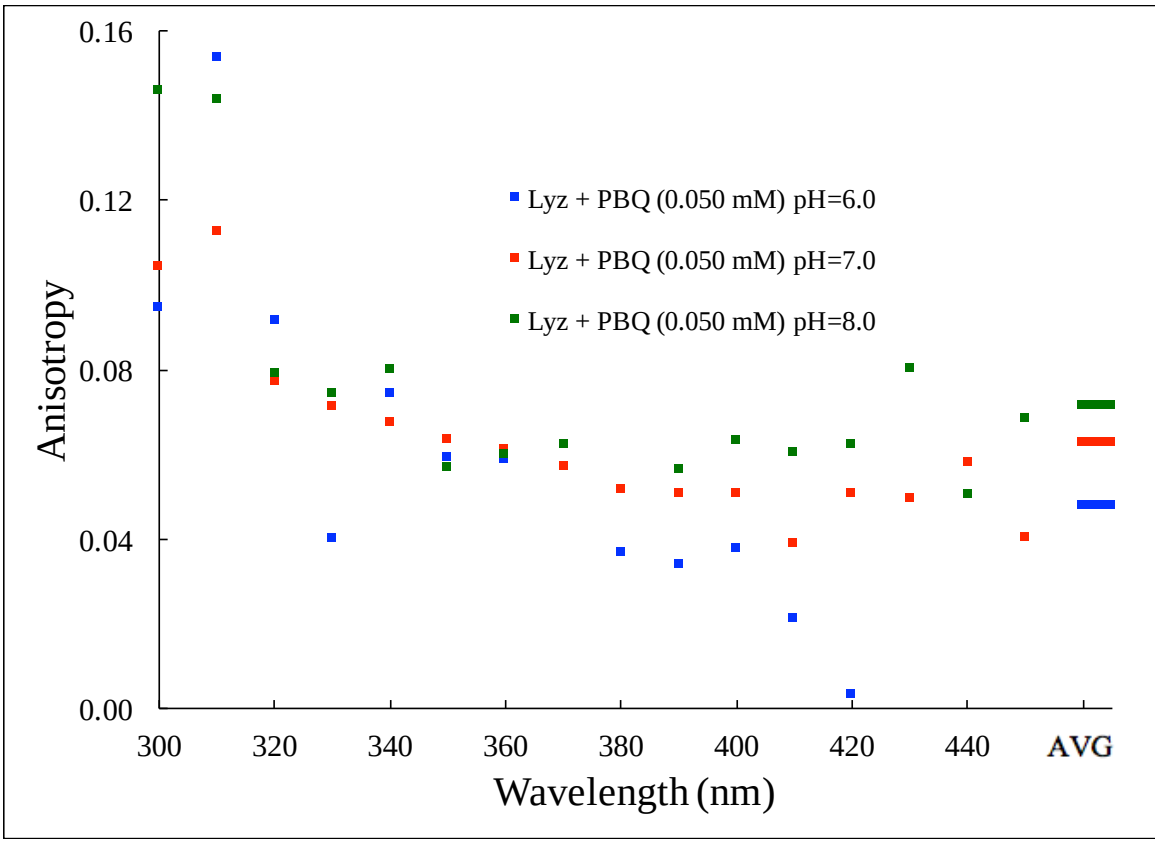

Figure A.5 Anisotropy values recorded from 300-450 nm with an average anisotropy value of Lyz (0.010 mM) modified by PBQ (0.050 mM) at pH=6.0, pH=7.0, and pH=8.0 for 24 h at 37°C.

A general trend of increasing anisotropy with increasing pH of reaction solution is observed. These results suggest increasing the pH of the reaction solution influences the modification of PBQ resulting in an overall non-spherical shape of the protein. In contrast, decreasing the pH of the reaction solution influences the modification of PBQ resulting in an increased spherical shape of the protein.

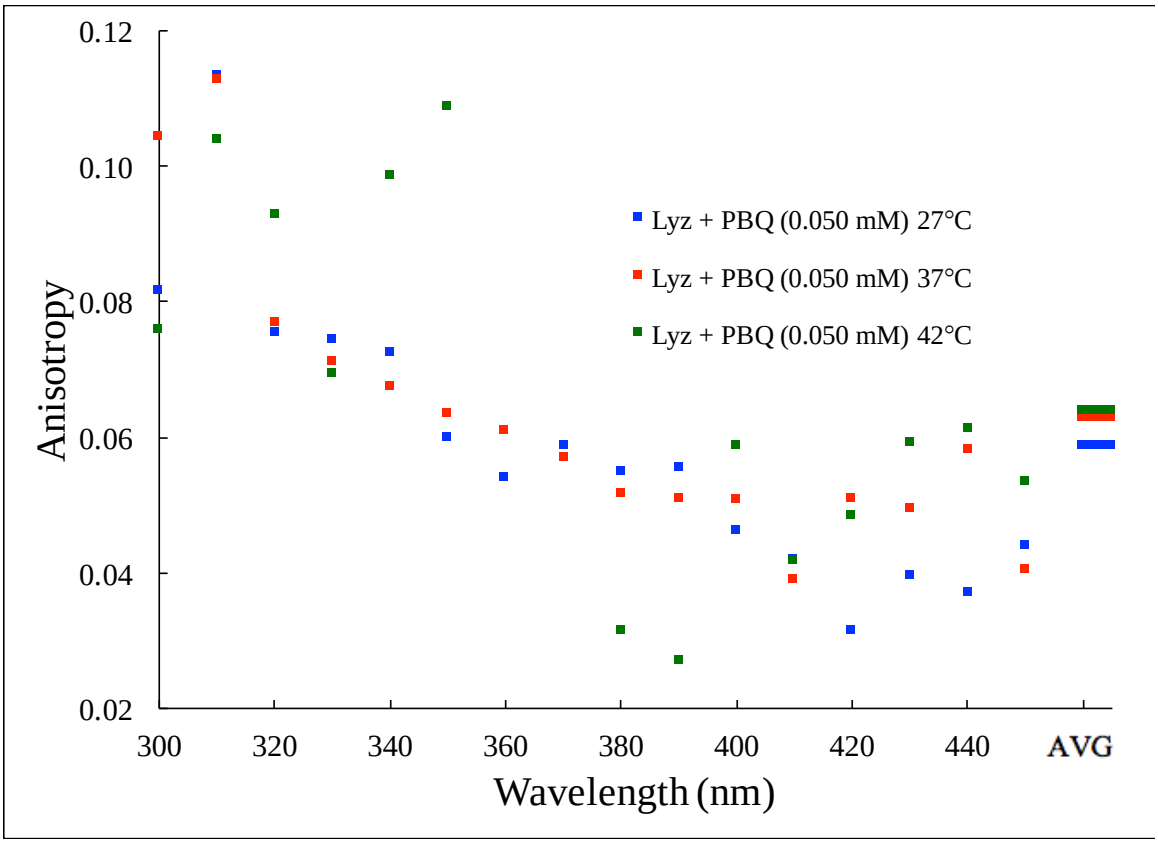

Figure A.6 Anisotropy values recorded from 300-450 nm with an average anisotropy value of Lyz (0.010 mM) modified by PBQ (0.050 mM) at 27°C, 37°C, and 42°C for 24 h at pH=7.0.

A general trend of increasing anisotropy with increasing temperature of reaction solution is observed. These results suggest increasing the temperature of the reaction solution influences the modification of PBQ resulting in an overall non-spherical shape of the protein. In contrast, decreasing the temperature of the reaction solution influences the modification of PBQ resulting in an increased spherical shape of the protein.

APPENDIX B

Anisotropy measures the non-sphericity of a molecule by recording the amount of emitted light that passes through different polarized planes. In these studies, larger values of anisotropy correspond to Ribonuclease A that has been modified resulting in an overall non-spherical shape, while smaller values of anisotropy correspond to Ribonuclease A that has been modified resulting in an increased spherical shape.

Anisotropy values of post-dialysis Ribonuclease A recorded from 300-450 nm corresponding to the different studies performed are presented in the following pages. These values were averaged and general trends in anisotropy were observed as result.

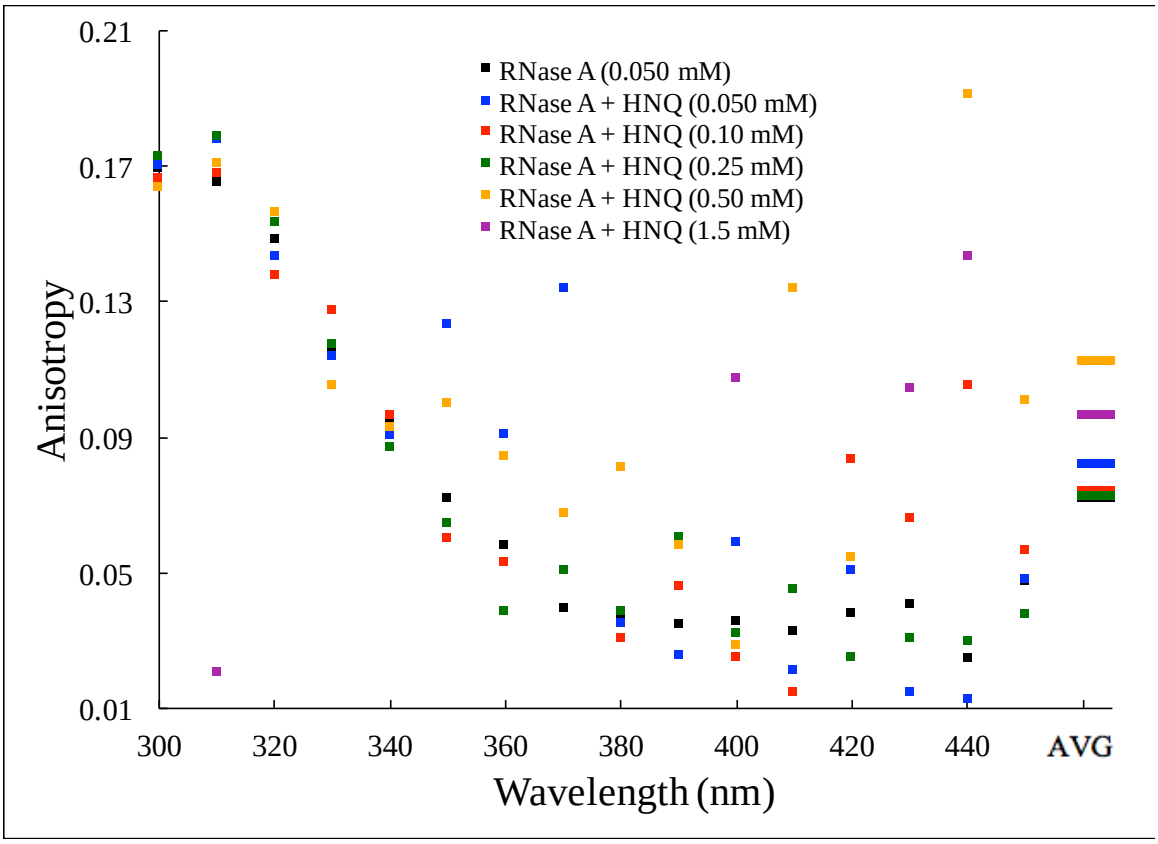

Figure B.1 Anisotropy values recorded from 300-450 nm with an average anisotropy value of RNase A (0.050 mM) and RNase A (0.050 mM) modified by HNQ (0.050, 0.10, 0.25, 0.50, or 1.5 mM) for 24 h at 37°C.

The results of these studies display no clear trend of increasing or decreasing anisotropy with increasing concentration of HNQ. This suggests HNQ does not modify Ribonuclease A in a consistent manner in regard to HNQ concentration.

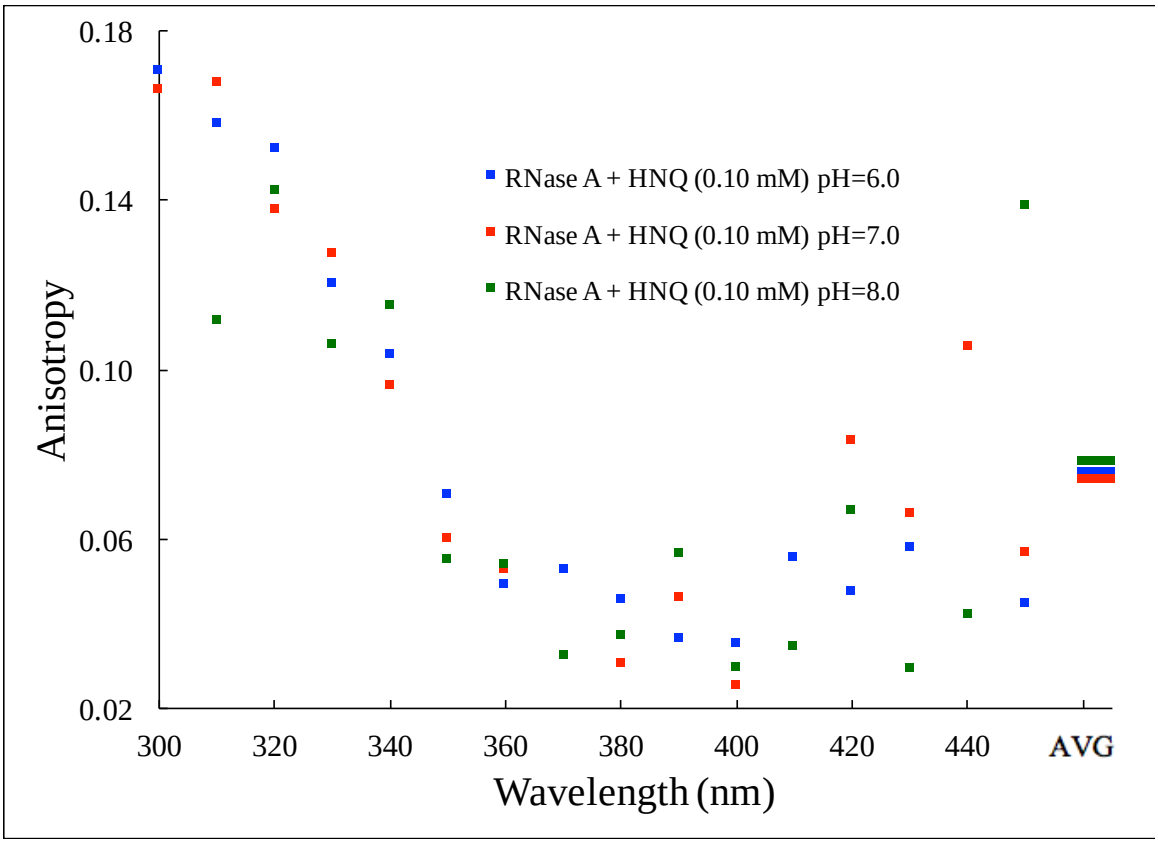

Figure B.2 Anisotropy values recorded from 300-450 nm with an average anisotropy value of RNase A (0.050 mM) modified by HNQ (0.10 mM) at pH=6.0, pH=7.0, and pH=8.0 for 24 h at 37°C.

The results of these studies display no clear trend of increasing or decreasing anisotropy with changes in pH. Similar to the studies performed with Lysozyme, increasing the pH of the reaction solution causes an overall increased non-spherical shape of Ribonuclease A. However, regarding decreases in the pH of the reaction solution, these results do not follow a similar trend as seen in Figure A.5.

APPENDIX C

Pre-dialysis and post-dialysis fluorescence scans of Lysozyme (incubated with PBQ) and Ribonuclease A (incubated with HNQ) from 290-600 nm are presented below. These scans are non-normalized and reflect the changes in fluorescence intensity over the initial 24 h incubation with quinone. The post-dialysis fluorescence scans are represented by the dark blue line denoted "AD".

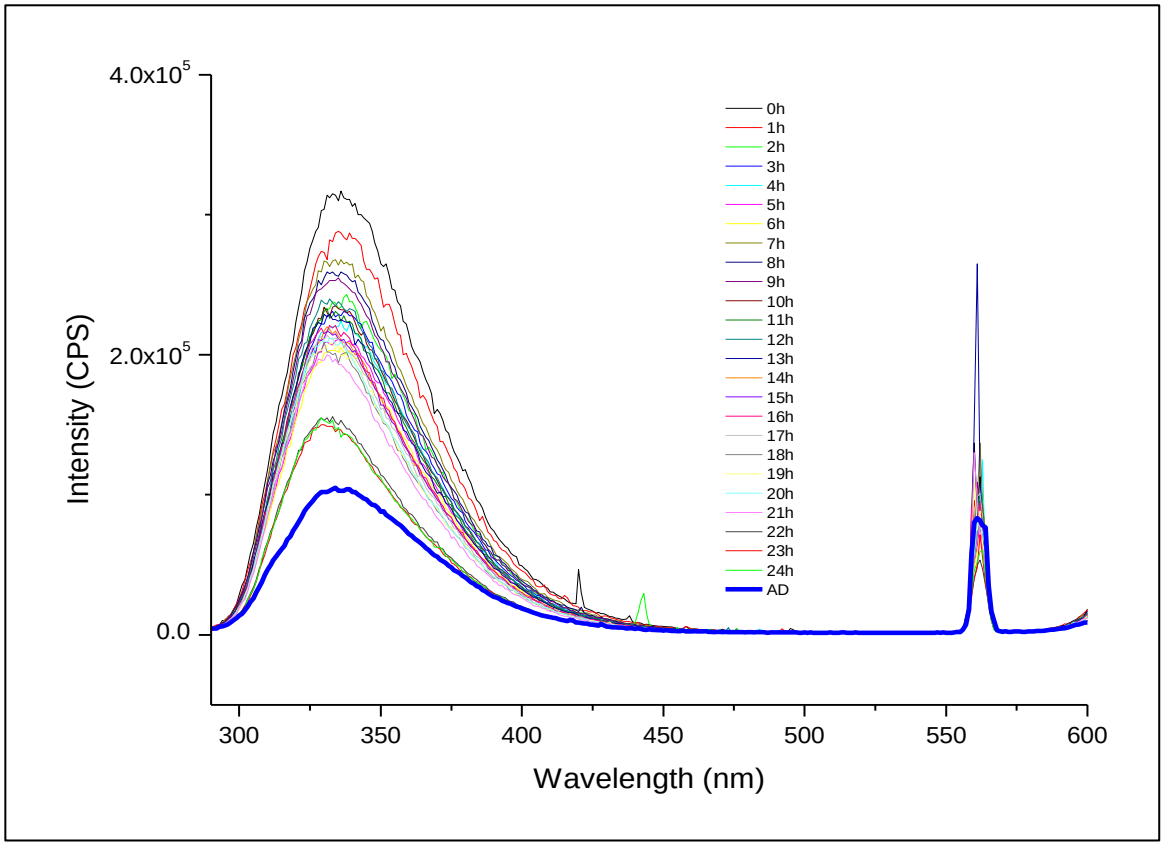

Figure C.1 Pre-dialysis and post-dialysis fluorescence scans of Lyz + PBQ (0.050 mM) for 24 h at 37°C.

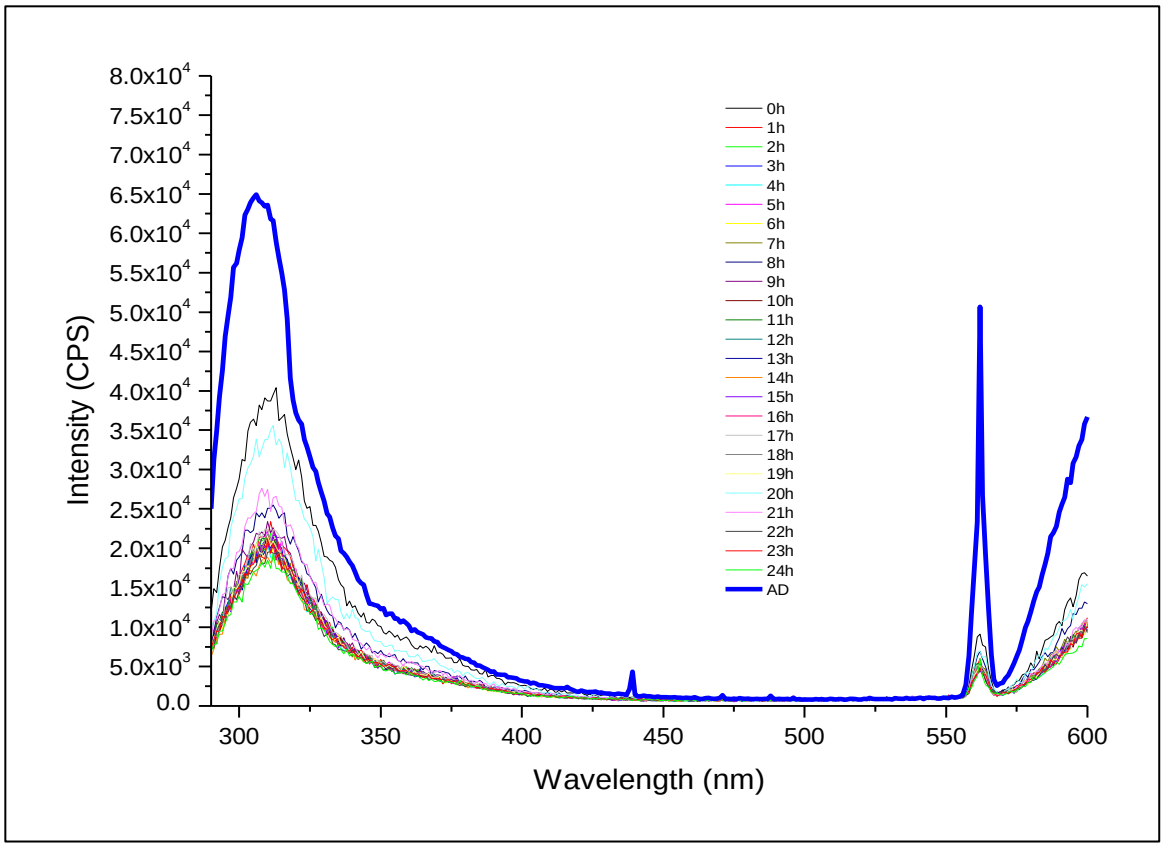

Figure C.2 Pre-dialysis and post-dialysis fluorescence scans of RNase A + HNQ (0.10 mM) for 24 h at 37°C. (The apparent increase of fluorescence intensity of post-dialysis RNase A is representative of initial fluorescence quenching by the concentrated HNQ solution.)